Appendix I
Discrete-Data Control Systems

TO ACCOMPANY

AUTOMATIC CONTROL SYSTEMS
EIGHTH EDITION

BY

BENJAMIN C. KUO

FARID GOLNARAGHI

Discrete-Data Control Systems

▶ I-1 INTRODUCTION

In recent years discrete-data and digital control systems have become more important in industry, mainly because of advances made in microprocessors and microcomputers. In addition, there are distinct advantages working with digital versus analog signals.

The block diagram of a typical digital control system is shown in Fig. I-1. The system is characterized by digitally coded signals at various parts of the system. However, the output device of the system is usually an analog component, such as a dc motor, driven by analog signals. Therefore, a digital control system often requires the use of digital-to-analog (D/A) and analog-to-digital (A/D) converters.

▶ I-2 THE z-TRANSFORM

Just as linear continuous-data systems are described by differential equations, linear digital control systems are described by difference equations (see Appendix B). We have seen that Laplace transform is a powerful method of solving linear time-invariant differential equations. Similarly, z-transform is an operational method of solving linear time-invariant difference equations.

I-2-1 Definition of the z-Transform

Consider the sequence $y(k)$, $k = 0, 1, 2, \ldots$, where $y(k)$ could represent a sequence of numbers or events. The z-transform of $y(k)$ is defined as

$$Y(z) = z\text{-transform of } y(k) = \mathcal{Z}[y(k)]$$

$$= \sum_{k=0}^{\infty} y(k)z^{-k} \tag{I-1}$$

where z is a complex variable with real and imaginary parts. The significance of this definition will become clear later. One important property of the z-transform is that it can
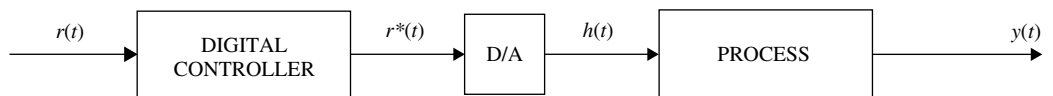
| $r(t)$ | DIGITAL CONTROLLER | $r^*(t)$ | D/A | $h(t)$ | PROCESS | $y(t)$ |

Figure I-1 Block diagram of a typical digital control system.

convert a sequence of numbers in the real domain into an expression in the complex z-domain. The following examples illustrate the derivation of the z-transforms of two simple functions.

► **EXAMPLE I-1** Consider the sequence

$$y(k) = e^{-\alpha k} \qquad k = 0, 1, 2, \dots \tag{I-2}$$

where α is a real constant. Applying Eq. (I-1), the z-transform of $y(k)$ is written

$$Y(z) = \sum_{k=0}^{\infty} e^{-\alpha k} z^{-k} = 1 + e^{-\alpha} z^{-1} + e^{-2\alpha} z^{-2} + \cdots \tag{I-3}$$

which converges for $|e^{-\alpha} z^{-1}| < 1$.

Multiplying both sides of the last equation by $e^{-\alpha} z^{-1}$, subtracting the resulting equation from Eq. (I-3), and solving for $Y(z)$, the latter is expressed in closed form as

$$Y(z) = \frac{1}{1 - e^{-\alpha} z^{-1}} = \frac{z}{z - e^{-\alpha}} \tag{I-4}$$

for $|e^{-\alpha} z^{-1}| < 1$. ◄

► **EXAMPLE I-2** In Example I-1, if $\alpha = 0$, we have

$$y(k) = 1 \qquad k = 0, 1, 2, \dots \tag{I-5}$$

which represents a sequence of ones. Then, the z-transform of $y(k)$ is

$$Y(z) = 1 + z^{-1} + z^{-2} + \cdots = \frac{z}{z - 1} \tag{I-6}$$

which converges for $|z| > 1$. ◄

I-2-2 Relationship between the Laplace Transform and the *z*-Transform

While the mathematicians like to talk about sequences, engineers feel more at home dealing with signals. It may be useful to represent the sequence $y(kT)$, $k = 0, 1, 2, \dots$ as a train of impulses separated by the time interval T. The latter is defined as the **sampling period**. The impulse at the kth time instant, $\delta(t - kT)$, carries the value of $y(kT)$. This situation occurs quite often in digital and sampled-data control systems in which a signal $y(t)$ is digitized or sampled every T seconds to form a time sequence that represents the signal at the sampling instants. Thus, we can relate the sequence $y(kT)$ with a signal that can be expressed as

$$y*(t) = \sum_{k=0}^{\infty} y(kT)\delta(t - kT) \tag{I-7}$$

Taking the Laplace transform on both sides of Eq. (I-7), we have

$$Y*(s) = \mathcal{L}[y*(t)] = \sum_{k=0}^{\infty} y(kT)e^{-kTs} \tag{I-8}$$

Comparing Eq. (I-8) with Eq. (I-1), we see that the z-transform may be related to the Laplace transform through

$$z = e^{Ts} \tag{I-9}$$

In fact, the *z*-transform as defined in Eq. (I-1) may be regarded as a special case with $T = 1$. The definition of the *z*-transform in Eq. (I-9) allows us to treat sampled systems and perform digital simulation of continuous-data systems. Thus, we can summarize the definition of the *z*-transform as

$$Y(z) = \mathcal{Z}[y(kT)] = \mathcal{Z}[y*(t)] = \mathcal{Z}[Y*(s)] \tag{I-10}$$

Or, we can write

$$Y(z) = \mathcal{Z}[y(t)] = \mathcal{Z}[Y(s)] \tag{I-11}$$

with the understanding that the function $y(t)$ is first sampled or discretized to get $y*(t)$ before taking the *z*-transform.

► **EXAMPLE I-3** Consider the time function

$$y(t) = e^{-\alpha t} u_s(t) \tag{I-12}$$

The *z*-transform of $y(t)$ is obtained by performing the following steps:

1. Represent the values of $y(t)$ at the time instants $t = kT$, $k = 0, 1, 2, \ldots$, to form the function $y*(t)$:

$$y*(t) = \sum_{k=0}^{\infty} e^{-\alpha kT} \delta(t - kT) \tag{I-13}$$

2. Take the Laplace transform on both sides of Eq. (I-13):

$$Y*(s) = \sum_{k=0}^{\infty} e^{-\alpha kT} e^{-kTs} = \sum_{k=0}^{\infty} e^{-(s+\alpha)kT} \tag{I-14}$$

3. Express $Y*(s)$ in closed form and apply Eq. (I-9), giving the *z*-transform,

$$Y(z) = \frac{z}{z - e^{-\alpha T}} \tag{I-15}$$

In general, the *z*-transforms of more complex functions may be obtained with the help of some of the *z*-transform theorems that follow. For engineering purposes, a *z*-transform table such as that in Appendix J may be used to transform from $y(k)$ to $Y(z)$.   ◄

I-2-3   Some Important Theorems of the *z*-Transform

Some of the commonly used theorems of the *z*-transform are stated in the following without proof. Just as in the case of the Laplace transform, these theorems are useful in many aspects of the *z*-transform analysis. For uniformity, the real sequence is expressed as $y(kT)$, and if a sampling period is not involved, T can be set to unity.

■ **Theorem 1.** *Addition and Subtraction*

If $y_1(kT)$ and $y_2(kT)$ have z-transforms $Y_1(z)$ and $Y_2(z)$, respectively, then
$$\mathcal{Z}[y_1(kT) \pm y_2(kT)] = Y_1(z) \pm Y_2(z) \tag{I-16}$$

■ **Theorem 2.** *Multiplication by a Constant*

$$\mathcal{Z}[\alpha y(kT)] = \alpha \mathcal{Z}[y(kT)] = \alpha Y(z) \tag{I-17}$$

where α is a constant.

■ **Theorem 3.** *Real Translation (Time Delay and Time Advance)*

$$\mathcal{Z}[y(kT - nT)] = z^{-n}Y(z) \tag{I-18}$$

and

$$\mathcal{Z}[y(kT + nT)] = z^n\left[Y(z) - \sum_{k=0}^{n-1} y(kT)z^{-k}\right] \tag{I-19}$$

where n is a positive integer.

Equation (I-18) represents the *z*-transform of a time sequence that is shifted to the right by *nT*, and Eq. (I-19) denotes that of a time sequence shifted to the left by *nT*. The reason that the right-hand side of Eq. (I-19) is not just $z^nY(z)$ is because the one-sided *z*-transform, similar to the Laplace transform, is defined only for $k \geq 0$. Thus, the second term on the right-hand side of Eq. (I-19) simply represents the sequence that is lost after it is shifted to the left of $k = 0$.

■ **Theorem 4.** *Complex Translation*

$$\mathcal{Z}[e^{\mp\alpha kT}y(kT)] = Y(ze^{\pm\alpha T}) \tag{I-20}$$

where α is a constant. Y(z) is the z-transform of y(kT).

■ **Theorem 5.** *Initial-Value Theorem*

$$\lim_{k\to 0} y(kT) = \lim_{z\to\infty} Y(z) \tag{I-21}$$

if the limit exists.

• The final-value theorem is valid only if $(1 - z^{-1})Y(z)$ does not have poles on or inside the unit circle $|z| = 1$.

■ **Theorem 6.** *Final-Value Theorem*

$$\lim_{k\to\infty} y(kT) = \lim_{z\to 1}(1 - z^{-1})Y(z) \tag{I-22}$$

if the function $(1 - z^{-1})Y(z)$ has no poles on or outside the unit circle $|z| = 1$ in the z-plane.

■ **Theorem 7.** *Real Convolution*

$$Y_1(z)Y_2(z) = \mathcal{Z}\left[\sum_{k=0}^{N} y_1(kT)y_2(NT - kT)\right] = \mathcal{Z}\left[\sum_{k=0}^{N} y_2(kT)y_1(NT - kT)\right]$$
$$= \mathcal{Z}[y_1(kT) * y_2(kT)] \tag{I-23}$$

where "" denotes real convolution in the discrete-time domain.*

Thus, we see that as in the Laplace transform, the *z*-transform of the product of two real functions $y_1(k)$ and $y_2(k)$ is **not** equal to the product of the *z*-transforms $Y_1(z)$ and $Y_2(z)$. One exception to this in the case of the *z*-transform is if one of the two functions is the delay e^{-NTs}, where *N* is a positive integer, then

$$\mathcal{Z}[e^{-NTs}Y(s)] = \mathcal{Z}[e^{-NTs}]\mathcal{Z}[Y(s)] = z^{-N}Y(z) \tag{I-24}$$

Table I-1 summarizes the theorems on the *z*-transform just given. The following examples illustrate the usefulness of some of these theorems.

TABLE I-1 Theorems of *z*-Transforms

Addition and subtraction	$\mathcal{Z}[y_1(kT) \pm y_2(kT)] = Y_1(z) \pm Y_2(z)$
Multiplication by a constant	$\mathcal{Z}[\alpha y(kT)] = \alpha \mathcal{Z}[y(kT)] = \alpha Y(z)$
Real translation	$\mathcal{Z}[y(k - n)T] = z^{-n}Y(z)$ **(time delay)**
	$\mathcal{Z}[y(k + n)T] = z^n \left[Y(z) - \sum_{k=0}^{n-1} y(kT)z^{-k} \right]$ **(time advance)**
	where n = positive integer
Complex translation	$\mathcal{Z}[e^{\mp \alpha kT}y(kT)] = Y(ze^{\pm \alpha T})$
Initial-value theorem	$\lim_{k \to 0} y(kT) = \lim_{z \to \infty} Y(z)$
Final-value theorem	$\lim_{k \to \infty} y(kT) = \lim_{z \to 1}(1 - z^{-1})Y(z)$
	if $(1 - z^{-1})Y(z)$ has no poles on or inside $|z| = 1$.
	$Y_1(z)Y_2(z) = \mathcal{Z}\left[\sum_{k=0}^{n} y_1(kT)y_2(NT - kT) \right]$
Real convolution	$= \mathcal{Z}\left[\sum_{k=0}^{n} y_2(kT)y_1(NT - kT) \right]$
	$= \mathcal{Z}[y_1(kT) * y_2(kT)]$

▶ **EXAMPLE I-4** (*complex translation theorem*) To find the *z*-transform of $y(t) = te^{-\alpha t}$, let $f(t) = t$, $t \geq 0$; then

$$F(z) = \mathcal{Z}[tu_s(t)] = \mathcal{Z}(kT) = \frac{Tz}{(z - 1)^2} \tag{I-25}$$

Using the complex translation theorem in Eq. (I-20), we obtain

$$Y(z) = \mathcal{Z}[te^{-\alpha t}u_s(t)] = F(ze^{\alpha T}) = \frac{Tze^{-\alpha T}}{(z - e^{-\alpha T})^2} \tag{I-26}$$

◀

▶ **EXAMPLE I-5** (*final-value theorem*) Given the function

$$Y(z) = \frac{0.792 z^2}{(z - 1)(z^2 - 0.146z + 0.208)} \tag{I-27}$$

determine the value of $y(kT)$ as k approaches infinity.

Since the function $(1 - z^{-1})Y(z)$ does not have any pole on or outside the unit circle $|z| = 1$ in the *z*-plane, the final-value theorem in Eq. (I-22) can be applied. Thus,

$$\lim_{k \to \infty} y(kT) = \lim_{z \to 1} \frac{0.792 z}{z^2 - 0.416z + 0.208} \tag{I-28}$$

◀

I-2-4 Inverse *z*-Transform

• The inverse *z*-transform of $Y(z)$ is $y(kT)$, not $y(t)$.

Just as in the Laplace transform, one of the major objectives of the *z*-transform is that algebraic manipulations can be made first in the *z*-domain, and then the final time response determined by the inverse *z*-transform. *In general, the inverse z-transform of a function Y(z) yields information on y(kT) only, not on y(t). In other words, the z-transform carries*

information only at the sampling instants. With this in mind, the inverse z-transform can be carried out by one of the following three methods:

1. Partial-fraction expansion
2. Power-series method
3. The inverse formula

Partial-Fraction Expansion Method

• If $Y(s)$ has at least one zero at $z = 0$, the partial-fraction expansion of $Y(z)/z$ should first be performed.

The z-transform function $Y(z)$ is expanded by partial-fraction expansion into a sum of simple recognizable terms, and the z-transform table is used to determine the corresponding $y(kT)$. In carrying out the partial-fraction expansion, there is a slight difference between the z-transform and the Laplace transform procedures. With reference to the z-transform table, we note that practically all the z-transform functions have the term z in the numerator. Therefore, we should expand $Y(z)$ into the form of

$$Y(z) = \frac{K_1 z}{z - e^{-\alpha T}} + \frac{K_2 z}{z - e^{-\beta T}} + \cdots \tag{I-29}$$

To do this, first expand $Y(z)/z$ into fractions and then multiply by z to obtain the final expression. The following example will illustrate this procedure.

▶ **EXAMPLE I-6** Given the z-transform function

$$Y(z) = \frac{(1 - e^{-\alpha T})z}{(z - 1)(z - e^{-\alpha T})} \tag{I-30}$$

find the inverse z-transform. Expanding $Y(z)/z$ by partial-fraction expansion, we have

$$\frac{Y(z)}{z} = \frac{1}{z - 1} - \frac{1}{z - e^{-\alpha T}} \tag{I-31}$$

The final expanded expression for $Y(z)$ is

$$Y(z) = \frac{z}{z - 1} - \frac{z}{z - e^{-\alpha T}} \tag{I-32}$$

From the z-transform table in Appendix J, the corresponding inverse z-transform of $Y(z)$ is found to be

$$y(kT) = 1 - e^{-\alpha kT} \quad k = 0, 1, 2, \ldots \tag{I-33}$$

◀

• If $Y(s)$ does not have any zeros at $z = 0$, then perform the partial-fraction expansion of $Y(z)$ directly.

It should be pointed out that if $Y(z)$ does not contain any factors of z in the numerator, this usually means that the time sequence has a delay, and the partial-fraction expansion of $Y(z)$ should be carried out without first dividing the function by z. The following example illustrates this situation.

▶ **EXAMPLE I-7** Consider the function

$$Y(z) = \frac{(1 - e^{-\alpha T})}{(z - 1)(z - e^{-\alpha T})} \tag{I-34}$$

which does not contain any powers of z as a factor in the numerator. In this case, the partial-fraction expansion of $Y(z)$ is carried out directly. We have

$$Y(z) = \frac{1}{z - 1} - \frac{1}{z - e^{-\alpha T}} \tag{I-35}$$

Although the z-transform table does not contain exact matches for the components in Eq. (I-35), we recognize that the inverse z-transform of the first term on the right-hand side can be written as

$$\mathcal{Z}^{-1}\left[\frac{1}{z-1}\right] = \mathcal{Z}^{-1}\left[z^{-1}\frac{z}{z-1}\right] = \sum_{k=1}^{\infty} z^{-1}$$
$$= u_k[(k-1)T] \qquad k = 1, 2, \ldots \qquad \text{(I-36)}$$

Similarly, the second term on the right-hand side of Eq. (I-35) can be identified with a time delay of T seconds. Thus, the inverse z-transform of $Y(z)$ is written

$$y(kT) = (1 - e^{-\alpha(k-1)T})u[(k-1)T] \qquad k = 1, 2, \ldots \qquad \text{(I-37)}$$

◀

I-2-5 Computer Solution of the Partial-Fraction Expansion of $Y(z)/z$

Whether the function to be expanded by partial fraction is in the form of $Y(z)/z$ or $Y(z)$, the computer programs designed for performing the partial-fraction of Laplace transform functions can still be applied.

Power-Series Method
The definition of the z-transform in Eq. (I-1) gives a straightforward method of carrying out the inverse z-transform. Based on Eq. (I-1) we can clearly see that in the sampled case the coefficient of z^{-k} in $Y(z)$ is simply $y(kT)$. Thus, if we expand $Y(z)$ into a power series in powers of z^{-k}, we can find the values of $y(kT)$ for $k = 0, 1, 2, \ldots$.

▶ **EXAMPLE I-8** Consider the function $Y(z)$ given in Eq. (I-30), which can be expanded into a power series of z^{-1} by dividing the numerator polynomial by the denominator polynomial by long division. The result is

$$Y(z) = (1 - e^{-\alpha T})z^{-1} + (1 - e^{-2\alpha T})z^{-2} + \cdots + (1 - e^{-k\alpha T})z^{-k} + \cdots \qquad \text{(I-38)}$$

Thus, it is apparent that

$$y(kT) = 1 - e^{-\alpha kT} \qquad k = 0, 1, 2, \ldots \qquad \text{(I-39)}$$

which is the same result as in Eq. (I-33). ◀

Inversion Formula
The time sequence $y(kT)$ can be determined from $Y(z)$ by use of the inversion formula:

$$y(kT) = \frac{1}{2\pi j}\oint_{\Gamma} Y(z)z^{k-1}dz \qquad \text{(I-40)}$$

which is a contour integration along the path Γ, that is, a circle of radius $|z| = e^{cT}$ centered at the origin in the z-plane, and c is a value such that the poles of $Y(z)z^{k-1}$ are inside the circle. The inversion formula of the z-transform is similar to that of the inverse Laplace-transform integral given in Eq. (2-10). One way of evaluating the contour integration of Eq. (I-40) is to use the residue theorem of complex-variable theory (the details are not covered here).

I-2-6 Application of the z-Transform to the Solution of Linear Difference Equations

The z-transform can be used to solve linear difference equations. As a simple example, let us consider the first-order unforced difference equation

$$y(k+1) + y(k) = 0 \qquad \text{(I-41)}$$

To solve this equation, we take the z-transform on both sides of the equation. By this, we mean that we multiply both sides of the equation by z^{-k} and take the sum from $k = 0$ to $k = \infty$. We have

$$\sum_{k=0}^{\infty} y(k+1)z^{-k} + \sum_{k=0}^{\infty} y(k)z^{-k} = 0 \tag{I-42}$$

By using the definition of $Y(z)$ and the real translation theorem of Eq. (I-19) for time advance, the last equation is written

$$z[Y(z) - y(0)] + Y(z) = 0 \tag{I-43}$$

Solving for $Y(z)$, we get

$$Y(z) = \frac{z}{z+1}y(0) \tag{I-44}$$

The inverse z-transform of the last equation can be obtained by expanding $Y(z)$ into a power series in z^{-1} by long division. We have

$$Y(z) = (1 - z^{-1} + z^{-2} - z^{-3} + \cdots)x(0) \tag{I-45}$$

Thus, $y(k)$ is written

$$y(k) = (-1)^k y(0) \qquad k = 0, 1, 2, \ldots \tag{I-46}$$

Equation (I-41) is recognized as a single state equation. The z-transform solution of high-order discrete-data systems described by state equations is treated in Section I-3.

The following example shows the z-transform solution of a second-order difference equation.

▶ **EXAMPLE I-9** Consider the second-order difference equation

$$y(k+2) + 0.5y(k+1) + 0.2y(k) = u(k) \tag{I-47}$$

where

$$u(k) = u(k) = 1 \qquad \text{for } k = 0, 1, 2, \ldots \tag{I-48}$$

The initial conditions of $y(k)$ are: $y(0) = 0$ and $y(1) = 0$.

Taking the z-transform on both sides of Eq. (I-47), we get

$$[z^2 Y(z) - z^2 y(0) - zy(1)] + 0.5[zY(z) - zy(0)] + 0.2Y(z) = U(z) \tag{I-49}$$

The z-transform of $u(k)$ is $U(z) = z/(z - 1)$. Substituting the initial conditions of $y(k)$ and the expression of $U(z)$ into Eq. (I-49) and solving for $Y(z)$, we have

$$Y(z) = \frac{z}{(z-1)(z^2 + 0.5z + 0.2)} \tag{I-50}$$

The partial-fraction expansion of $Y(z)/z$ is

$$\frac{Y(z)}{z} = \frac{0.588}{z-1} - \frac{1.036e^{j1.283}}{z + 0.25 + j0.37} - \frac{1.036e^{-j1.283}}{z + 0.25 - j0.37} \tag{I-51}$$

where the exponents in the numerator coefficients are in radians.

Taking the inverse z-transform of $Y(z)$, we get

$$\begin{aligned} y(k) &= 0.588 - 1.036(0.447)^k [e^{-j(2.165k - 1.283)} + e^{j(2.165k - 1.283)}] \\ &= 0.588 - 2.072(0.447)^k \cos(2.165k - 1.283) \qquad k \geq 0 \end{aligned} \tag{I-52}$$
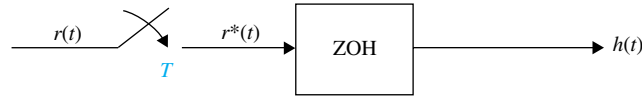
◀

Figure I-2 Sample-and-hold (S/H) device.

▶I-3 TRANSFER FUNCTIONS OF DISCRETE-DATA SYSTEMS

• The ideal sampler is not a physical entity. It is used only for the representation of discrete data.

Discrete-data control systems have the unique features that the signals in these systems either are in the form of pulse trains or are digitally coded, and the controlled processes often contain analog components. For instance, a dc motor, which is an analog device, can be controlled either by a controller that outputs analog signals or by a digital controller that outputs digital data. In the latter case, an interface such as a digital-to-analog (D/A) converter is necessary to couple the digital component to the analog devices. The input and output of the discrete-data system in Fig. I-1 can be represented by number sequences with the numbers separated by the sampling period T. For linear operation, the D/A converter can be represented by a **sample-and-hold (S/H)** device, which consists of a sampler and a data-hold device. The S/H that is most often used for the analysis of discrete-data systems consists of an **ideal sampler** and a **zero-order-hold (ZOH)** device. Thus, the system shown in Fig. I-1 can be functionally represented by the block diagram in Fig. I-2. Figure I-3 shows the typical operation of an ideal sampler and a ZOH. The continuous data $r(t)$ is sampled with a sampling period T by the ideal sampler. The output of the ideal sampler $r^*(t)$ is a train of impulses with the magnitudes of $r(t)$ at T carried by the strengths of the impulses. Note that the ideal sampler is not a physical entity. It is devised simply to represent the discrete-time signal mathematically. In Fig. I-3, the arrows at the sampling instants represent impulses. Since, by definition, an impulse has zero pulse width and infinite height, the lengths of the arrows simply represent the areas
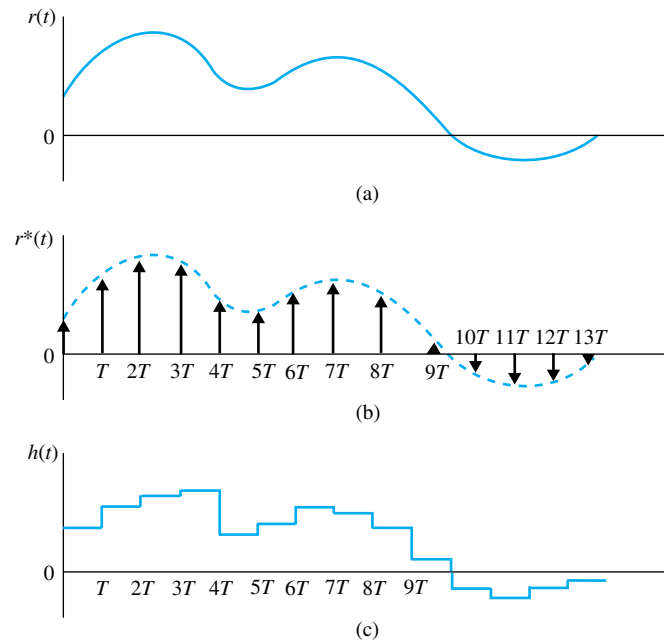

Figure I-3 (a) Input signal to an ideal sampler. (b) Output signal of an ideal sampler. (c) Output signal of a zero-order-hold (ZOH) device.
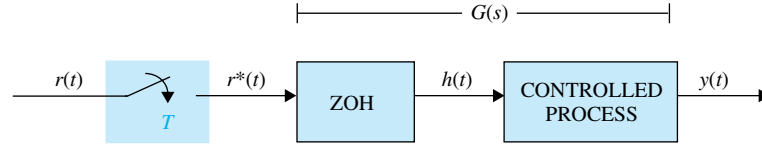
Figure I-4 Block diagram of a discrete-data system.

under the impulses and are the magnitudes of the input signal $r(t)$ at the sampling instants. The ZOH simply holds the magnitude of the signal carried by the incoming impulse at a given time instant, say, kT, for the entire sampling period t until the next impulse arrives at $t = (k + 1)T$. The output of the ZOH is a staircase approximation of the input to the ideal sampler, $r(t)$. As the sampling period T approaches zero, the output of the ZOH, $h(t)$ approaches $r(t)$, that is,

$$\lim_{T \to 0} h(t) = r(t) \tag{I-53}$$

However, since the output of the sampler, $r^*(t)$, is an impulse train, its limit as T approaches zero *does not* have any physical meaning. Based on the preceding discussions, a typical open-loop discrete-data system is modeled as shown in Fig. I-4.

There are several ways of deriving the transfer-function representation of the system in Fig. I-5. The following derivation is based on the Fourier-series representation of the signal $r^*(t)$. We begin by writing

$$r^*(t) = r(t)\delta_T(t) \tag{I-54}$$

where $\delta_T(t)$ is the unit-impulse train,

$$\delta_T(t) = \sum_{k=-\infty}^{\infty} \delta(t - kT) \tag{I-55}$$

Since $\delta_T(t)$ is a periodic function with period T, it can be expressed as a Fourier series:

$$\delta_T(t) = \sum_{n=-\infty}^{\infty} C_n e^{j2\pi nt/T} \tag{I-56}$$

where C_n is the Fourier coefficient, and is given by

$$C_n = \frac{1}{T} \int_0^T \delta_T(t) e^{-jn\omega_s t} dt \tag{I-57}$$

where $\omega_s = 2\pi/T$ is the **sampling frequency** in rad/sec.

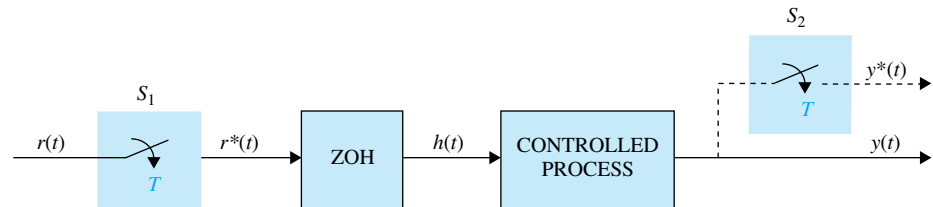**Figure I-5** Discrete-data system with a fictitious sampler.

Since the unit impulse is defined as a pulse with a width of δ and a height of $1/\delta$, and $\delta \to 0$, C_n is written

$$C_n = \lim_{\delta \to 0} \frac{1}{T\delta} \int_0^\delta e^{-jn\omega_s t}\, dt = \lim_{\delta \to 0} \frac{1 - e^{-jn\omega_s \delta}}{jn\omega_s T\delta} = \frac{1}{T} \tag{I-58}$$

Substituting Eq. (I-58) in Eq. (I-56), and then the latter in Eq. (I-54), we get

$$r^*(t) = \frac{1}{T} \sum_{n=-\infty}^{\infty} r(t) e^{jn\omega_s t} \tag{I-59}$$

Taking the Laplace transform on both sides of Eq. (I-59), and using the complex shifting property of Eq. (2-23), we get

$$R^*(s) = \frac{1}{T} \sum_{n=-\infty}^{\infty} R(s - jn\omega_s) = \frac{1}{T} \sum_{n=-\infty}^{\infty} R(s + jn\omega_s) \tag{I-60}$$

Equation (I-60) represents the Laplace transform of the sampled signal $r^*(t)$. It is an alternative expression to Eq. (I-8). From Eq. (I-8), $R^*(s)$ can be written as

$$R^*(s) = \sum_{k=0}^{\infty} r(kT) e^{-kTs} \tag{I-61}$$

Since the summing limits of $R^*(s)$ range from $-\infty$ to ∞, if s is replaced by $s + jm\omega_s$ in Eq. (I-60), where m is any integer, we have

$$R^*(s + jm\omega_s) = R^*(s) \tag{I-62}$$

Pulse-Transfer Function

Now we are ready to derive the transfer function of the discrete-data system shown in Fig. I-4. The Laplace transform of the system output $y(t)$ is written

$$Y(s) = G(s)R^*(s) \tag{I-63}$$

Although the output $y(t)$ is obtained from $Y(s)$ by taking the inverse Laplace transform on both sides of Eq. (I-63), this step is difficult to execute because $G(s)$ and $R^*(s)$ represent different types of signals. To overcome this problem, we apply a fictitious sampler at the output of the system, as shown in Fig. I-5. The fictitious sampler S_2 has the same sampling period T and is synchronized to the original sampler S_1. The sampled form of $y(t)$ is $y^*(t)$. Applying Eq. (I-60) to $y^*(t)$, and using Eq. (I-63), we have

$$Y^*(s) = \frac{1}{T} \sum_{n=-\infty}^{\infty} G(s + jn\omega_s)R^*(s + jn\omega_s) \tag{I-64}$$

In view of the relationship in Eq. (I-62), Eq. (64) is written

$$Y^*(s) = R^*(s)\frac{1}{T} \sum_{n=-\infty}^{\infty} G(s + jn\omega_s) = R^*(s)G^*(s) \tag{I-65}$$

where $G^*(s)$ is defined the same way as $R^*(s)$ in Eq. (I-60), and is called the **pulse-transfer function** of $G(s)$.

z-Transfer Function

Now that all the functions in Eq. (I-65) are in sampled form, where $R^*(s)$, $G^*(s)$, and $Y^*(s)$ all have the form of Eq. (I-61), we can take the z-transform on both sides of the
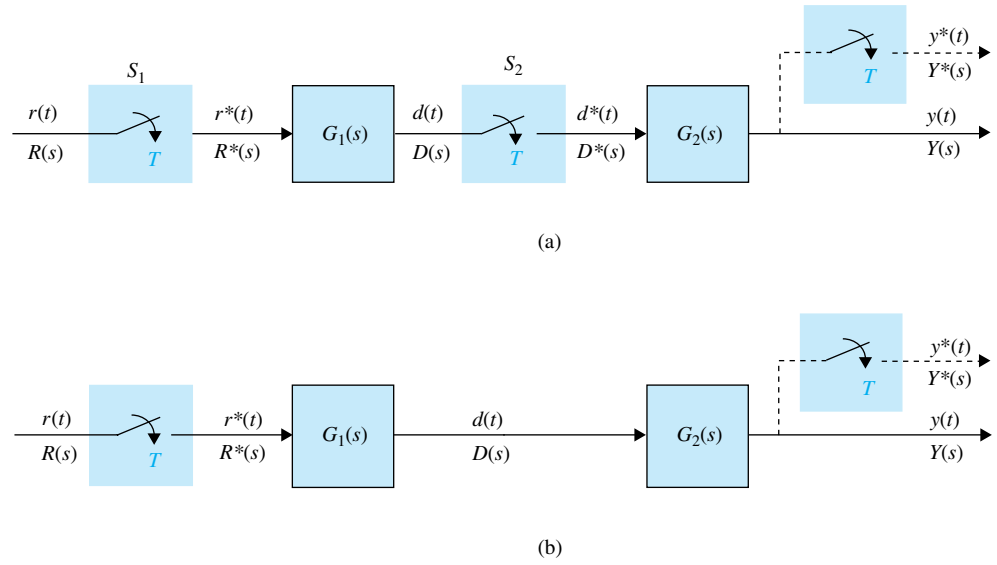
(a)

(b)

Figure I-6 (a) Discrete-data system with cascaded elements and a sampler separating the two elements. (b) Discrete-data system with cascaded elements and no sampler in between.

equation by substituting $z = e^{Ts}$. We have

$$Y(z) = G(z)R(z) \tag{I-66}$$

where $G(z)$ is defined as the **z-transfer function** of $G(s)$, and is given by

$$G(z) = \sum_{k=0}^{\infty} g(kT)z^{-k} \tag{I-67}$$

Thus, for the discrete-data system shown in Figs. I-5 and I-6, the z-transform of the output is equal to the z-transfer function of the process and the z-transform of the input.

I-3-1 Transfer Functions of Discrete-Data Systems with Cascade Elements

The transfer-function representation of discrete-data systems with elements connected in cascade is slightly more involved than that for continuous-data systems, because of the variation of having or not having samplers in between the elements. Figure I-6 shows two different discrete-data systems that contain two elements connected in cascade. In the system of Fig. I-6(a), the two elements are separated by the sampler S_2, which is synchronized to, and has the same period as, the sampler S_1. The two elements in the system of Fig. I-6(b) are connected directly together. It is important to distinguish these two cases when deriving the pulse-transfer function and the z-transfer function. For the system in Fig. I-6(a), the output of $G_1(s)$ is written

$$D(s) = G_1(s)R^*(s) \tag{I-68}$$

and the system output is

$$Y(s) = G_2(s)D^*(s) \tag{I-69}$$

Taking the pulse transform on both sides of Eq. (I-68), and using Eq. (I-62), we have

$$D^*(s) = G_1^*(s)R^*(s) \tag{I-70}$$

Now substituting Eq. (I-70) in Eq. (I-69) and taking the pulse transform, we get

$$Y^*(s) = G_1^*(s)G_2^*(s)R^*(s) \tag{I-71}$$

The corresponding z-transform expression of Eq. (I-71) is

$$Y(z) = G_1(z)G_2(z)R(z) \tag{I-72}$$

• The z-transform of two systems separated by a sampler is equal to the product of the z-transforms of the two systems.

We conclude that *the z-transform of two systems separated by a sampler is equal to the product of the z-transforms of the two systems.*

The Laplace transform of the output of the system in Fig. I-6(b) is

$$Y(s) = G_1(s)G_2(s)R^*(s) \tag{I-73}$$

Taking the pulse transform on both sides of the last equation, we get

$$Y^*(s) = [G_1(s)G_2(s)]^*R^*(s) \tag{I-74}$$

where

$$[G_1(s)G_2(s)]^* = \frac{1}{T}\sum_{n=-\infty}^{\infty} G_1(s + jn\omega_s)G_2(s + jn\omega_s) \tag{I-75}$$

Notice that since $G_1(s)$ and $G_2(s)$ are not separated by a sampler, they have to be treated as one system when taking the pulse transform.

Taking the z-transform on both sides of Eq. (I-74) gives

$$Y(z) = \mathcal{Z}\{[G_1(s)G_2(s)]^*\}R(z) \tag{I-76}$$

Let

$$\mathcal{Z}\{[G_1(s)G_2(s)]^*\} = G_1G_2(z) \tag{I-77}$$

Then, Eq. (I-76) is written

$$Y(z) = G_1G_2(z)R(z) \tag{I-78}$$

I-3-2   Transfer Function of the Zero-Order-Hold

Based on the description of the ZOH given earlier, its impulse response is shown in Fig. I-7. The transfer function of the ZOH is written

$$G_h(s) = \mathcal{L}[g_h(t)] = \frac{1 - e^{-Ts}}{s} \tag{I-79}$$

Thus, if the ZOH is connected in cascade with a linear process using transfer function $G_p(s)$, as shown in Fig. I-5, the z-transform of the combination is written

$$G(z) = \mathcal{Z}[G_h(s)G_p(s)] = \mathcal{Z}\left(\frac{1 - e^{-Ts}}{s}G_p(s)\right) \tag{I-80}$$
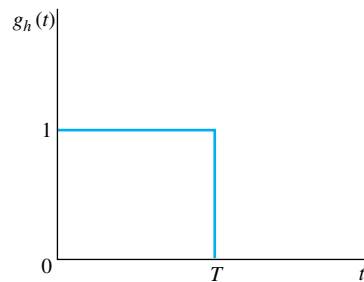

Figure I-7   Impulse response of the ZOH.

By using the time-delay property of z-transforms, Eq. (I-18), Eq. (I-80) is simplified to

$$G(z) = (1 - z^{-1})\mathcal{Z}\left(\frac{G_p(s)}{s}\right) \tag{I-81}$$

▶ **EXAMPLE I-10** Consider that for the system shown in Fig. I-5,

$$G_p(s) = \frac{1}{s(s + 0.5)} \tag{I-82}$$

The sampling period is 1 second. The z-transfer function of the system between the input and the output is determined using Eq. (I-81).

$$G(z) = (1 - z^{-1})\mathcal{Z}\left(\frac{1}{s^2(s + 0.5)}\right)$$

$$= (1 - z^{-1})\mathcal{Z}\left(\frac{2}{s^2} - \frac{4}{s} + \frac{4}{s + 0.5}\right) = \frac{0.426z + 0.361}{z^2 - 1.606z + 0.606} \tag{I-83}$$

◀

I-3-3   Transfer Functions of Closed-Loop Discrete-Data Systems

The transfer functions of closed-loop discrete-data systems are derived using the following procedures:

1. Regard the outputs of samplers as inputs to the system.
2. All other noninputs of the system are treated as outputs.
3. Write cause-and-effect equations between the inputs and the outputs of the system using the SFG gain formula.
4. Take the pulsed transform or the z-transform of the equations obtained in step 3, and manipulate these equations to get the pulse-transfer function or the z-transfer function.

Reference [1] describes the sampled signal flow graph that can be used to implement step 4 using the SFG gain formula.

The following examples illustrate the algebraic procedure of finding the transfer functions of closed-loop discrete-data systems.

▶ **EXAMPLE I-11** Consider the closed-loop discrete-data system shown in Fig. I-8. The output of the sampler is regarded as an input to the system. Thus, the system has inputs $R(s)$ and $E^*(s)$. The signals $E(s)$ and $Y(s)$ are regarded as the outputs of the system.

Writing the cause-and-effect equations for $E(s)$ and $Y(s)$ using the gain formula, we get

$$E(s) = R(s) - G(s)H(s)E^*(s) \tag{I-84}$$
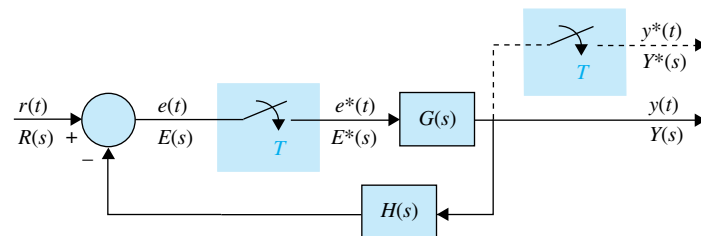$$Y(s) = G(s)E^*(s) \tag{I-85}$$

Figure I-8   Closed-loop discrete-data system.

Notice that the right-hand side of the last two equations contains only the inputs $R(s)$ and $E^*(s)$ and the transfer functions. Taking the pulse transform on both sides of Eq. (I-60) and solving for $E^*(s)$, we get

$$E^*(s) = \frac{R^*(s)}{1 + [G(s)H(s)]^*} \qquad (I\text{-}86)$$

Substituting $E^*(s)$ from Eq. (I-86) into Eq. (I-85), we get

$$Y(s) = \frac{G(s)}{1 + [G(s)H(s)]^*} R^*(s) \qquad (I\text{-}87)$$

Taking the pulse transform on both sides of Eq. (I-87), and using Eq. (I-62), we arrive at the pulse-transfer function of the closed-loop system,

$$\frac{Y^*(s)}{R^*(s)} = \frac{G^*(s)}{1 + [G(s)H(s)]^*} \qquad (I\text{-}88)$$

Taking the z-transform on both sides of the last equation, we have

$$\frac{Y(z)}{R(z)} = \frac{G(z)}{1 + GH(z)} \qquad (I\text{-}89)$$

◀

▶ **EXAMPLE I-12** We show in this example that although it is possible to define an input-output transfer function for the system in Fig. I-8, this may not be possible for all discrete-data systems. Let us consider the system shown in Fig. I-9, which has a sampler in the feedback path. In this case, the outputs of the sampler $Y^*(s)$ and $R(s)$ are the inputs of the system; $Y(s)$ and $E(s)$ are regarded as the outputs. Writing $E(s)$ and $Y(s)$ in terms of the inputs using the gain formula, we get

$$Y(s) = G(s)E(s) \qquad (I\text{-}90)$$
$$E(s) = R(s) - H(s)Y^*(s) \qquad (I\text{-}91)$$

Taking the pulse transform on both sides of the last two equations and after simple algebraic manipulations, the pulse transform of the output is written

$$Y^*(s) = \frac{[G(s)R(s)]^*}{1 + [G(s)H(s)]^*} \qquad (I\text{-}92)$$

Note that the input $R(s)$ and the transfer function $G(s)$ are now combined as one function, $[G(s)R(s)]^*$, and we cannot define a transfer function in the form of $Y^*(s)/R^*(s)$. The z-transform of the output is written

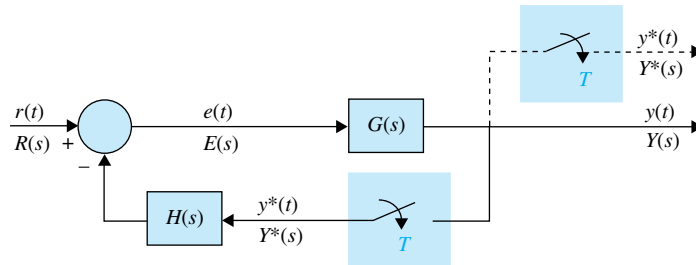$$Y(z) = \frac{GR(z)}{1 + GH(z)} \qquad (I\text{-}93)$$

Figure I-9   Closed-loop discrete-data system.

◀

Although we have been able to arrive at the input-output transfer function and transfer relation of the systems in Figs. I-8 and I-9 by algebraic means without difficulty, for more complex system configurations, the algebraic method may become tedious. The signal-flow graph method may be extended to the analysis of discrete-data systems; the reader may refer to [1] for details.

▶ I-4 STATE EQUATIONS OF LINEAR DISCRETE-DATA SYSTEMS

Just as for continuous-data systems, the modern way of modeling a discrete-data system is by discrete state equations. As described earlier, when dealing with discrete-data systems, we often encounter two situations. The first one is that the system contains continuous-data components, but the signals at certain points of the system are discrete with respect to time because of sample-and-hold (S/H) operations. In this case, the components of the system are still described by differential equations, but because of the discrete-time data, the differential equations are discretized to yield a set of difference equations. The second situation involves systems that are completely discrete with respect to time, and the system dynamics should be difference equations from the outset.

I-4-1 Discrete State Equations

Let us consider the discrete-data control system with an S/H device, as shown in Fig. I-10. Typical signals that appear at various points in the system are shown in the figure. The output signal $y(t)$ ordinarily is a continuous-data signal. The output of the S/H, $h(t)$, is a sequence of steps. Therefore, we can write

$$h(t) = h(kT) = r(kT) \tag{I-94}$$

for $kT \le t < (k + 1)T$, $k = 0, 1, 2, \ldots$.

Now we let the linear process G be described by the state equation and output equation:

$$\frac{d\mathbf{x}(t)}{dt} = \mathbf{A}\mathbf{x}(t) + \mathbf{B}h(t) \tag{I-95}$$

$$y(t) = \mathbf{C}\mathbf{x}(t) + \mathbf{D}h(t) \tag{I-96}$$

where $\mathbf{x}(t)$ is the $n \times n$ state vector, and $h(t)$ and $y(t)$ are the scalar input and output, respectively. The matrices $\mathbf{A}$, $\mathbf{B}$, $\mathbf{C}$, and $\mathbf{D}$ are coefficient matrices. By using Eq. (5-44), the state transition equation is

$$\mathbf{x}(t) = \boldsymbol{\phi}(t - t_0)\mathbf{x}(t_0) + \int_{t_0}^{t} \boldsymbol{\phi}(t - \tau)\mathbf{B}h(\tau)d\tau \tag{I-97}$$

for $t \ge t_0$. If we are interested only in the responses at the sampling instants, we let $t = (k + 1)T$ and $t_0 = kT$. Then Eq. (I-97) becomes

$$\mathbf{x}[(k + 1)T] = \boldsymbol{\phi}(T)\mathbf{x}(kT) + \int_{kT}^{(k+1)T} \boldsymbol{\phi}[(k + 1)T - \tau]\mathbf{B}h(\tau)d\tau \tag{I-98}$$

Since $h(t)$ is piecewise constant, as defined in Eq. (I-95), the input $h(\tau)$ in Eq. (I-98) can be taken outside of the integral sign. Equation (I-98) is written

$$\mathbf{x}[(k + 1)T] = \boldsymbol{\phi}(T)\mathbf{x}(kT) + \int_{kT}^{(k+1)T} \boldsymbol{\phi}[(k + 1)T - \tau]\mathbf{B}d\tau \, h(kT) \tag{I-99}$$

or

$$\mathbf{x}[(k + 1)T] = \boldsymbol{\phi}(T)\mathbf{x}(kT) + \boldsymbol{\theta}(T)h(kT) \tag{I-100}$$
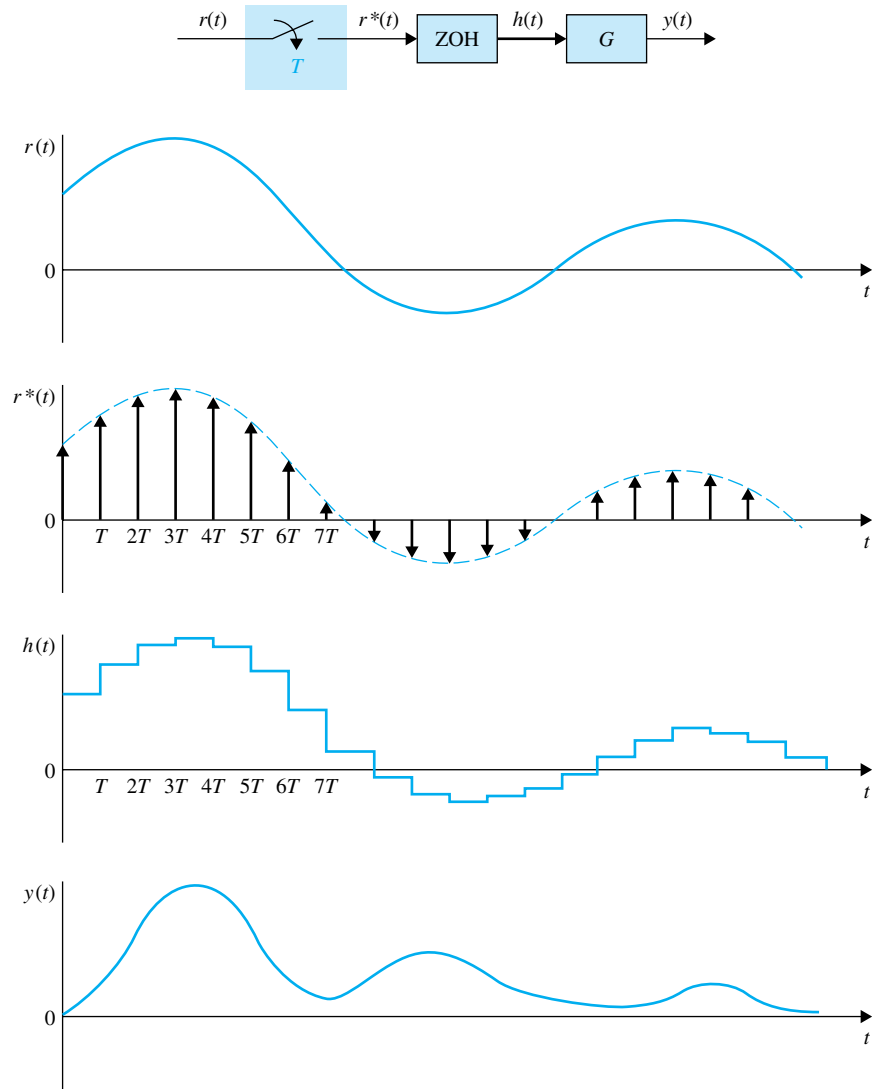
Figure I-10   Discrete-data system with sample-and-hold (S/H).

where

$$\theta(T) = \int_{kT}^{(k+1)T} \boldsymbol{\phi}[(k+1)T - \tau]\mathbf{B}d\tau = \int_{0}^{T} \boldsymbol{\phi}(T - \tau)\mathbf{B}d\tau \qquad \text{(I-101)}$$

Equation (I-100) is of the form of a set of linear first-order difference equations in vector-matrix form, and is referred to as the **vector-matrix discrete state equation**.

I-4-2   Solutions of the Discrete State Equations: Discrete State-Transition Equations

The discrete state equations represented by Eq. (I-100) can be solved by using a simple recursion procedure. By setting $k = 0, 1, 2, \ldots$ successively in Eq. (I-100), the following

equations result:

$$k = 0: \qquad \mathbf{x}(T) = \boldsymbol{\phi}(T)\mathbf{x}(0) + \boldsymbol{\theta}(T)h(0) \qquad \text{(I-102)}$$

$$k = 1: \qquad \mathbf{x}(2T) = \boldsymbol{\phi}(2T) = \boldsymbol{\phi}(T)\mathbf{x}(T) + \boldsymbol{\theta}(T)h(T) \qquad \text{(I-103)}$$

$$k = 2: \qquad \mathbf{x}(3T) = \boldsymbol{\phi}(3T) = \boldsymbol{\phi}(T)\mathbf{x}(2T) + \boldsymbol{\theta}(T)h(2T) \qquad \text{(I-104)}$$

$$\vdots \qquad\qquad \vdots$$

$$k = n - 1: \qquad \mathbf{x}(nT) = \boldsymbol{\phi}(T)\mathbf{x}[(n-1)T] + \boldsymbol{\theta}(T)h[(n-1)T] \qquad \text{(I-105)}$$

Substituting Eq. (I-102) into Eq. (I-103), then Eq. (I-103) into Eq. (I-104), and so on, we obtain the following solution for Eq. (I-100):

$$\mathbf{x}(nT) = \boldsymbol{\phi}^n(T)\mathbf{x}(0) + \sum_{i=0}^{n-1} \boldsymbol{\phi}^{n-i-1}(T)\boldsymbol{\theta}(T)h(iT) \qquad \text{(I-106)}$$

where, from Eq. (5-36), $\boldsymbol{\phi}^n(T) = [\boldsymbol{\phi}(T)]^n = \boldsymbol{\phi}(nT)$.

Equation (I-106) is defined as the **discrete state-transition equation** of the discrete-data system. It is interesting to note that Eq. (I-106) is analogous to its continuous-data counterpart in Eq. (5-41). The state-transition equation of Eq. (I-97) describes the state of the system of Fig. I-10 for all values of t, whereas the discrete state-transition equation in Eq. (I-106) describes the states only at the sampling instants $t = nT$, $n = 0, 1, 2, \ldots$.

With nT considered as the initial time, where n is any positive integer, the state-transition equation is

$$\mathbf{x}[(n + N)T] = \boldsymbol{\phi}^N(T)\mathbf{x}(nT) + \sum_{i=0}^{N-1} \boldsymbol{\phi}^{N-i-1}(T)\boldsymbol{\theta}(T)h[(n+i)T] \qquad \text{(I-107)}$$

where N is a positive integer.

The output of the system at the sampling instants is obtained by substituting $t = nT$ and Eq. (I-106) into Eq. (I-96), yielding

$$y(nT) = \mathbf{C}\mathbf{x}(nT) + \mathbf{D}h(nT)$$

$$= \mathbf{C}\boldsymbol{\phi}(nT)\mathbf{x}(0) + \mathbf{C}\sum_{i=0}^{n-1} \boldsymbol{\phi}[(n-i-1)T]\boldsymbol{\theta}(T)h(iT) + \mathbf{D}h(nT) \qquad \text{(I-108)}$$

An important advantage of the state-variable method over the z-transform method is that it can be modified easily to describe the states and the output between sampling instants. In Eqs. (I-97), if we let $t = (n + \Delta)T$, where $0 < \Delta \le 1$ and $t_0 = nT$, we get

$$\mathbf{x}[(n + \Delta)T] = \boldsymbol{\phi}(\Delta T)\mathbf{x}(nT) + \int_{nT}^{(n+\Delta)T} \boldsymbol{\phi}[(n+\Delta)T - \tau]\mathbf{B}d\tau h(nT)$$

$$= \boldsymbol{\phi}(\Delta T)\mathbf{x}(nT) + \boldsymbol{\theta}(\Delta T)h(nT) \qquad \text{(I-109)}$$

By varying the value of Δ between 0 and 1, the information on the state variables between the sampling instants is completely described by Eq. (I-109).

When a linear system has only discrete data through the system, its dynamics can be described by a set of discrete state equations:

$$\mathbf{x}[(k + 1)T] = \mathbf{A}\mathbf{x}(kT) + \mathbf{B}r(kT) \qquad \text{(I-110)}$$

and output equations:

$$\mathbf{y}(kT) = \mathbf{C}\mathbf{x}(kT) + \mathbf{D}r(kT) \qquad \text{(I-111)}$$

where $\mathbf{A}$, $\mathbf{B}$, $\mathbf{C}$, and $\mathbf{D}$ are coefficient matrices of the appropriate dimensions. Notice that Eq. (I-110) is basically of the same form as Eq. (I-100). The only difference in the two

situations is the starting point of system representation. In the case of Eq. (I-100), the starting point is the continuous-data state equations of Eq. (I-95); $\phi(T)$ and $\theta(T)$ are determined from the **A** and **B** matrices, and must satisfy the conditions and properties of the state transition matrix. In the case of Eq. (I-110), the equation itself represents an outright description of the discrete-data system, and there are no restrictions on the matrices **A** and **B**.

The solution of Eq. (I-110) follows directly from that of Eq. (I-100), and is

$$\mathbf{x}(nT) = \mathbf{A}^n\mathbf{x}(0) + \sum_{i=0}^{n-1}\mathbf{A}^{n-i-1}\mathbf{Br}(iT) \tag{I-112}$$

where

$$\mathbf{A}^n = \mathbf{AAAA}\cdots\mathbf{A}$$
$$|\leftarrow \ n \ \rightarrow| \tag{I-113}$$

I-4-3   *z*-Transform Solution of Discrete State Equations

In Section I-1-5, we illustrated the solution of a simple discrete state equation by the *z*-transform method. In this section, the discrete state equations in vector-matrix form of an *n*th-order system are solved by *z*-transformation. Consider the discrete state equations

$$\mathbf{x}[(k+1)T] = \mathbf{Ax}(kT) + \mathbf{Br}(kT) \tag{I-114}$$

Taking the *z*-transform on both sides of the last equation, we get

$$z\mathbf{X}(z) - z\mathbf{x}(0) = \mathbf{AX}(z) + \mathbf{BR}(z) \tag{I-115}$$

Solving for $\mathbf{X}(z)$ from Eq. (I-115), we get

$$\mathbf{X}(z) = (z\mathbf{I} - \mathbf{A})^{-1}z\mathbf{x}(0) + (z\mathbf{I} - \mathbf{A})^{-1}\mathbf{BR}(z) \tag{I-116}$$

Taking the inverse *z*-transform on both sides of Eq. (I-116), we have

$$\mathbf{x}(nT) = \mathcal{Z}^{-1}[(z\mathbf{I} - \mathbf{A})^{-1}z]\mathbf{x}(0) + \mathcal{Z}^{-1}[(z\mathbf{I} - \mathbf{A})^{-1}\mathbf{BR}(z)] \tag{I-117}$$

In order to carry out the inverse *z*-transform operation of the last equation, we write the *z*-transform of $\mathbf{A}^n$ as

$$\mathcal{Z}(\mathbf{A}^n) = \sum_{n=0}^{\infty}\mathbf{A}^nz^{-n} = \mathbf{I} + \mathbf{A}z^{-1} + \mathbf{A}^2z^{-2} + \cdots \tag{I-118}$$

Premultiplying both sides of Eq. (I-118) by $\mathbf{A}z^{-1}$ and subtracting the result from the last equation, we get

$$(\mathbf{I} - \mathbf{A}z^{-1})\mathcal{Z}(\mathbf{A}^n) = \mathbf{I} \tag{I-119}$$

Therefore, solving for $\mathcal{Z}(\mathbf{A}^n)$ from the last equation yields

$$\mathcal{Z}(\mathbf{A}^n) = (\mathbf{I} - \mathbf{A}z^{-1})^{-1} = (z\mathbf{I} - \mathbf{A})^{-1}z \tag{I-120}$$

or

$$\mathbf{A}^n = \mathcal{Z}^{-1}[(z\mathbf{I} - \mathbf{A})^{-1}z] \tag{I-121}$$

Equation (I-121) represents a way of finding $\mathbf{A}^n$ by using the *z*-transform method. Similarly, we can prove that

$$\mathcal{Z}^{-1}[(z\mathbf{I} - \mathbf{A})^{-1}\mathbf{BR}(z)] = \sum_{i=0}^{n-1}\mathbf{A}^{n-i-1}\mathbf{Br}(iT) \tag{I-122}$$

Now we substitute Eqs. (I-121) and (I-122) into Eq. (I-117), $\mathbf{x}(nT)$ becomes

$$\mathbf{x}(nT) = \mathbf{A}^n\mathbf{x}(0) + \sum_{i=0}^{n-1} \mathbf{A}^{n-i-1}\mathbf{Br}(iT) \tag{I-123}$$

which is identical to Eq. (I-112).

I-4-4 Transfer-Function Matrix and the Characteristic Equation

Once a discrete-data system is modeled by the dynamic equations of Eqs. (I-110) and (I-111), the transfer-function relation of the system can be expressed in terms of the coefficient matrices. By setting the initial state $\mathbf{x}(0)$ to zero, Eq. (I-116) becomes

$$\mathbf{X}(z) = (z\mathbf{I} - \mathbf{A})^{-1} \mathbf{BR}(z) \tag{I-124}$$

Substituting Eq. (I-124) into the z-transformed version of Eq. (I-111), we have

$$\mathbf{Y}(z) = [\mathbf{C}(z\mathbf{I} - \mathbf{A})^{-1} \mathbf{B} + \mathbf{D}]\mathbf{R}(z) = \mathbf{G}(z)\mathbf{R}(z) \tag{I-125}$$

where the transfer-function matrix of the system is defined as

$$\mathbf{G}(z) = \mathbf{C}(z\mathbf{I} - \mathbf{A})^{-1} \mathbf{B} + \mathbf{D} \tag{I-126}$$

or

$$\mathbf{G}(z) = \frac{\mathbf{C}[\mathrm{adj}(z\mathbf{I} - \mathbf{A})\mathbf{B} + |z\mathbf{I} - \mathbf{A}|\mathbf{D}]}{|z\mathbf{I} - \mathbf{A}|} \tag{I-127}$$

The characteristic equation of the system is defined as

$$|z\mathbf{I} - \mathbf{A}| = 0 \tag{I-128}$$

In general, a linear time-invariant discrete-data system with one input and one output can be described by the following difference equation with constant coefficients:

$$\begin{aligned}
y[(k+n)T] &+ a_{n-1}y[(k+n-1)T] + a_{n-2}y[(k+n-2)T] \\
&+ \cdots + a_1y[((k+1))T] + a_0y(kT) \\
&= b_mr[(k+m)T] + b_{m-1}r[(k+m-1)T] \\
&+ \cdots + b_1r[((k+1))T] + b_0r(kT) \qquad n \ge m
\end{aligned} \tag{I-129}$$

Taking the z-transform on both sides of Eq. (I-129) and setting zero initial conditions, the transfer function of the system is written

$$\frac{Y(z)}{R(s)} = \frac{b_mz^m + b_{m-1}z^{m-1} + \cdots + b_1z + b_0}{z^n + a_{n-1}z^{n-1} + \cdots + a_1z + a_0} \qquad n \ge m \tag{I-130}$$

The characteristic equation is obtained by equating the denominator polynomial of the transfer function to zero.

$$z^n + a_{n-1}z^{n-1} + \cdots + a_1z + a_0 = 0 \tag{I-131}$$

► **EXAMPLE I-13** Consider that a discrete-data system is described by the difference equation

$$y(k+2) + 5y(k+1) + 3y(k) = r(k+1) + 2r(k) \tag{I-132}$$

The transfer function of the system is simply

$$\frac{Y(z)}{R(z)} = \frac{z+2}{z^2 + 5z + 3} \tag{I-133}$$

The characteristic equation is

$$z^2 + 5z + 3 = 0 \tag{I-134}$$

The state variables of the system may be defined as

$$x_1(k) = y(k) \tag{I-135}$$
$$x_2(k) = x_1(k + 1) - r(k) \tag{I-136}$$

Substituting the last two equations into Eq. (I-132) gives the two state equations as

$$x_1(k + 1) = x_2(k) + r(k) \tag{I-137}$$
$$x_2(k + 1) = -3x_1(k) - 5x_2(k) - 3r(k) \tag{I-138}$$

from which we have the matrices **A** and **B**:

$$\mathbf{A} = \begin{bmatrix} 0 & 1 \\ -3 & -5 \end{bmatrix} \qquad \mathbf{B} = \begin{bmatrix} 1 \\ -3 \end{bmatrix} \tag{I-139}$$

The same characteristic equation as in Eq. (I-134) is obtained by using $|z\mathbf{I} - \mathbf{A}| = 0$. ◀

I-4-5 State Diagrams of Discrete-Data Systems

When a discrete-data system is described by difference or discrete state equations, a **discrete state diagram** may be constructed for the system. Similar to the relations between the analog-computer block diagram and the state diagram for continuous-data systems, the elements of a discrete state diagram resemble the computing elements of a digital computer. Some of the operations of a digital computer are **multiplication by a constant**, **addition of several variables**, and **time delay** or **shifting**. The discrete state diagram can be used to determine the transfer functions as well as for digital implementation of the system. The mathematical description of these basic digital computations and their corresponding z-transform expressions are as follows:

1. *Multiplication by a constant*:

$$x_2(kT) = ax_1(kT) \tag{I-140}$$
$$X_2(z) = aX_1(z) \tag{I-141}$$

2. *Summing*:

$$x_2(kT) = x_1(kT) + x_3(kT) \tag{I-142}$$
$$X_2(z) = X_1(z) + X_3(z) \tag{I-143}$$

3. *Shifting or time delay*:

$$x_2(kT) = x_1[(k + 1)T] \tag{I-144}$$
$$X_2(z) = zX_1(z) - zx_1(0) \tag{I-145}$$

or

$$X_1(z) = z^{-1}X_2(z) + x_1(0) \tag{I-146}$$

The state diagram representation of these operations are illustrated in Fig. I-11. The initial time $t = 0$ in Eqs. (I-145) and (I-146) can be generalized to $t = t_0$. Then the equations represent the discrete-time state transition from $t \geq t_0$.
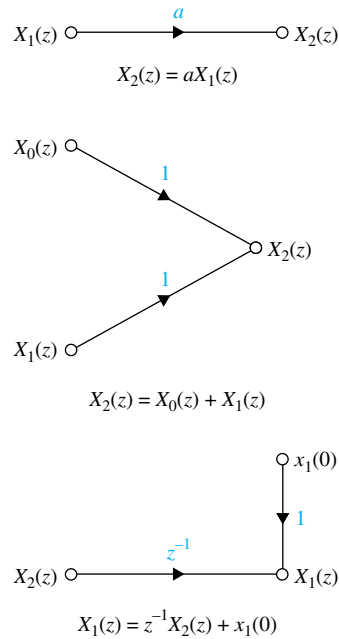
$X_2(z) = aX_1(z)$

$X_2(z) = X_0(z) + X_1(z)$

$X_1(z) = z^{-1}X_2(z) + x_1(0)$

Figure I-11 Basic elements of a discrete state diagram.

▶ **EXAMPLE I-14** Consider again the difference equation in Eq. (I-132), which is

$$y(k + 2) + 5y(k + 1) + 3y(k) = r(k + 1) + 2r(k) \qquad \text{(I-147)}$$

One way of constructing the discrete state diagram for the system is to use the state equations. In this case, the state equations are already defined in Eqs. (I-137) and (I-138). By using essentially the same principle as the state diagram for continuous-data systems, the state diagram for Eqs. (I-137) and (I-138) is shown in Fig. I-12. The time delay unit z^{-1} is used to relate $x_1(k + 1)$ to $x_2(k)$. *The state variables are defined as the outputs of the delay units in the state diagram.*

• The state variables are defined as the outputs of the delay units in the state diagram.

The state-transition equations of the system can be obtained directly from the state diagram using the SFG gain formula. By referring to $X_1(z)$ and $X_2(z)$ as the output nodes and $x_1(0)$, $x_2(0)$, and $R(z)$ as input nodes in Fig. I-12, the state-transition equations are written as

$$\begin{bmatrix} X_1(z) \\ X_2(z) \end{bmatrix} = \frac{1}{\Delta} \begin{bmatrix} 1 + 5z^{-1} & z^{-1} \\ -3z^{-1} & 1 \end{bmatrix} \begin{bmatrix} x_1(0) \\ x_2(0) \end{bmatrix} + \frac{1}{\Delta} \begin{bmatrix} z^{-1}(1 + 5z^{-1}) - 3z^{-2} \\ -3z^{-1} - 3z^{-2} \end{bmatrix} R(z) \qquad \text{(I-148)}$$
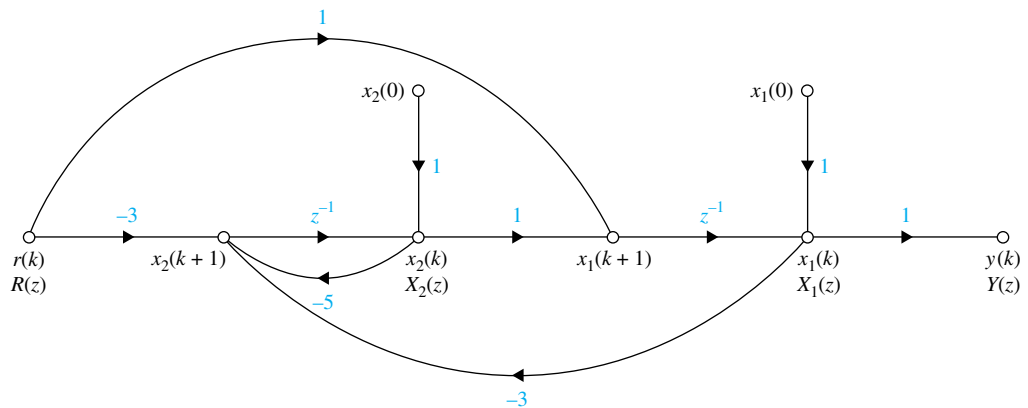

Figure I-12 Discrete state diagram of the system described by the difference equation of Eq. (I-132) or by the state equations of Eqs. (I-137) and (I-138).

(a) Direct decomposition

(b) Cascade decomposition
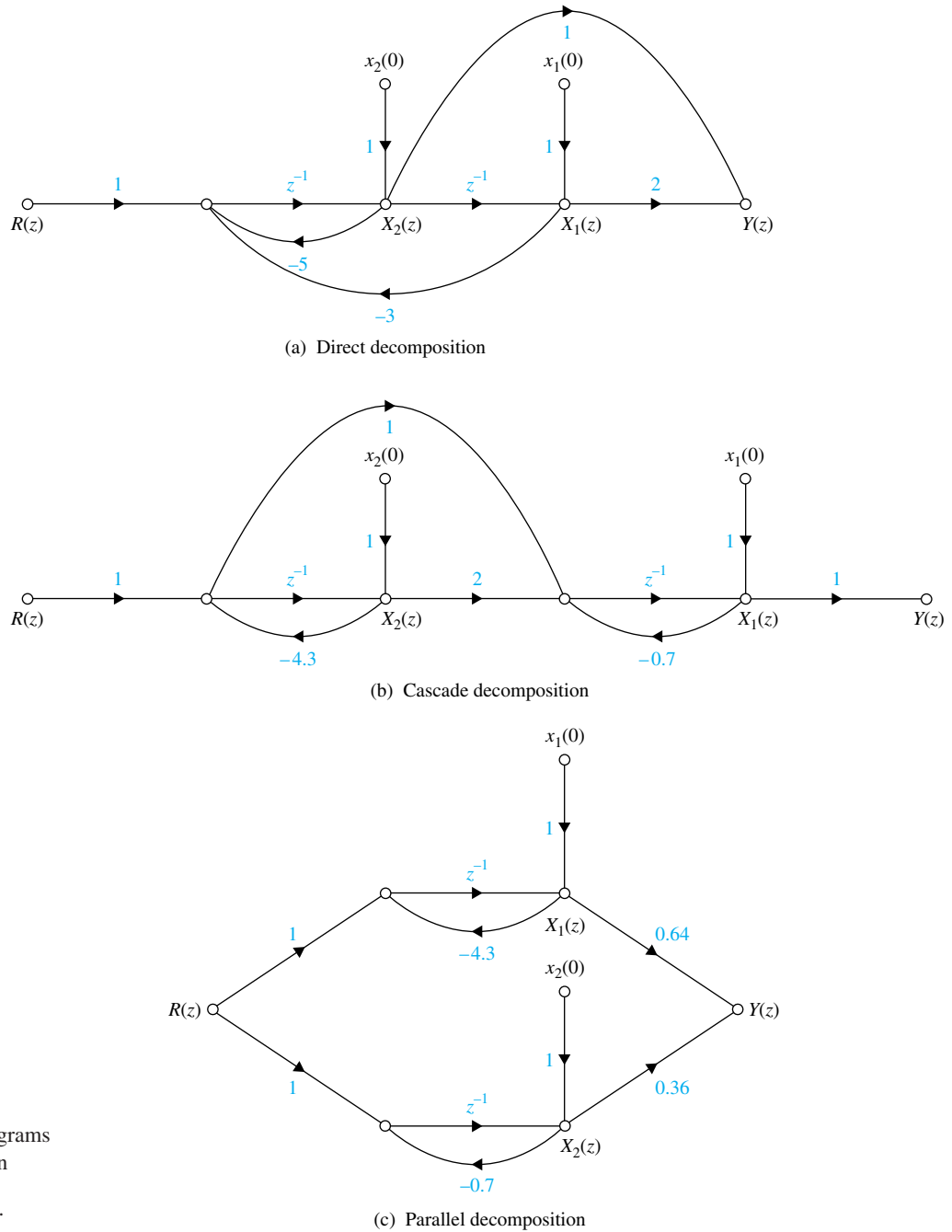
Figure I-13 State diagrams of the transfer function $\dfrac{Y(z)}{R(z)} = \dfrac{(z + 2)}{(z^2 + 5z + 3)}$.

(c) Parallel decomposition

where

$$\Delta = 1 + 5z^{-1} + 3z^{-2} \tag{I-149}$$

The same transfer function between $R(z)$ and $Y(z)$ as in Eq. (I-133) can be obtained directly from the state diagram in Fig. I-13 by applying the SFG gain formula between these two nodes.

As an alternative, the discrete state diagram can be drawn directly from the difference equation via the transfer function, using the decomposition schemes (Fig. I-13). The decomposition of a discrete-data transfer function follows basically the same procedure as that of an analog transfer function covered in Section 5-9, and so the details are not repeated here. ◀
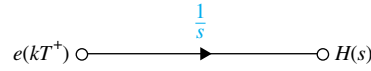
$$e(kT^+) \circ \xrightarrow{\quad \dfrac{1}{s} \quad} \circ H(s)$$

Figure I-14 State-diagram representation of the zero-order-hold (ZOH).

I-4-6 State Diagrams for Sampled-Data Systems

When a discrete-data system has continuous-data as well as discrete-data elements, with the two types of elements separated by sample-and-hold devices, a state diagram model for the sample-and-hold (zero-order-hold) must be established.

Consider that the input of the ZOH is denoted by $e^*(t)$, which is a train of impulses, and the output by $h(t)$. Since the ZOH simply holds the strength of the input impulse at the sampling instant until the next input comes, the signal $h(t)$ is a sequence of steps. The input-output relation in the Laplace domain is

$$H(s) = \frac{1 - e^{-Ts}}{s} E^*(s) \tag{I-150}$$

In the time domain, the relation is simply

$$h(t) = e(kT^+) \tag{I-151}$$

for $kT \le t < (k + 1)T$.

In the state-diagram notation, we need the relation between $H(s)$ and $e(kT^+)$. For this purpose, we take the Laplace transform on both sides of Eq. (I-151) to give

$$H(s) = \frac{e(kT^+)}{s} \tag{I-152}$$

for $kT \le t < (k + 1)T$. The state-diagram representation of the zero-order-hold is shown in Fig. I-14.

▶ **EXAMPLE I-15** As an illustrative example on how the state diagram of a sampled-data system is constructed, let us consider the system in Fig. I-15. We shall demonstrate the various ways of modeling the input-output relations of the system. First, the Laplace transform of the output of the system is written in terms of the input to the ZOH.

$$Y(s) = \frac{1 - e^{-Ts}}{s} \frac{1}{s + 1} E^*(s) \tag{I-153}$$

Taking the z-transform on both sides of Eq. (I-153), we get

$$Y(z) = \frac{1 - e^{-T}}{z - e^{-T}} E(z) \tag{I-154}$$

Figure I-16 shows the state diagram for Eq. (I-154). The discrete dynamic equations of the system are written directly from the state diagram.

$$x_1[(k + 1)T] = -e^{-T}x_1(kT) + (1 - e^{-T})e(kT^+) \tag{I-155}$$
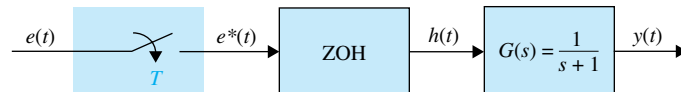$$y(kT) = x_1(kT) \tag{I-156}$$
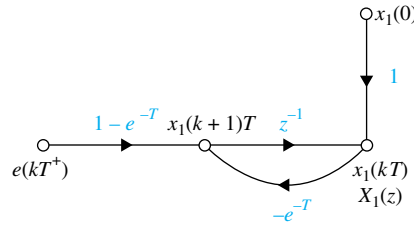

Figure I-15 Sampled-data system.

Figure I-16 Discrete state diagram of the system in Fig. I-15. ◄

► I-5 STABILITY OF DISCRETE-DATA SYSTEMS

The definitions of BIBO and zero-input stability can be readily extended to linear time-invariant SISO discrete-data control systems.

I-5-1 BIBO Stability

Let $u(kT)$, $y(kT)$, and $g(kT)$ be the input, output, and impulse sequence of a linear time-invariant SISO discrete-data system, respectively. With *zero initial conditions, the system is said to be BIBO stable, or simply stable, if its output sequence $y(kT)$ is bounded to a bounded input $u(kT)$*. As with the treatment in Section 6-1, we can show that for the system to be BIBO stable, the following condition must be met:

$$\sum_{k=0}^{\infty} |g(kT)| < \infty \tag{I-157}$$

I-5-2 Zero-Input Stability

For zero-input stability, the output sequence of the system must satisfy the following conditions:

1. $|y(kT)| \leq M < \infty$ (I-158)

2. $\lim_{k \to \infty} |y(kT)| = 0$ (I-159)

Thus, zero-input stability can also be referred to as **asymptotic stability**. We can show that *both the BIBO stability and the zero-input stability of discrete-data systems require that the roots of the characteristic equation lie inside the unit circle $|z| = 1$ in the z-plane.* This is not surprising, since the $j\omega$-axis of the s-plane is mapped onto the unit circle in the z-plane. The regions of stability and instability for discrete-data systems in the z-plane are shown in Fig. I-17. Let the characteristic equation roots of a linear discrete-data time-invariant SISO system be z_i, $i = 1, 2, \ldots, n$. The possible stability conditions of the system are summarized in Table I-2 with respect to the roots of the characteristic equation.

TABLE I-2 Stability Conditions of Linear Time-Invariant Discrete-Data SISO Systems

| Stability condition	Root values
Asymptotically stable or simply stable	$|z_i| < 1$ for all i, $i = 1, 2, \ldots, n$ (all roots inside the unit circle)
Marginally stable or marginally unstable	$|z_i| = 1$ for any i for simple roots, and no $|z_i| > 1$ for $i = 1, 2, \ldots, n$ (at least one simple root, no multiple-order roots on the unit circle, and no roots outside the unit circle)
Unstable	$|z_i| > 1$ for any i, or $|z_i| = 1$ for any multiple-order root. $i = 1, 2, \ldots, n$ (at least one simple root outside the unit circle and at least one multiple-order root on the unit circle)
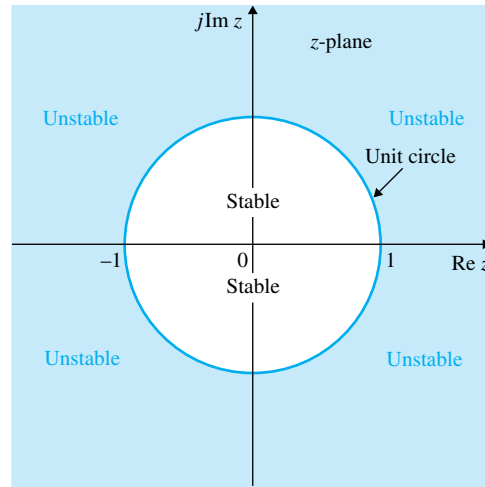
Figure I-17 Stable and unstable regions for discrete-data systems in the z-plane.

The following example illustrates the relationship between the closed-loop transfer-function poles, which are the characteristic equation roots, and the stability condition of the system.

▶ **EXAMPLE I-16**

$$M(z) = \frac{5z}{(z - 0.2)(z - 0.8)} \qquad \text{Stable system}$$

$$M(z) = \frac{5z}{(z + 1.2)(z - 0.8)} \qquad \text{Unstable system due to the pole at } z = -1.2$$

$$M(z) = \frac{5(z + 1)}{z(z - 1)(z - 0.8)} \qquad \text{Marginally stable due to } z = 1$$

$$M(z) = \frac{5(z + 1.2)}{z^2(z + 1)^2\,(z + 0.1)} \qquad \text{Unstable due to second-order pole at } z = -1$$

◀

I-5-3   Stability Tests of Discrete-Data Systems

We pointed out in Section I-5 that the stability test of a linear discrete-data system is essentially a problem of investigating whether all the roots of the characteristic equation are inside the unit circle $|z| = 1$ in the z-plane. The Nyquist criterion, root-locus diagram, and Bode diagram, originally devised for continuous-data systems, can all be extended to the stability studies of discrete-data systems. One exception is the Routh-Hurwitz criterion, which in its original form is restricted to only the imaginary axis of the s-plane as the stability boundary, and thus can be applied only to continuous-data systems.

Bilinear Transformation Method [1]
We can still apply the Routh-Hurwitz criterion to discrete-data systems if we can find a transformation that transforms the unit circle in the z-plane onto the imaginary axis of another complex plane. We cannot use the z-transform relation $z = \exp(Ts)$ or $s = (\ln z)/T$,

since it would transform an algebraic equation in z into a nonalgebraic equation in s, and the Routh test still cannot be applied. However, there are many bilinear transformations of the form of

$$z = \frac{ar + b}{cr + d} \tag{I-160}$$

where a, b, c, d are real constants, *and* r is a complex variable, that will transform circles in the z-plane onto straight lines in the r-plane. One such transformation that transforms the interior of the unit circle of the z-plane onto the left half of the r-plane is

$$z = \frac{1 + r}{1 - r} \tag{I-161}$$

which is referred to as the **r-transformation**. Once the characteristic equation in z is transformed into the r domain using Eq. (I-161), the Routh-Hurwitz criterion can again be applied to the equation in r.

The r-transformation given in Eq. (I-161) is probably the simplest form that can be used for manual transformation of an equation $F(z)$ to an equation in r. Another transformation that is often used in discrete-data control-system design in the frequency domain is

$$z = \frac{(2/T) + w}{(2/T) - w} \tag{I-162}$$

or

$$w = \frac{2}{T}\frac{z - 1}{z + 1} \tag{I-163}$$

which is called the **w-transformation**. Note that the w-transformation becomes the r-transformation when $T = 2$. The advantage of the w-transformation over the r-transformation is that the imaginary axis of the w-plane resembles that of the s-plane. To show this, we substitute

$$z = e^{j\omega T} = \cos \omega T + j \sin \omega T \tag{I-164}$$

into Eq. (I-163), and we get

$$w = \frac{2}{T}\frac{\cos wT + j \sin \omega T - 1}{\cos \omega T + j \sin \omega T + 1} \tag{I-165}$$

Rationalizing the last equation, and simplifying, we get

$$w = j\omega_w = j\frac{2}{T}\tan\frac{\omega T}{2} \tag{I-166}$$

Thus, the unit circle in the z-plane is mapped onto the imaginary axis $w = j\omega_w$ in the w-plane. the relationship between ω_w and ω, the real frequency, is

$$\omega_w = \frac{2}{T}\tan\frac{\omega T}{2} = \frac{\omega_s}{\pi}\tan\frac{\pi\omega}{\omega_s} \tag{I-167}$$

where ω_s is the sampling frequency in rad/sec. The correlation between ω and ω_w is that they both go to 0 and ∞ at the same time. For Routh-Hurwitz criterion, of course, the w-transformation is more difficult to use, especially since the sampling period T appears in Eq. (I-163). However, if computer programs are available for the transformations, the difference is insignificant.

The following examples illustrate the application of the r-transformation to a characteristic equation in z so that the equation can be tested by Routh-Hurwitz criterion in the r-domain.

▶ **EXAMPLE I-17** Consider that the characteristic equation of a discrete-data control system is

$$z^3 + 5.94z^2 + 7.7z - 0.368 = 0 \tag{I-168}$$

Substituting Eq. (I-161) into the last equation and simplifying, we get

$$3.128r^3 - 11.74r^2 + 2.344r + 14.27 = 0 \tag{I-169}$$

Routh's tabulation of the last equation is

r^3	3.128	2.344
Sign change		
r^2	-11.74	14.27
Sign change		
r^1	6.146	0
r^0	14.27	

Since there are two sign changes in the first column of the tabulation, Eq. (I-169) has two roots in the right half of the r-plane. This corresponds to Eq. (I-168) having two roots outside the unit circle in the z-plane. This result can be checked by solving the two equations in z and r. For Eq. (I-168), the roots are: $z = -2.0$, $z = -3.984$, and $z = 0.0461$. The three corresponding roots in the r-plane are: $r = 3.0$, $r = 1.67$, and $r = -0.9117$, respectively. ◀

▶ **EXAMPLE I-18** Let us consider a design problem using the bilinear transformation and Routh-Hurwitz criterion. The characteristic equation of a linear discrete-data control system is given as

$$F(z) = z^3 + z^2 + z + K = 0 \tag{I-170}$$

where K is a real constant. The problem is to find the range of values of K so that the system is stable. We first transform $F(z)$ into an equation in r using the bilinear transformation of Eq. (I-161). The result is

$$(1 - K)r^3 + (1 + 3K)r^2 + 3(1 - K)r + 3 + K = 0 \tag{I-171}$$

Routh's tabulation of the last equation is

r^3	$1 - K$	$3(1 - K)$
r^2	$1 + 3K$	$3 + K$
r^1	$\dfrac{8K(1 - K)}{1 + 3K}$	0
r^0	$3 + K$	

For a stable system, the numbers in the first column of the tabulation must be of the same sign. We can show that these numbers cannot be all negative, since the conditions contradict each other. Next, for all the numbers to be positive, we have the following conditions:

$$1 - K > 0 \qquad 1 + 3K > 0 \qquad K > 0 \qquad 3 + K > 0$$

which lead to the condition for stability:

$$0 < K < 1 \tag{I-172}$$

◀

Direct Stability Tests

There are stability tests that can be applied directly to the characteristic equation in z with reference to the unit circle in the z-plane. One of the first methods that gives the necessary

and sufficient conditions for the characteristic equation roots to lie inside the unit circle is the Schur-Cohn criterion [2]. A simpler tabulation method was devised by Jury and Blanchard [3, 4] and is called **Jury's stability criterion** [6]. R. H. Raible [5] devised an alternate tabular form of Jury's stability test. Unfortunately, these analytical tests all become very tedious for equations higher than the second order, especially when the equation has unknown parameter(s) in it. Then, there is no reason to use any of these tests if all the coefficients of the equation are known, since we can always use a root-finding program on a computer. Weighing all the pros and cons, this author believes that when the characteristic equation has at least one unknown parameter, the bilinear transformation method is still the best manual method for determining stability of linear discrete-data systems. However, it is useful to introduce the necessary condition of stability that can be checked by inspection.

Consider that the characteristic equation of a linear time-invariant discrete-data system is

$$F(z) = a_n z^n + a_{n-1} z^{n-1} + \cdots + a_1 z + a_0 = 0 \tag{I-173}$$

where all the coefficients are real. Among all the conditions provided in Jury's test, the following *necessary* conditions must be satisfied for $F(z)$ to have no roots on or outside the unit circle.

$$
\begin{aligned}
&F(1) > 0 \\
&F(-1) > 0 \qquad \text{if } n = \text{even integer} \\
&F(-1) < 0 \qquad \text{if } n = \text{odd integer} \\
&|a_0| < a_n
\end{aligned}
\tag{I-174}
$$

If an equation of the form of Eq. (I-173) violates any one of these conditions, then not all of the roots are inside the unit circle, and the system would not be stable. Apparently, these necessary conditions can be checked easily by inspection.

▶ **EXAMPLE I-19** Consider the equation

$$F(z) = z^3 + z^2 + 0.5z + 0.25 = 0 \tag{I-175}$$

Applying the conditions in Eq. (I-174), we have

$$
\begin{aligned}
&F(1) = 2.75 > 0 \qquad \text{and} \qquad F(-1) = -0.25 < 0 \qquad \text{for } n = 3, \text{ which is odd} \\
&|a_0| = 0.25 < a_3 = 1
\end{aligned}
$$

Thus, the conditions in Eq. (I-174) are all satisfied, but nothing can be said about the stability of the system. ◀

▶ **EXAMPLE I-20** Consider the equation

$$F(z) = z^3 + z^2 + 0.5z + 1.25 = 0 \tag{I-176}$$

The conditions in Eq. (6-58) are

$$
\begin{aligned}
&F(-1) = 0.75 > 0 \qquad \text{for } n = 3, \text{ which is odd} \\
&|a_0| = 1.25, \text{ which is not less than } a_3, \text{ which equals 1.}
\end{aligned}
$$

Since for odd n $F(-1)$ must be negative, the equation in Eq. (I-176) has at least one root outside the unit circle. The condition on the absolute value of a_0 is also not met. ◀

Second-Order Systems

The conditions in Eq. (I-174) become *necessary and sufficient* when the system is of the second order. That is, the necessary and sufficient conditions for the second-order equation

$$F(z) = a_2 z^2 + a_1 z + a_0 = 0 \tag{I-177}$$

to have no roots on or outside the unit circle are

$$
\begin{aligned}
F(1) &> 0 \\
F(-1) &> 0 \\
|a_0| &< a_2
\end{aligned}
\tag{I-178}
$$

▶ **EXAMPLE I-21** Consider the equation

$$
F(z) = z^2 + z + 0.25 = 0
\tag{I-179}
$$

Applying the conditions in Eq. (I-178), we have

$$
F(1) = 2.25 > 0 \qquad F(-1) = 0.25 > 0 \qquad \text{for } n = 2, \text{ which is even}
$$
$$
|a_0| = 0.25 < a_2 = 1
$$

Thus, the conditions in Eq. (I-178) are all satisfied. The two roots in Eq. (I-179) are all inside the unit circle, and the system is stable. ◀

▶ I-6 TIME-DOMAIN PROPERTIES OF DISCRETE-DATA SYSTEMS

I-6-1 Time Response of Discrete-Data Control Systems

To carry out the design of discrete-data control systems in the time domain or the z-domain, we must first study the time- and z-domain properties of these systems. We learned from the previous sections that the output responses of most discrete-data control systems are functions of the continuous-time variable t. Thus, the time-domain specifications such as the maximum overshoot, rise time, damping ration, and so forth, can still be applied to discrete-data systems. The only difference is that in order to make use of the analytical tools such as z-transforms, the continuous data found in a discrete-data system are sampled so that the independent time variable is kT, where T is the sampling period in seconds. Also, instead of working in the s-plane, the transient performance of a discrete-data system is characterized by poles and zeros of the transfer function in the z-plane.

The objectives of the following sections are as follows:

1. To present methods of finding the discretized time responses of discrete-data control systems
2. To describe the important characteristics of the discretized time response $y(kT)$
3. To establish the significance of pole and zero locations in the z-plane
4. To provide comparison between time responses of continuous-data and discrete-data control systems

Let us refer to the block diagram of the discrete-data control system shown in Fig. I-18. The transfer function of the system is

$$
\frac{Y(z)}{R(z)} = \frac{G(z)}{1 + GH(z)}
\tag{I-180}
$$

where $GH(z)$ denotes the z-transform of $G(s)H(s)$. Once the input $R(z)$ is given, the output sequence $y(kT)$ can be determined using one of the following two methods:

1. Take the inverse z-transform of $Y(z)$ using the z-transform table.
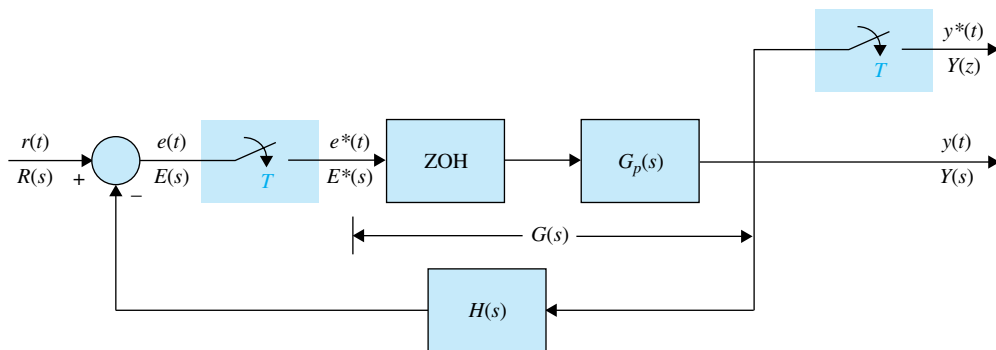2. Expand $Y(z)$ into a power series of z^{-k}.

Figure I-18 Block diagram of a discrete-data control system.

The z-transform of the output is defined as

$$Y(z) = \sum_{k=0}^{\infty} y(kT)z^{-k} \tag{I-181}$$

The discrete-time response $y(kT)$ can be determined by referring to the coefficient of z^{-k} for $k = 0, 1, 2, \ldots$. Remember that $y(kT)$, $k = 0, 1, 2, \ldots$ contains only the sampled information on $y(t)$ at the sampling instants. If the sampling period is large relative to the most significant time constant of the system, $y(kT)$ may not be an accurate representation of $y(t)$.

▶ **EXAMPLE I-22** Consider that the position-control system described in Section 7-7 has discrete data in the forward path, so that the system is now described by the block diagram of Fig. I-18. For $K = 14.5$, the transfer function of the controlled process is

$$G_p(s) = \frac{65,250}{s(s + 361.2)} \tag{I-182}$$

The forward-path transfer function of the discrete-data system is

$$G_{h0}G_p(z) = \mathcal{Z}[G_{h0}G_p(s)] = (1 - z^{-1})\mathcal{Z}\left[\frac{G_p(s)}{s}\right] \tag{I-183}$$

For a sampling period of $T = 0.001$ second, the z-transfer function in Eq. (I-183) is evaluated as

$$G_{h0}G_p(z) = \frac{0.029z + 0.0257}{z^2 - 1.697z + 0.697} \tag{I-184}$$

The closed-loop transfer function of the system is

$$\frac{Y(z)}{R(z)} = \frac{G_{h0}G_p(z)}{1 + G_{h0}G_p(z)} = \frac{0.029z + 0.0257}{z^2 - 1.668z + 0.7226} \tag{I-185}$$

where $R(z)$ and $Y(z)$ represent the z-transforms of the input and the output, respectively. For a unit-step input, $R(z) = z/(z - 1)$. The output transform $Y(z)$ becomes

$$Y(z) = \frac{z(0.029z + 0.0257)}{(z - 1)(z^2 - 1.668z + 0.7226)} \tag{I-186}$$

The output sequence $y(kT)$ can be determined by dividing the numerator polynomial of $Y(z)$ by its denominator polynomial to yield a power series in z^{-1}. Figure I-20 shows the plot of $y(kT)$ (dots) versus kT, when $T = 0.001$ second. For comparison, the unit-step response of the continuous-data system in Section 7-6 with $K = 14.5$ is shown in the same figure. As seen in Fig. I-19, when the sampling period is small, the output responses of the discrete-data and the continuous-data systems are very similar. The maximum value of $y(kT)$ is 1.0731, or a 7.31 percent maximum overshoot, as against the 4.3 percent maximum overshoot for the continuous-data system.
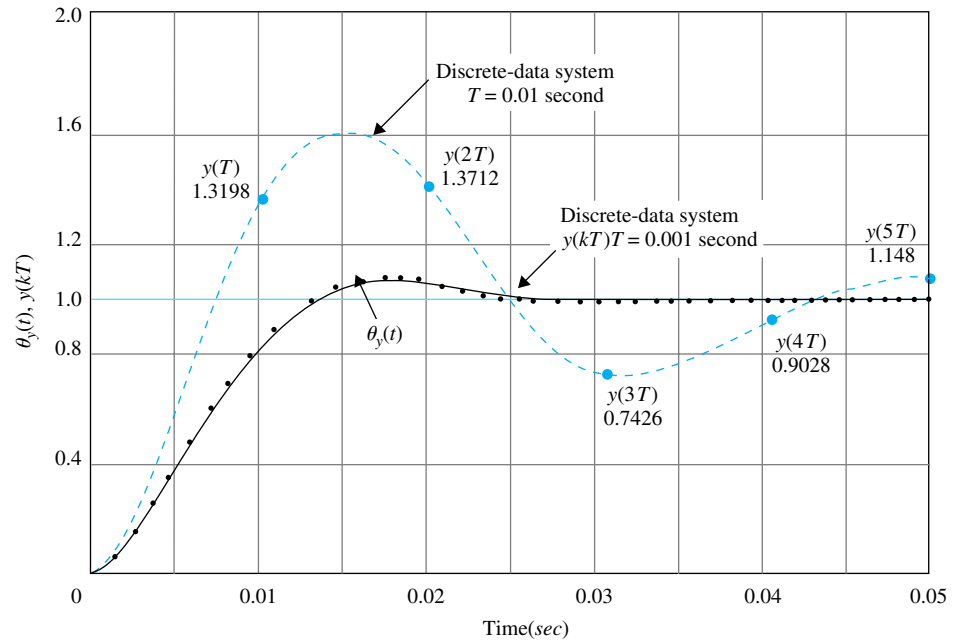
Figure I-19 Comparison of unit-step responses of discrete-data and continuous-data systems.

When the sampling period is increased to 0.01 second, the forward-path transfer function of the discrete-data system is

$$G_{h0}G_p(z) = \frac{1.3198z + 0.4379}{z^2 - 1.027z + 0.027} \tag{I-187}$$

and the closed-loop transfer function is

$$\frac{Y(z)}{R(z)} = \frac{1.3198z + 0.4379}{z^2 + 0.2929z + 0.4649} \tag{I-188}$$

• Two equal characteristic equation roots on the negative real axis in the z-plane do not correspond to critical damping.

The output sequence $y(kT)$ with $T = 0.01$ second is shown in Fig. I-19 with $k = 0, 1, 2, 3, 4,$ and 5. The true continuous-time output of the discrete-data system is shown as the dotted curve. Notice that the maximum value of $y(kT)$ is 1.3712, but the true maximum overshoot is considerably higher than that. Thus, the larger sampling period only makes the system less stable, but the sampled output no longer gives an accurate measure of the true output.

When the sampling period is increased to 0.01658 second, the characteristic equation of the discrete-data system is

$$z^2 + 1.4938z + 0.4939 = 0 \tag{I-189}$$

• When one or more characteristic equation roots lie on the negative axis in the z-plane, response will oscillate with positive and negative peaks.
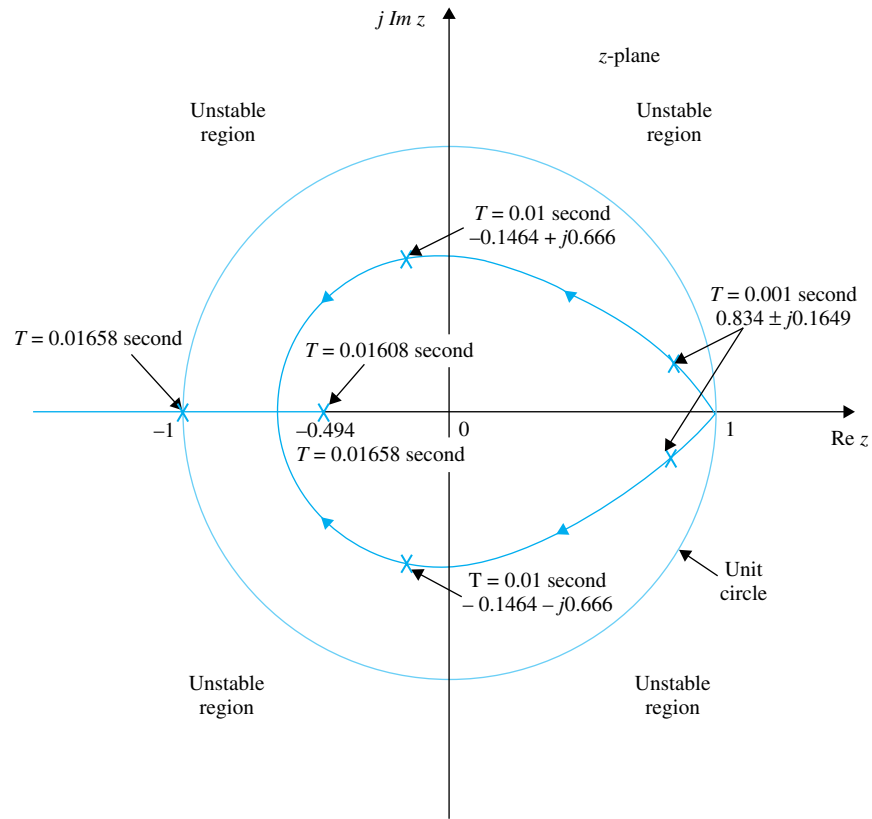
which has roots at $z = -0.494$ and $z = -1.000$. The root at -1.000 causes the step response of the system to oscillate with a constant amplitude, and the system is marginally stable. Thus, for all sampling periods greater than 0.01658 second, the discrete-data system will be unstable. From Section 7-6, we learned that the second-order continuous-data system is always stable for finite positive values of K. For the discrete-data system, the sample-and-hold has the effect of making the system less stable, and if the value of T is too large, the second-order system can become unstable. Figure I-20 shows the trajectories of the two characteristic-equation roots of the discrete-data system as the sampling period T varies. Notice that when the sampling period is very small, the two characteristic-equation roots are very close to the $z = 1$ point and are complex. When $T = 0.01608$ second, the two roots become equal and real and are negative. Unlike the continuous-data system, the case of two identical roots on the *negative* real axis in the z-plane *does not* correspond to critical damping. For discrete-data systems, when one or more characteristic-equation roots lie on the negative real axis of the z-plane, the system response will oscillate with positive and negative peaks. Figure I-21 shows the oscillatory response of $y(kT)$ when $T = 0.01658$ second, which is the critical value for stability. Beyond this value of T, one root will move outside the unit circle, and the system will become unstable.

Figure I-20 Trajectories of roots of a second-order discrete-data control system as the sampling period T varies.
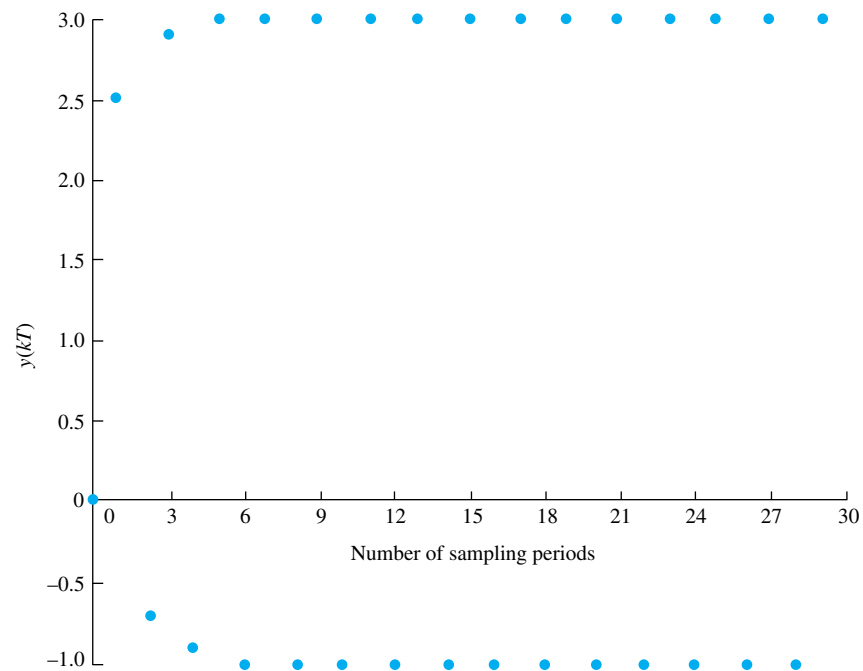

Figure I-21 Oscillatory response of a discrete-data system with a sampling period $T = 0.01658$ second.

I-6-2 Mapping between s-Plane and z-Plane Trajectories

For analysis and design purposes, it is important to study the relation between the location of the characteristic-equation roots in the z-plane and the time response of the discrete-data system. In Section I-2, the periodic property of the Laplace transform of the Laplace transform of the sampled signal $R^*(s)$ is established by Eq. (I-62); that is, $R^*(s + jm\omega_s) = R^*(s)$, where m is an integer. In other words, given any point s_1 in the s-plane, the function $R^*(s)$ has the same value at all periodic points $s = s_1 + jm\omega_s$. Thus, the s-plane is divided into an infinite number of periodic strips, as shown in Fig. I-22(a). The strip between

(a)

(b)
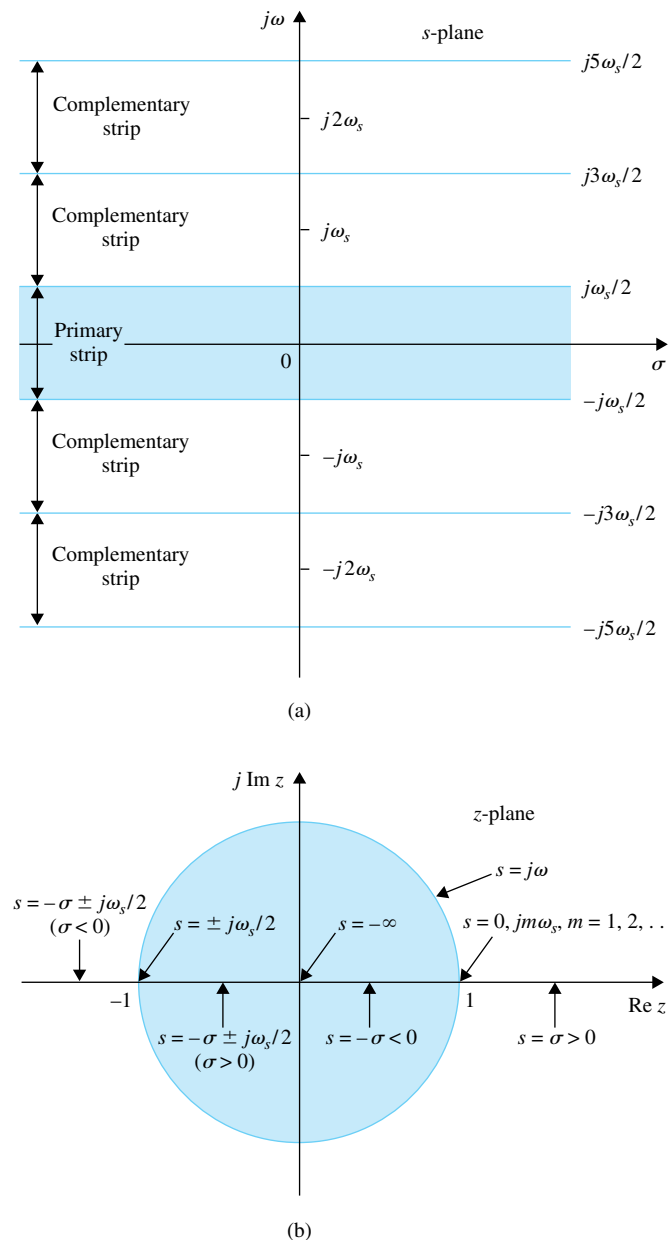
Figure I-22 Periodic strips in the s-plane and the corresponding points and lines between the s-plane and the z-plane.

$\omega = \omega_s/2$ is called the **primary strip**, and all others at higher frequencies are called the **complementary strips**. Figure I-22(b) shows the mapping of the periodic strips from the s-plane to the z-plane, and the details are explained as follows.

1. The $j\omega$-axis in the s-plane is mapped onto the unit circle $|z| = 1$ in the z-plane.
2. The boundaries of the period strips, $s = jm\omega_s/2$, $m = \pm1, \pm3, \pm5, \ldots$, are mapped onto the negative real axis of the z-plane. The portion inside the unit circle corresponds to $\sigma < 0$, and the portion outside the unit circle corresponds to $\sigma > 0$.
3. The center lines of the periodic strips, $s = jm\omega_s$, $m = 0, \pm2, \pm4, \ldots$, are mapped onto the positive real axis of the z-plane. The portion inside the unit circle corresponds to $\sigma < 0$, and the portion outside the unit circle corresponds to $\sigma > 0$.
4. Regions shown in the periodic strips in the left-half s-plane are mapped onto the interior of the unit circle in the z-plane.
5. The point $z = 1$ in the z-plane corresponds to the origin, $s = 0$, in the x-plane.
6. The origin, $z = 0$, in the z-plane corresponds to $s = -\infty$ in the s-plane.

In the time-domain analysis of continuous-data systems, we devise the damping factor α, the damping ratio ζ, and the natural undamped frequency ω_n to characterize the system dynamics. The same parameters can be defined for discrete-data systems with respect to the characteristic-equation roots in the z-plane. The loci of the constant-α, constant-ζ, constant-ω, and constant-ω_n in the z-plane are described in the following sections.

Constant-Damping Loci: For a constant-damping factor $\sigma = \alpha$ in the s-plane, the corresponding trajectory in the z-plane is described by

$$z = e^{\alpha T} \tag{I-190}$$

which is a circle centered at the origin with a radius of $e^{\alpha T}$, as shown in Fig. I-23.

Constant-Frequency Loci: The constant-frequency $\omega = \omega_1$ locus in the s-plane is a horizontal line parallel to the σ-axis. The corresponding z-plane locus is a straight line emanating from the origin at an angle of $\theta = \omega_1 T$ radians, measured from the real axis, as shown in Fig. I-24.
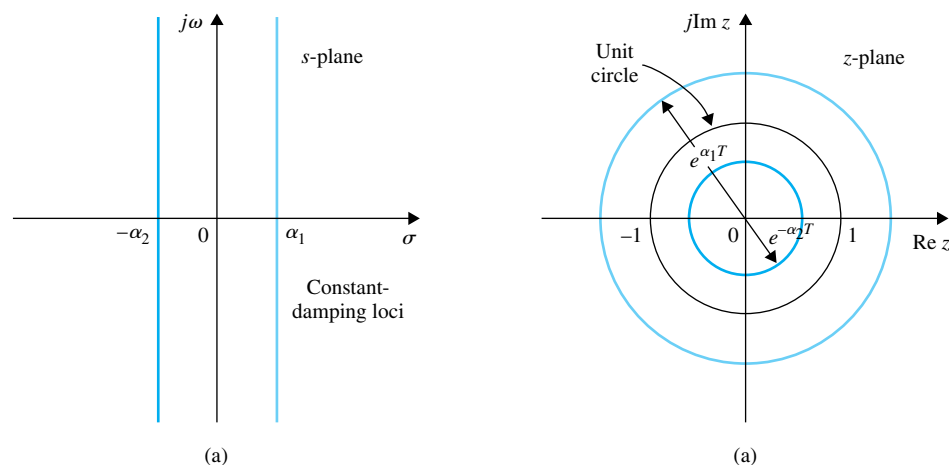

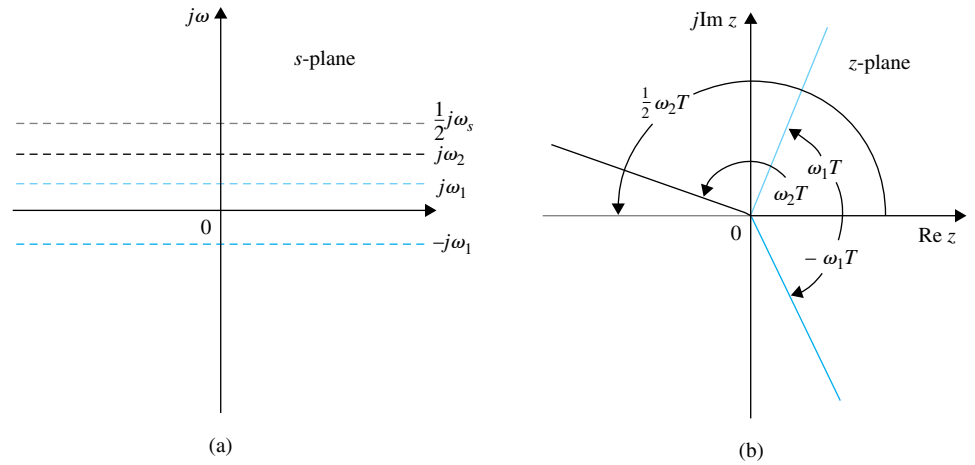**Figure I-23** Constant-damping loci in the s-plane and the z-plane.

Figure I-24 Constant-frequency loci in the s-plane and the z-plane.

Constant Natural-Undamped Frequency Loci: The constant-ω_n loci in the s-plane are concentric circles with the center at the origin, and the radius is ω_n. The corresponding constant-ω_n loci in the z-plane are shown in Fig. I-25 for $\omega_n = \omega_s/16$ to $\omega_s/2$. Only the loci inside the unit circle are shown.

Constant-Damping Ratio Loci: For a constant-damping ratio ζ, the s-plane loci are described by

$$s = -\omega \tan \beta + j\omega \qquad (\text{I-191})$$

The constant-ζ loci in the z-plane are described by

$$z = e^{Ts} = e^{-2\pi(\tan\beta)/\omega_s} \angle 2\pi\omega/\omega_s \qquad (\text{I-192})$$
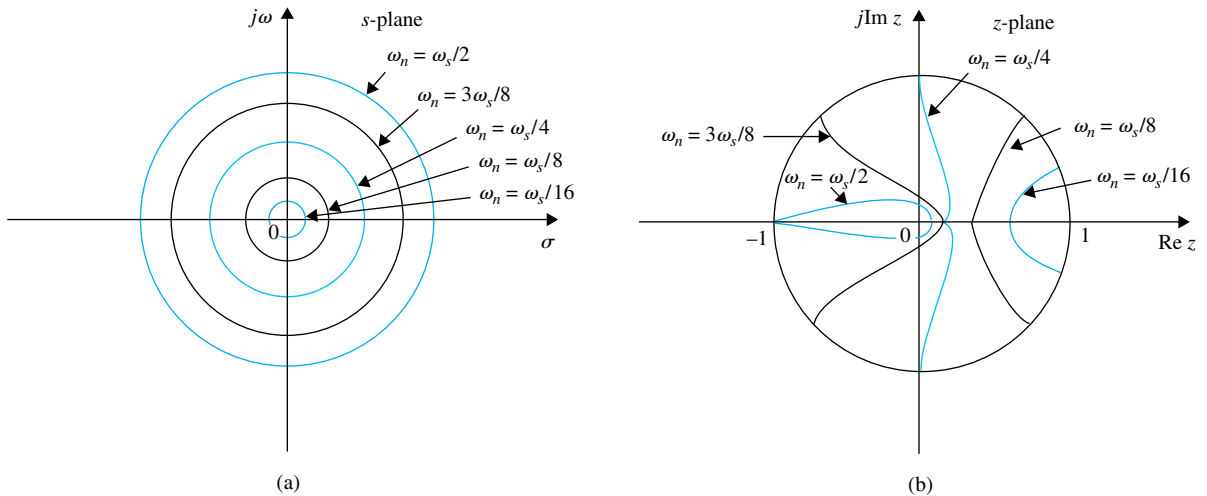
Figure I-25 Constant-natural-undamped frequency loci in the s-plane and the z-plane.
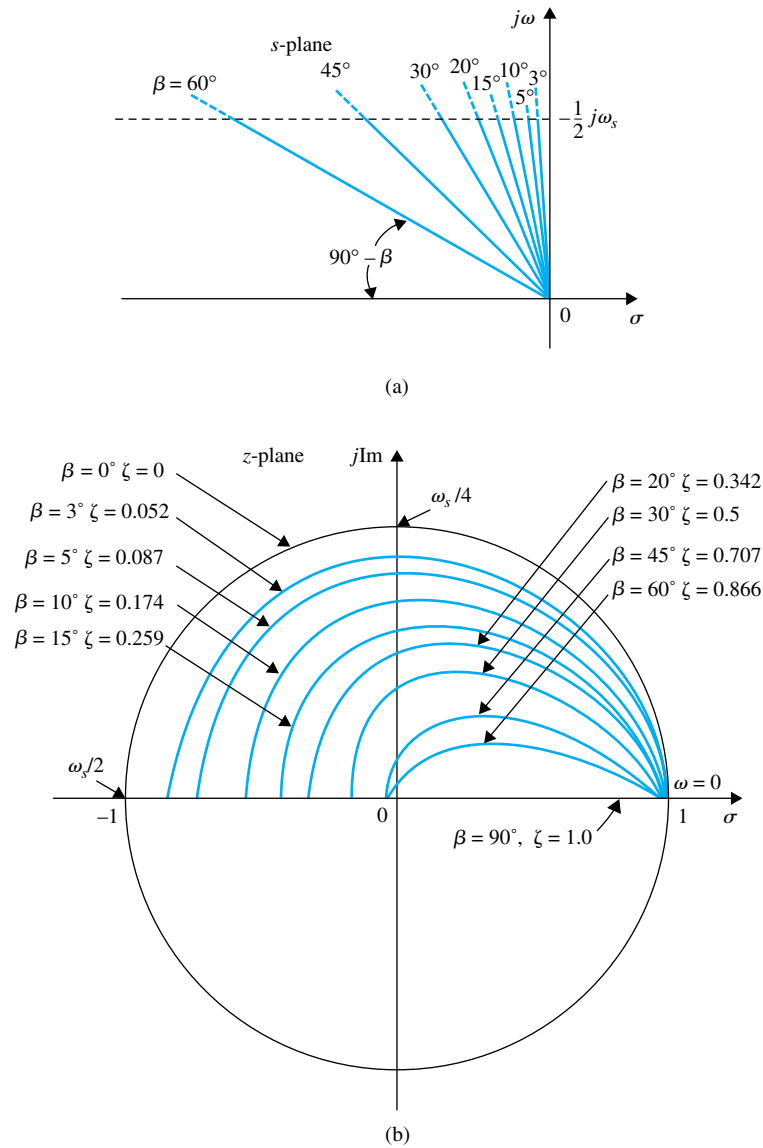
Figure I-26 Constant-damping-ratio loci in the s-plane and the z-plane.

where

$$\beta = \sin^{-1}\zeta = \text{constant} \tag{I-193}$$

For a given value of β, the constant-ζ locus in the z-plane, described by Eq. (I-193), is a logarithmic spiral for $0° < \beta < 90°$. Figure I-26 shows several typical constant-ζ loci in the top half of the z-plane.

I-6-3 Relation between Characteristic-Equation Roots and Transient Response

Based on the discussions given in the last section, we can establish the basic relation between the characteristic-equation roots and the transient response of a discrete-data system,
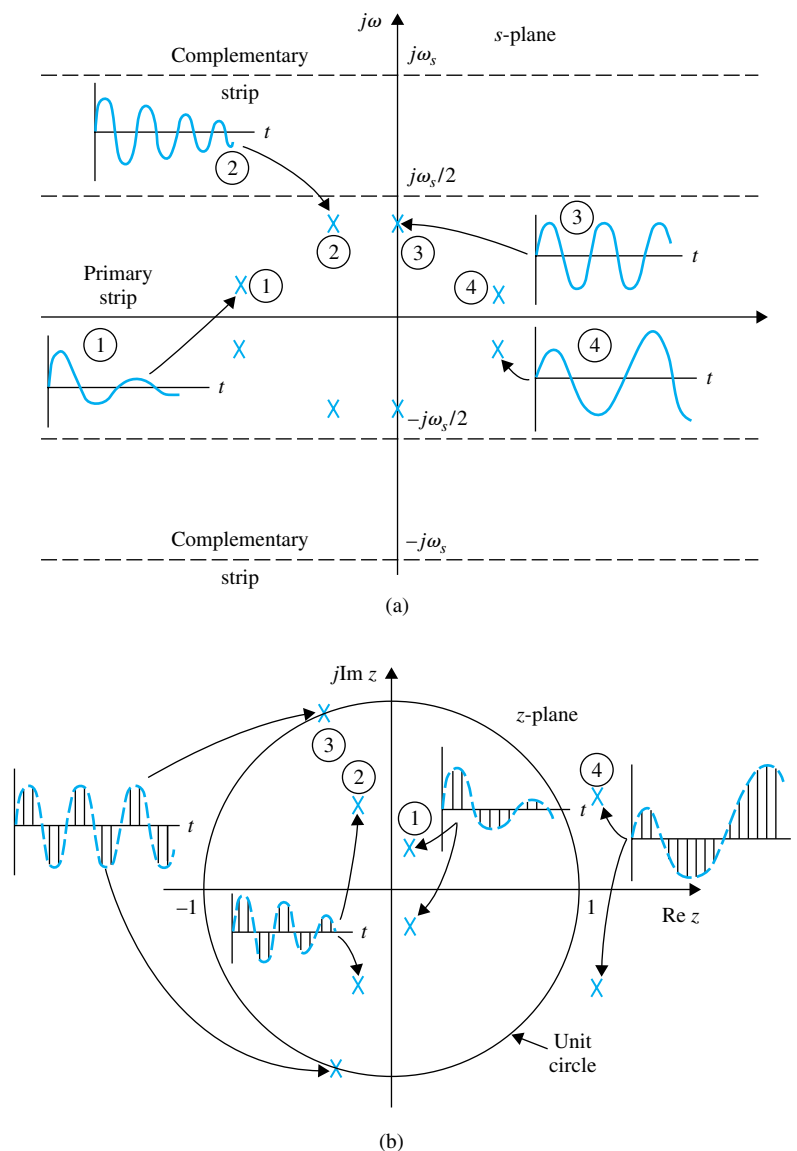
Figure I-27 (a) Transient responses corresponding to various pole locations of $Y^*(s)$ in the s-plane (complex-conjugate poles only). (b) Transient-response sequence corresponding to various pole locations of $Y(z)$ in the z-plane.

keeping in mind that, in general, the zeros of the closed-loop transfer function will also play an important role on the response, but not on the stability, of the system.

Roots on the Positive Real Axis in the z-Plane: Roots on the positive real axis inside the unit circle of the z-plane give rise to responses that decay exponentially with an increase of kT. Typical responses relative to the root locations are shown in Figs. I-27 and I-28. The roots closer to the unit circle will decay slower. When the root is at $z = 1$, the response has a constant amplitude. Roots outside the unit circle correspond to unstable systems, and the responses will increase with kT.

Roots on the Negative Real Axis in the z-Plane: The negative real axis of the z-plane corresponds to the boundaries of the periodic strips in the s-plane. For example, when
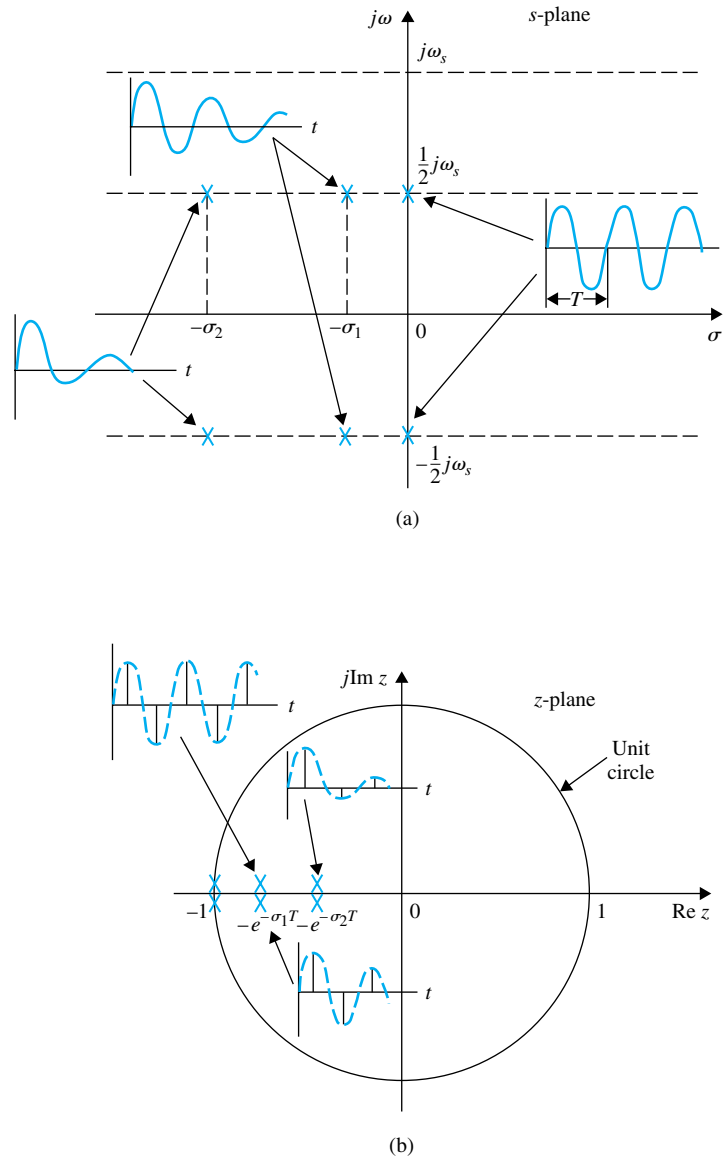
(a)

(b)

Figure I-28 (a) Transient responses corresponding to various pole loca-
tions of $Y^*(s)$ in the s-plane (complex-conjugate poles on the boundaries
between periodic strips). (b) Transient-response sequence corresponding
to various pole locations of $Y(z)$ in the z-plane.

$s = -\sigma_1 \pm j\omega_s/2$, the complex-conjugate points are on the boundaries of the primary
strip in the s-plane. The corresponding z-plane points are

$$z = e^{-\sigma_1 T} e^{\pm j\omega_s T/2} = -e^{-\sigma_1 T} \qquad \text{(I-194)}$$

which are on the negative real axis of the z-plane. For the frequency of $\omega_s/2$, the output
sequence will have exactly one sample in each one-half period of the envelope. Thus,
the output sequence will occur in alternating positive and negative pulses, as shown in
Fig. I-28(b).

Complex-Conjugate Roots in the z-Plane: Complex-conjugate roots inside the unit circle in the z-plane correspond to oscillatory responses that decay with an increase in kT. Roots that are closer to the unit circle will decay slower. As the roots move toward the second and the third quadrants, the frequency of oscillation of the response increases. Refer to Figs. I-27 and I-28 for typical examples.

▶ I-7 STEADY-STATE ERROR ANALYSIS OF DISCRETE-DATA CONTROL SYSTEMS

Since the input and output signals of a typical discrete-data control system are continuous-time functions, as shown in the block diagram of Fig. I-19, the error signal should still be defined as

$$e(t) = r(t) - y(t) \tag{I-195}$$

where $r(t)$ is the input, $y(t)$ is the output. The error analysis conducted here is only for unity-feedback systems with $H(s) = 1$. Due to the discrete data that appear inside the system, z-transform or difference equations are often used, so that the input and output are represented in sampled form, $r(kT)$ and $y(kT)$, respectively. Thus, the error signal is more appropriately represented by $e^*(t)$ or $e(kT)$. That is,

$$e^*(t) = r^*(t) - y^*(t) \tag{I-196}$$

or

$$e(kT) = r(kT) - y(kT) \tag{I-197}$$

The steady-state error at the sampling instants is defined as

$$e_{ss}^* = \lim_{t \to \infty} e^*(t) = \lim_{k \to \infty} e(kT) \tag{I-198}$$

By using the final-value theorem of the z-transform, the steady-state error is

$$e_{ss}^* = \lim_{k \to \infty} e(kT) = \lim_{z \to 1}(1 - z^{-1})E(z) \tag{I-199}$$

provided that the function $(1 - z^{-1})E(z)$ does not have any pole on or outside the unit circle in the z-plane. It should be pointed out that since the true error of the system is $e(t)$, e_{ss}^* predicts only the steady-state error of the system at the sampling instants.

By expressing $E(z)$ in terms of $R(z)$ and $G_{ho}G_p(z)$, Eq. (I-199) is written

$$e_{ss}^* = \lim_{k \to \infty} e(kT) = \lim_{z \to 1}(1 - z^{-1})\frac{R(z)}{1 + G_{ho}G_p(z)} \tag{I-200}$$

This expression shows that the steady-state error depends on the reference input $R(z)$ as well as the forward-path transfer function $G_{ho}G_p(z)$ Just as in the continuous-data systems, we shall consider only the three basic types of input signals and the associated error constants and relate e_{ss}^* to these and the type of the system.

Let the transfer function of the controlled process in the system of Fig. I-18 be of the form

$$G_p(s) = \frac{K(1 + T_a s)(1 + T_b s)\cdots(1 + T_m s)}{s^j(1 + T_1 s)(1 + T_2 s)\cdots(1 + T_n s)} \tag{I-201}$$

where $j = 0, 1, 2, \ldots$. The transfer function $G_{ho}G_p(z)$ is

$$G_{h0}G_p(z) = (1 - z^{-1})\mathcal{Z}\left[\frac{K(1 + T_a s)(1 + T_b s)\cdots(1 + T_m s)}{s^{j+1}(1 + T_1 s)(1 + T_2 s)\cdots(1 + T_n s)}\right] \tag{I-202}$$

Steady-State Error Due to a Step-Function Input

When the input to the system, $r(t)$, in Fig. I-18 is a step function with magnitude R, the z-transform of $r(t)$ is

$$R(z) = \frac{Rz}{z-1} \tag{I-203}$$

Substituting $R(z)$ into Eq. (I-200), we get

$$e_{ss}^* = \lim_{z \to 1} \frac{R}{1 + G_{ho}G_p(z)} = \frac{R}{1 + \lim_{z \to 1} G_{ho}G_p(z)} \tag{I-204}$$

Let the **step-error constant** be defined as

$$K_p^* = \lim_{z \to 1} G_{ho}G_p(z) \tag{I-205}$$

Equation (I-204) becomes

$$e_{ss}^* = \frac{R}{1 + K_p^*} \tag{I-206}$$

Thus, we see that the steady-state error of the discrete-data control system in Fig. I-18 is related to the step-error constant K_p^* in the same way as in the continuous-data case, except that K_p^* is given by Eq. (I-205).

We can relate K_p^* to the system type as follows.

For a type-0 system, $j = 0$ in Eq. (I-202), and the equation becomes

$$G_{ho}G_p(z) = (1 - z^{-1})\mathcal{Z}\left[\frac{K(1 + T_a s)(1 + T_b s)\cdots(1 + T_m s)}{s(1 + T_1 s)(1 + T_2 s)\cdots(1 + T_n s)}\right] \tag{I-207}$$

Performing partial-fraction expansion to the function inside the square brackets of the last equation, we get

$$G_{ho}G_p(z) = (1 - z^{-1})\mathcal{Z}\left[\frac{K}{s} + \text{terms due to the nonzero poles}\right]$$

$$= (1 - z^{-1})\left[\frac{Kz}{z-1} + \text{terms due to the nonzero poles}\right] \tag{I-208}$$

Since the terms due to the nonzero poles do not contain the term $(z - 1)$ in the denominator, the step-error constant is written

$$K_p^* = \lim_{z \to 1} G_{ho}G_p(z) = \lim_{z \to 1}(1 - z^{-1})\frac{Kz}{z-1} = K \tag{I-209}$$

Similarly, for a type-1 system, $G_{ho}G_p(z)$ will have an s^2 term in the denominator that corresponds to a term $(z - 1)^2$. This causes the step-error constant K_p^* to be infinite. The same is true for any system type greater than 1. The summary of the error constants and the steady-state error due to a step input is as follows:

System Type	K_p^*	e_{ss}^*
0	K	$R/(1 + K)$
1	∞	0
2	∞	0

Steady-State Error Due to a Ramp-Function Input

When the reference input to the system in Fig. I-18 is a ramp function of magnitude R, $r(t) = Rtu_s(t)$. The steady-state error in Eq. (I-200) becomes

$$e_{ss}^* = \lim_{z \to 1} \frac{RT}{(z-1)[1 + G_{ho}G_p(z)]} \tag{I-210}$$

$$= \frac{R}{\lim_{z \to 1} \dfrac{z-1}{T} G_{ho}G_p(z)}$$

Let the **ramp-error constant** be defined as

$$K_v^* = \frac{1}{T} \lim_{z \to 1} [(z-1)G_{ho}G_p(z)] \tag{I-211}$$

Then, Eq. (I-210) becomes

$$e_{ss}^* = \frac{R}{K_v^*} \tag{I-212}$$

The ramp-error constant K_v^* is meaningful only when the input $r(t)$ is a ramp function and if the function $(z-1)G_{ho}G_p(z)$ in Eq. (I-211) does not have any poles on or outside the unit circle $|z| = 1$. The relations between the steady-state error e_{ss}^*, K_v^* and the system type when the input is a ramp function with magnitude R are summarized as follows.

System Type	K_v^*	e_{ss}^*
0	0	∞
1	K	R/K
2	∞	0

Steady-State Error Due to a Parabolic-Function Input

When the input is a parabolic function, $r(t) = Rtu_s(t)/2$; the z-transform of $r(t)$ is

$$R(z) = \frac{RT^2 z(z+1)}{2(z-1)^3} \tag{I-213}$$

From Eq. (I-200), the steady-state error at the sampling instants is

$$e_{ss}^* = \frac{T^2}{2} \lim_{z \to 1} \frac{R(z+1)}{(z-1)^2 [1 + G_{ho}G_p(z)]} \tag{I-214}$$

$$= \frac{R}{\dfrac{1}{T^2} \lim_{z \to 1} (z-1)^2 G_{ho}G_p(z)}$$

By defining the **parabolic-error constant** as

$$K_a^* = \frac{1}{T^2} \lim_{z \to 1} [(z-1)^2 G_{ho}G_p(z)] \tag{I-215}$$

the steady-state error due to a parabolic-function input is

$$e_{ss}^* = \frac{R}{K_a^*} \tag{I-216}$$

The relations between the steady-state error e_{ss}^*, K_a^*, and the system type when the input is a parabolic function with its z-transform described by Eq. (I-213) are summarized as follows.

System Type	K_a^*	e_{ss}^*
0	0	∞
1	0	∞
2	K	R/K
3	∞	0

▶ I-8 ROOT LOCI OF DISCRETE-DATA SYSTEMS

The root-locus technique can be can be applied to discrete-data systems without any complications. With the z-transformed transfer function, the root loci for discrete-data systems are plotted in the z-plane, rather than in the s-plane. Let us consider the discrete-data control system shown in Fig. I-29. The characteristic equation roots of the system satisfy the following equation:

$$1 + GH^*(s) = 0 \tag{I-217}$$

in the s-plane, or

$$1 + GH(z) = 0 \tag{I-218}$$

in the z-plane. From Eq (I-64) $GH^*(s)$ is written

$$GH^*(s) = \frac{1}{T} \sum_{n=-\infty}^{\infty} G(s + jn\omega_s)H(s + jn\omega_s) \tag{I-219}$$

which is an infinite series. Thus, the poles and zeros of $GH^*(s)$ in the s-plane will be infinite in number. This evidently makes the construction of the root loci of Eq. (I-217) in the s-plane quite complex. As an illustration, consider that for the system of Fig. I-29,

$$G(s)H(s) = \frac{K}{s(s + 1)} \tag{I-220}$$

Substituting Eq. (I-220) into Eq. (I-219), we get

$$GH^*(s) = \frac{1}{T} \sum_{n=-\infty}^{\infty} \frac{K}{(s + jn\omega_s)(s + jn\omega_s + 1)} \tag{I-221}$$

which has poles at $s = -jn\omega_s$ and $s = -1 -jn\omega_s$, where n takes on all integers between $-\infty$ and ∞. The pole configuration of $GH^*(s)$ is shown in Fig. I-30(a). By using the properties of the RL in the s-plane, RL of $1 + GH^*(s) = 0$ are drawn as shown in Fig. I-30(b) for the sampling period $T = 1$ s. The RL contain an infinite number of branches, and these
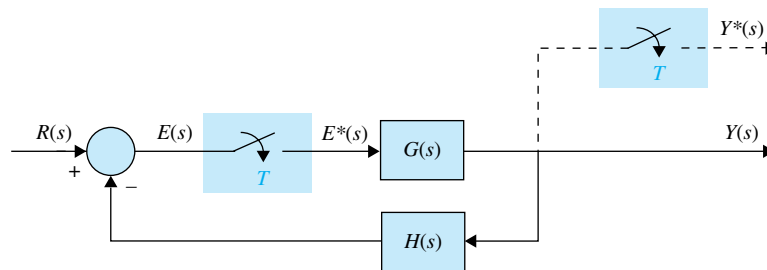

Figure I-29 Discrete-data control system.

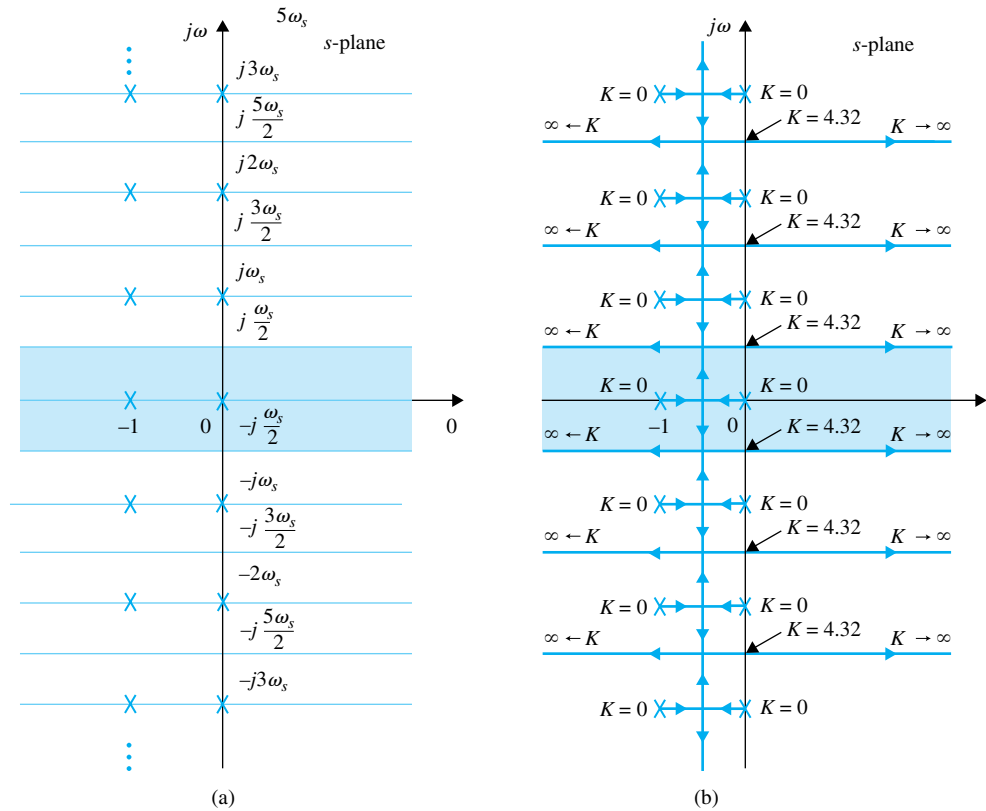(a)   (b)

Figure I-30 Pole configuration of $GH^*(s)$ and the root-locus diagram in the s-plane for the discrete-data system in Fig. I-29 with $G(s)H(s) = \dfrac{K}{s(s+1)}$, $T = 1$ sec.

clearly indicate that the closed-loop system is unstable for all values of K greater than 4.32. In contrast, it is well known that the same system without sampling is stable for all positive values of K.

• The same procedures of construction of root loci of continuous-data systems can be applied to root loci of discrete-data systems in the z-plane.

The root-locus problem for discrete-data systems is simplified if the root loci are constructed in the z-plane using Eq. (I-218). Since Eq. (I-218) is, in general, a rational function in z with constant coefficients, its poles and zeros are finite in number, and the number of root loci is finite in the z-plane. The same procedures of construction for continuous-data systems are directly applicable in the z-plane for discrete-data systems. The following examples illustrate the constructions of root loci for discrete-data systems in the z-plane.

► **EXAMPLE I-23** Consider that for the discrete-data system shown in Fig. I-29 the loop transfer function in the z domain is

$$GH(z) = \frac{0.632Kz}{(z-1)(z-0.368)} \tag{I-222}$$

The RL of the closed-loop characteristic equation are constructed based on the pole-zero configuration of $GH(z)$, as shown in Fig. I-31. Notice that when the value of K exceeds 4.32, one of the two roots moves outside the unit circle, and the system becomes unstable. The constant-damping-ratio locus may be superimposed on the RL to determine the required value of K for a specified damping ratio. In Fig. I-31, the constant-damping-ratio locus for $\zeta = 0.5$ is drawn, and the intersection with the RL gives the desired value of $K = 1$. For the same system, if the sampling period T is increased
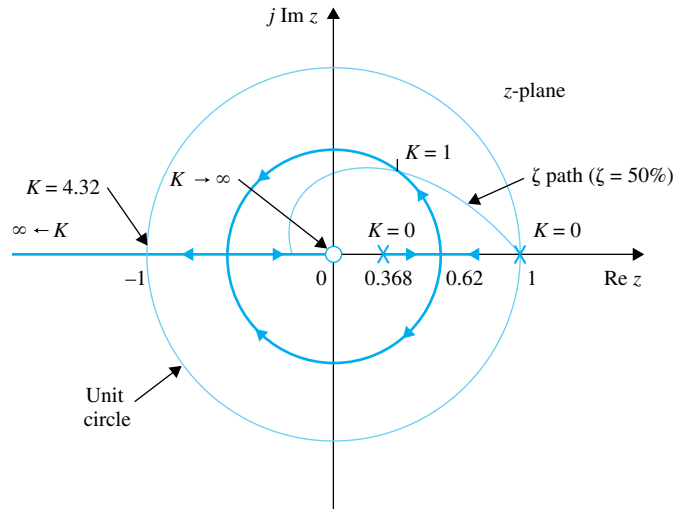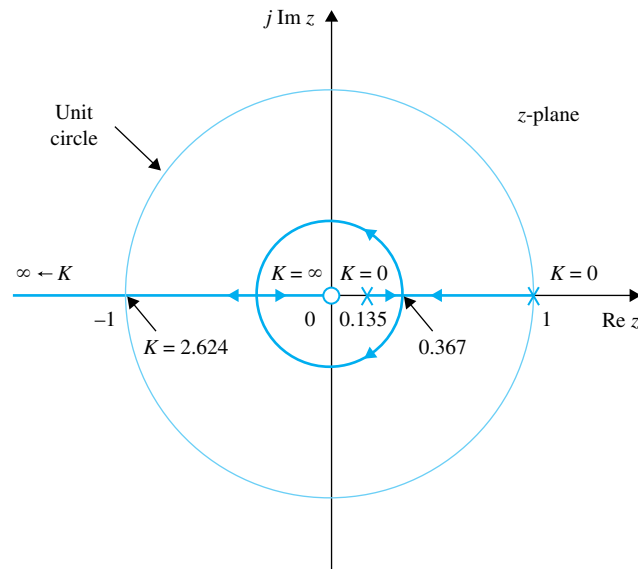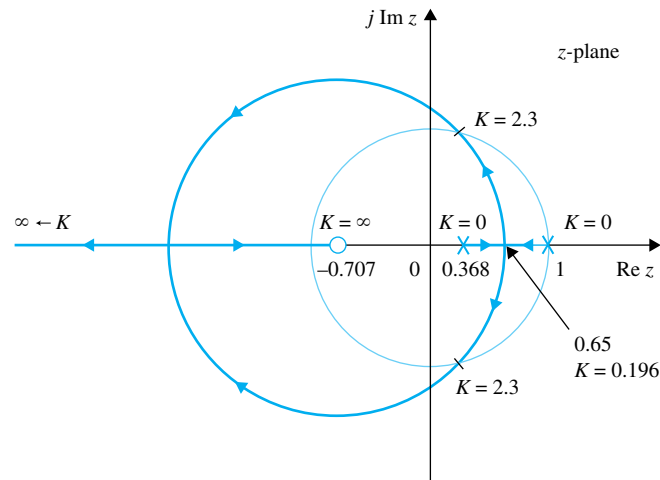
Figure I-31 Root-locus diagram of a discrete-data control system without zero-order-hold.

$$G(s)H(s) = \frac{K}{s(s + 1)},$$

$T = 1$ second.

to 2 seconds, the z-transform loop transfer function becomes

$$GH(z) = \frac{0.865Kz}{(z - 1)(z - 0.135)} \tag{I-223}$$

The RL for this case are shown in Fig. I-32. Note that although the complex part of the RL for $T = 2$ seconds takes the form of a smaller circle than that when $T = 1$ second, the system is actually less stable, since the marginal value of K for stability is 2.624, as compared with the marginal K of 4.32 for $T = $ second.

Next, let us consider that a zero-order-hold is inserted between the sampler and the controlled process $G(s)$ in the system of Fig. I-29. The loop transfer function of the system with the zero-order-hold is

$$G_{ho}GH(z) = \frac{K[(T - 1 + e^{-T})z - Te^{-T} + 1 - e^{-T}]}{(z - 1)(z - e^{-T})} \tag{I-224}$$
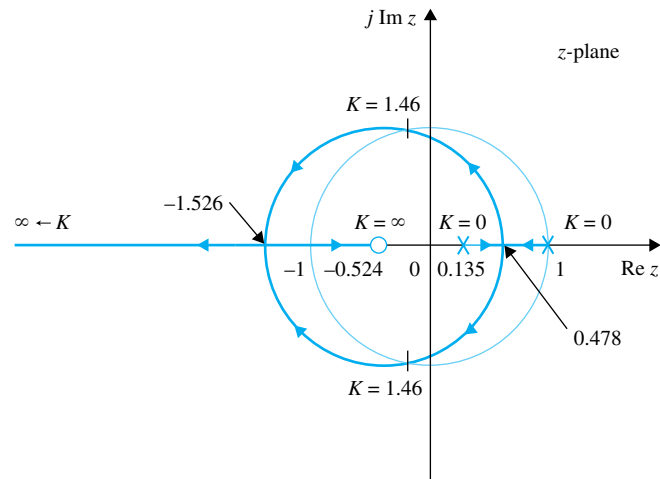

Figure I-32 Root-locus diagram of a discrete-data control system without zero-order-hold.

$$G(s)H(s) = \frac{K}{s(s+1)},$$

$T = 2$ seconds.

(a) Root loci for $T = 1$ second

(b) Root loci for $T = 2$ seconds

Figure I-33 Root-locus diagram of a discrete-data control system with zero-order-hold.

$$G(s)H(s) = \frac{K}{s(s + 1)}.$$

The RL of the system with ZOH for $T = 1$ and 2 seconds are shown in Fig. I-33(a) and I-33(b), respectively. In this case, the marginal value of stability for K is 2.3 for $T = 1$ second and 1.46 for $T = 2$ seconds. Comparing the root loci of the system with and without the ZOH, we see that the ZOH reduces the stability margin of the discrete-data system.

In conclusion, the root loci of discrete-data systems can be constructed in the z-plane using essentially the same properties as those of the continuous-data systems in the s-plane. However, the absolute and relative stability conditions of the discrete-data system must be investigated with respect to the unit circle and the other interpretation of performance with respect to the regions in the z-plane. ◀

▶ I-9 FREQUENCY-DOMAIN ANALYSIS OF DISCRETE-DATA CONTROL SYSTEMS

All the frequency-domain methods discussed in the preceding sections can be extended to the analysis of discrete-data systems. Consider the discrete-data system shown

Figure I-34 Closed-loop discrete-data control system.
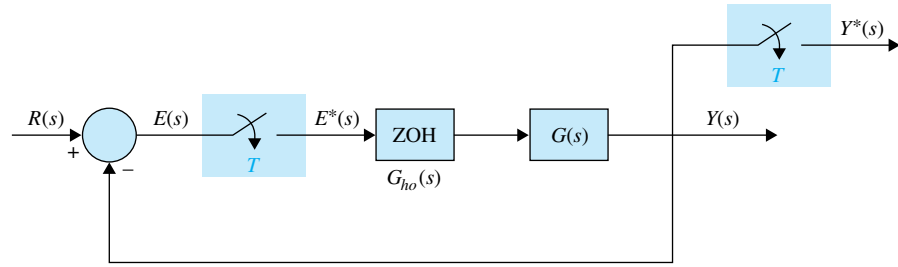
in Fig. I-34. The closed-loop transfer function of the system is

$$\frac{Y(z)}{R(z)} = \frac{G_{ho}G(z)}{1 + G_{ho}G(z)} \tag{I-225}$$

where $G_{ho}G(z)$ is the z-transform of $G_{ho}(s)G(s)$. Just as in the case of continuous-data systems, the absolute and relative stability conditions of the closed-loop discrete-data system can be investigated by making the frequency-domain plots of $G_{ho}G(z)$. Since the positive $j\omega$-axis of the s-plane corresponds to real frequency, the frequency-domain plots of $G_{ho}G(z)$ are obtained by setting $z = e^{j\omega T}$ and then letting ω vary from 0 to ∞. This is also equivalent to mapping the points on the unit circle, $|z| = 1$, in the z-plane onto the $G_{ho}G(e^{j\omega T})$-plane. Since the unit circle repeats for every sampling frequency $\omega_s (= 2\pi/T)$, as shown in Fig. I-35, when ω is varied along the $j\omega$-axis, the frequency-domain plot of $G(e^{j\omega T})$ repeats for $\omega = n\omega_s$ to $(n + 1)\omega_s$, $n = 0, 1, 2, \ldots$. Thus, it is necessary to plot $G_{ho}G(e^{j\omega T})$ only for the range of $\omega = 0$ to $\omega = \omega_s$. In fact, since the unit circle in the z-plane is symmetrical about the real axis, the plot of $G_{ho}G(e^{j\omega T})$ in the polar coordinates for $\omega = 0$ to $\omega_s/2$ needs to be plotted.

I-9-1 Bode Plot with the *w*-Transformation

The w-transformation introduced in Eq. (I-162) can be used for frequency-domain analysis and design of discrete-data control systems. The transformation is
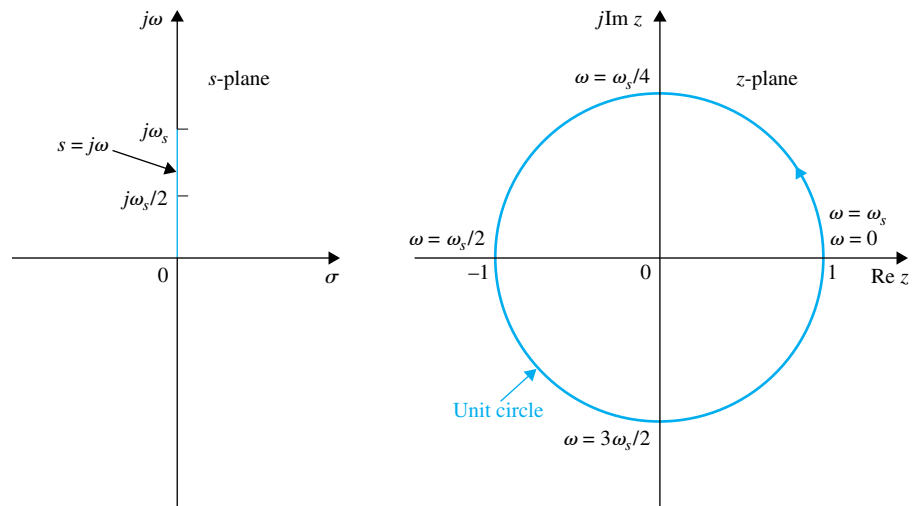
$$z = \frac{(2/T) + w}{(2/T) - w} \tag{I-226}$$

Figure I-35 Relation between the $j\omega$-axis in the s-plane and the unit circle in the z-plane.

In the frequency domain, we set [Eq. (I-166)],

$$w = j\omega_w = j\frac{2}{T}\tan\frac{\omega T}{2} \tag{I-227}$$

For frequency-domain analysis of a discrete-data system, we substitute Eqs. (I-226) and (I-227) in $G(z)$ to get $G(j\omega_w)$; the latter can be used to form the Bode plot or the polar plot of the system.

▶ **EXAMPLE I-24** As an illustrative example on frequency-domain plots of discrete-data control systems, let the transfer function of the process in the system in Fig. I-34 be

$$G(s) = \frac{1.57}{s(s + 1)} \tag{I-228}$$

and the sampling frequency is 4 rad/sec. Let us first consider that the system does not have a zero-order-hold, so that

$$G_{ho}G(z) = G(z) = \frac{1.243z}{(z - 1)(z - 0.208)} \tag{I-229}$$
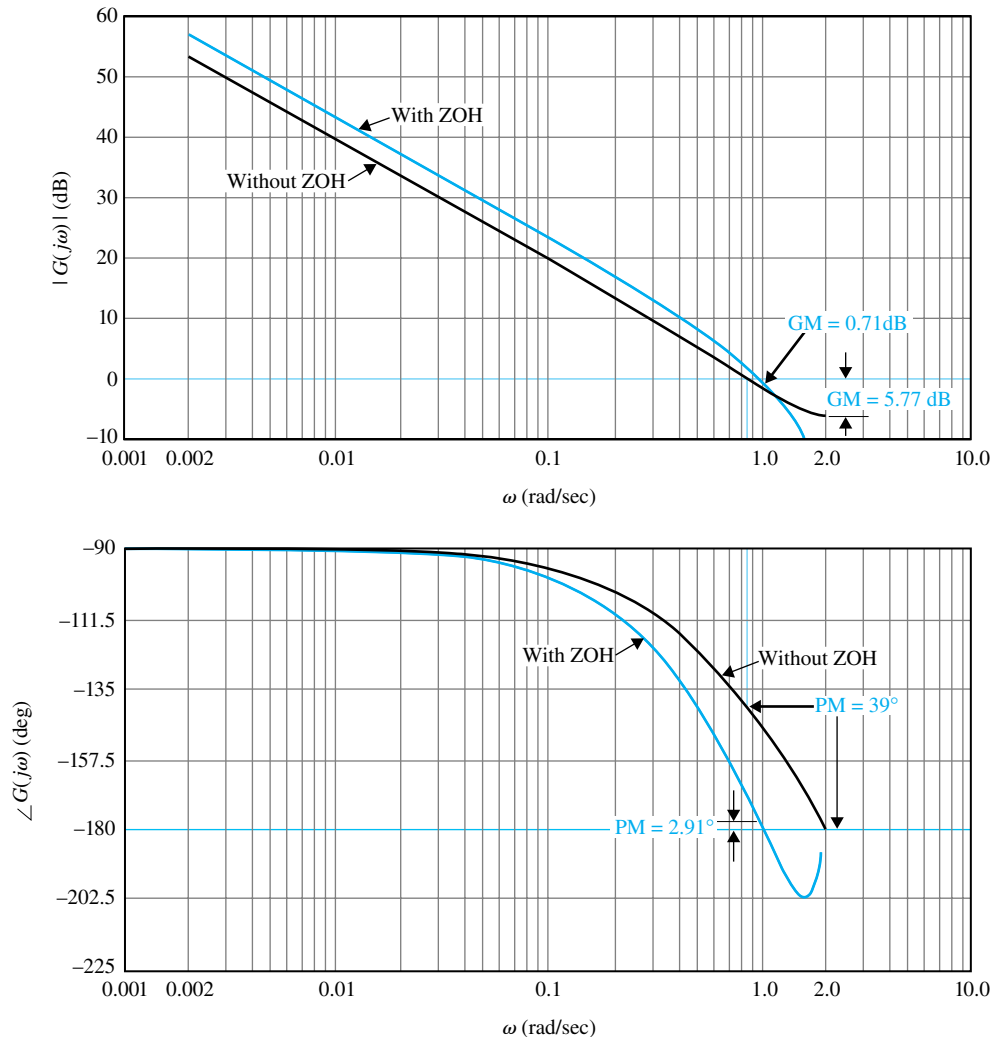

Figure I-36 Bode plot of $G_{ho}G(z)$ of the system in Fig. I-34, with $G(s) = 1.57/[s(s + 1)]$. $T = 1.57$ sec, and with and without ZOH.

The frequency response of $G_{ho}G(z)$ is obtained by substituting $z = e^{j\omega T}$ in Eq. (I-228). The polar plot of $G_{ho}G(e^{j\omega T})$ for $\omega = 0$ to $\omega_s/2$ is shown in Fig. I-36. The mirror image of the locus shown, with the mirror placed on the real axis, represents the plot for $\omega = \omega_s/2$ to ω_s.

The Bode plot of $G_{ho}G(e^{j\omega T})$ consists of the graphs of $|G_{ho}G(e^{j\omega T})|$ in dB versus ω, and $\angle G_{ho}G(e^{j\omega T})$ in degrees versus ω, as shown in Fig. I-37 for three decades of frequency with the plots ended at $\omega = \omega_s/2 = 2$ rad/sec.

For the sake of comparison, the forward-path transfer function of the system with a zero-order-hold is obtained:

$$G_{ho}G(z) = \frac{1.2215z + 0.7306}{(z - 1)(z - 0.208)} \tag{I-230}$$

The polar plot and the Bode plot of the last equation are shown in Figs. I-36 and I-37, respectively. Notice that the polar plot of the system with the ZOH intersects the negative real axis at a point that is closer to the $(-1, j0)$ point than that of the system without the ZOH. Thus, the system with the ZOH is less stable. Similarly, the phase of the Bode plot of the system with the ZOH is more negative than that of the system without the ZOH. The gain margin, phase margin, and peak resonance of the two systems are summarized as follows.

	Gain Margin (dB)	Phase Margin (deg)	M_r
Without ZOH	5.77	39.0	1.58
With ZOH	0.71	2.91	22.64

As an alternative, the Bode plot and polar plot of the forward-path transfer function can be done using the w-transformation of Eqs. (I-226). For the system with ZOH, the forward-path transfer
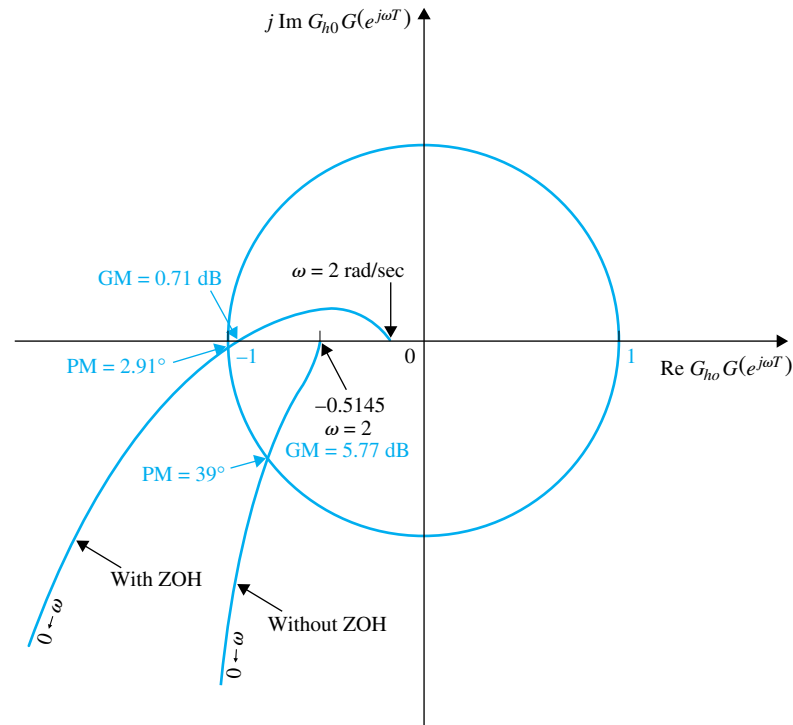

Figure I-37 Frequency-domain plot of $G(s) = \dfrac{1.57}{s(s + 1)}$, $T = 1.57$ seconds, and with and without ZOH.

function in the *w*-domain is

$$G_{ho}G(w) = \frac{1.57(1 + 0.504w)(1 - 1.0913w)}{w(1 + 1.197w)} \tag{I-231}$$
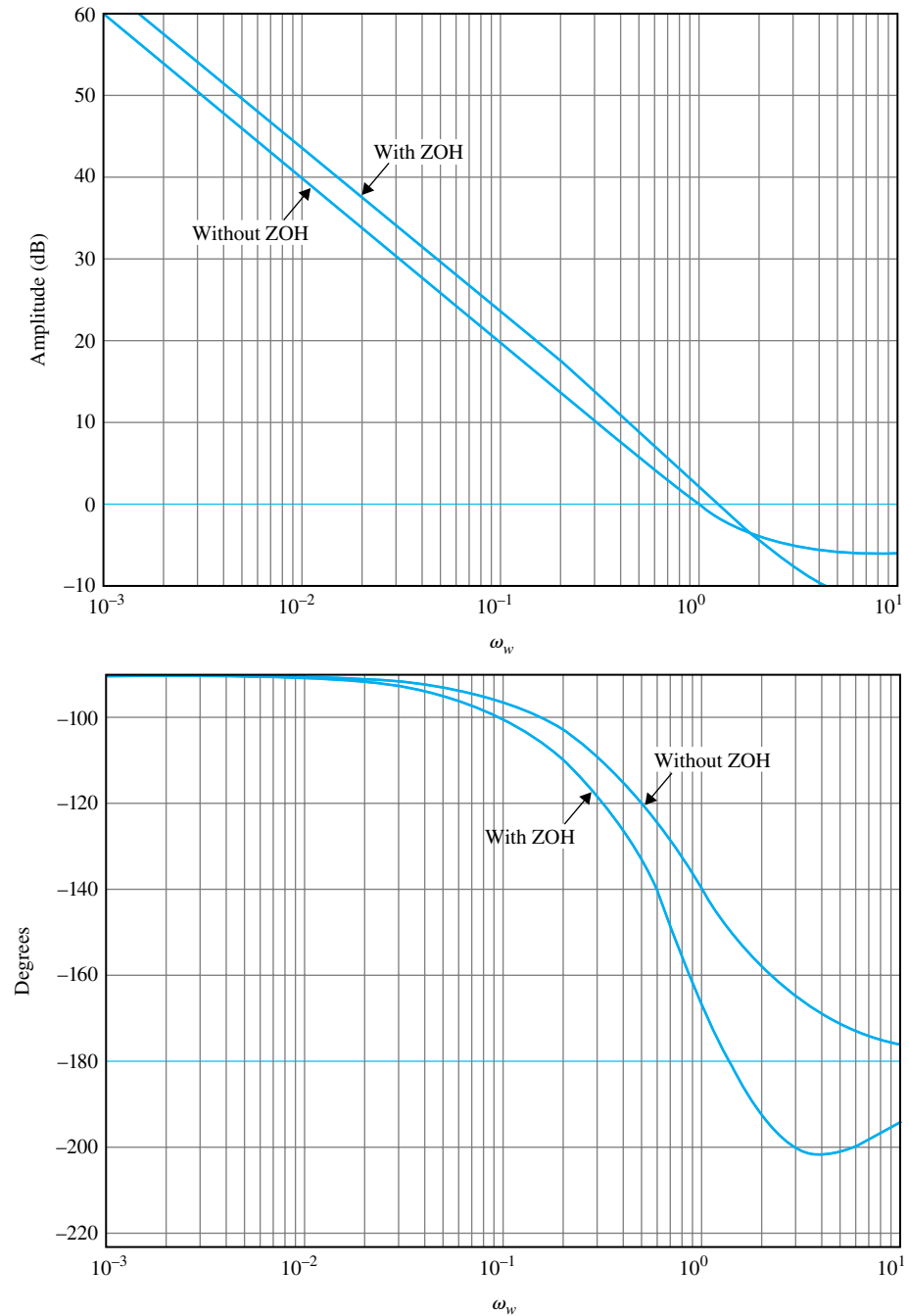

Figure I-38 Bode plot of $G_{ho}G(z)$ of the system in Fig. I-34 with $G(s) = \dfrac{1.57}{s(s + 1)}$, $T = 1.57$ seconds with and without ZOH. The plots are done with the *w*-transformation, $w = j\omega_w$.

For the system without ZOH,

$$G_{ho}G(jw) = \frac{1 - 0.6163w^2}{w(1 + 1.978w)} \tag{I-232}$$

Substituting $w = j\omega_w$ into Eq. (I-232), the Bode plots are made as shown in Fig. (I-38). Notice that the frequency coordinates in Fig. I-38 are ω_w, whereas those in Fig. I-36 are the real frequency ω. The two frequencies are related through Eq. (I-227).

The conclusion from this illustrative example is that once z is replaced by $e^{j\omega T}$ in the z-domain transfer function, or if the w-transform is used, all the frequency-domain analysis techniques available for continuous-data systems can be applied to discrete-data systems. ◄

► I-10 DESIGN OF DISCRETE-DATA CONTROL SYSTEMS

I-10-1   Introduction

The design of discrete-data control systems is similar in principle to the design of continuous-data control systems. The design objective is basically that of determining the controller so that the system will perform in accordance with specifications. In fact, in most situations, the controlled process is the same, except in discrete-data systems the controller is designed to process sampled or digital data.

The design of discrete-data control systems treated in this chapter is intended only for introductory purposes. An in-depth coverage of the subject may be found in books dedicated to digital control. In this chapter we deal only with the design of a control system with a cascade digital controller and a system with digital state feedback. Block diagrams of these systems are shown in Fig. I-39.

Just as with the design of continuous-data control systems, the design of discrete-data control systems can be carried out in either the frequency domain or the time domain. Using computer programs, digital control systems can be designed with a minimum amount of trial and error.
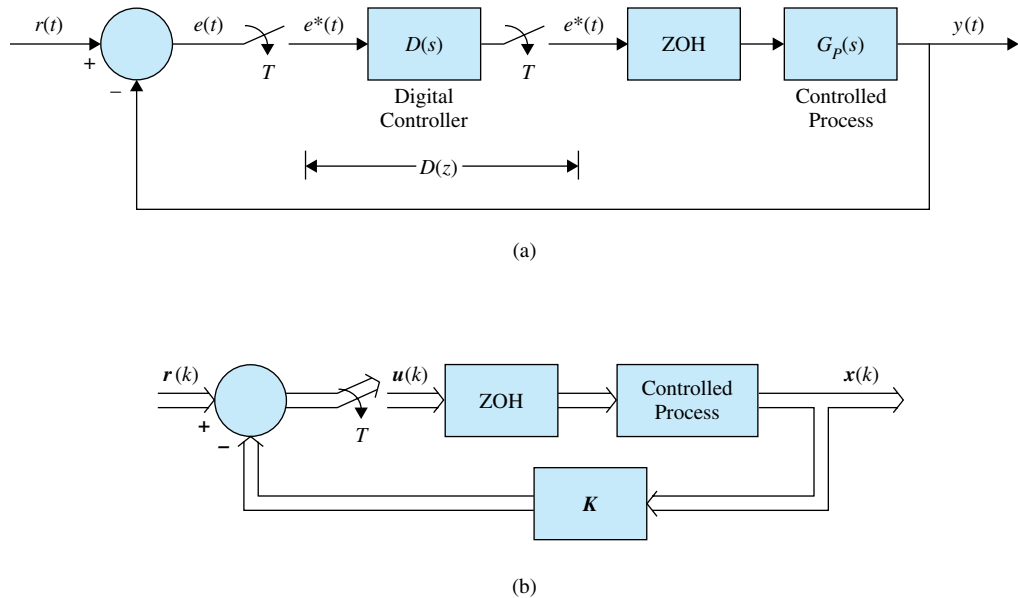

(a)

(b)

Figure I-39   (a) Digital control system with cascade digital controller. (b) Digital control system with state feedback.

I-10-2 Digital Implementation of Analog Controllers

It seems that most people learn how to design continuous-data systems before they learn to design digital systems, if at all. Therefore, it is not surprising that most engineers prefer to design continuous-data systems. Ideally, if the designer intends to use digital control, the system should be designed so that the dynamics of the controller can be described by a z-transfer function or difference equations. However, there are situations in which the analog controller is already designed, but the availability and advantages of digital control suggest that the controller be implemented by digital elements. Thus, the problems discussed in this section are twofold: first how continuous-data controllers such as PID, phase-lead or phase-lag controllers, and others can be approximated by digital controllers; and second, the problem of implementing digital controllers by digital processors.

I-10-3 Digital Implementation of the PID Controller

The PID controller in the continuous-data domain is described by

$$G_c(s) = K_P + K_D s + \frac{K_I}{s} \tag{I-233}$$

The proportional component K_P is implemented digitally by a constant gain K_P. Since a digital computer or processor has finite word length, the constant K_P cannot be realized with infinite resolution.

The time derivative of a function $f(t)$ at $t = kT$ can be approximated by the **backward-difference rule**, using the values of $f(t)$ measured at $t = kT$ and $(k - 1)T$, that is,

$$\left. \frac{df(t)}{dt} \right|_{t=kT} = \frac{1}{T}(f(kT) - f[(k - 1)T]) \tag{I-234}$$

To find the z-transfer function of the derivative operation described before, we take the z-transform on both sides of Eq. (I-234). We have

$$\mathcal{Z}\left(\left. \frac{df(t)}{dt} \right|_{t=kT} \right) = \frac{1}{T}(1 - z^{-1})F(z) = \frac{z - 1}{Tz}F(z) \tag{I-235}$$

Thus, the z-transfer function of the digital differentiator is

$$G_D(z) = K_D \frac{z - 1}{Tz} \tag{I-236}$$

where K_D is the proportional constant of the derivative controller. Replacing z by e^{Ts} in Eq. (I-236), we can show that as the sampling period T approaches zero, $G_D(z)$ approaches $K_D s$, which is the transfer function of the analog derivative controller. In general, the choice of the sampling period is extremely important. The value of T should be sufficiently small so that the digital approximation is adequately accurate.

There are a number of numerical integration rules that can be used to digitally approximate the integral controller K_I/s. The three basic methods of approximating the area of a function numerically are **trapezoidal integration**, **forward-rectangular integration**, and **backward-rectangular integration**. These are described as follows.

Trapezoidal Integration
The trapezoidal-integration rule approximates the area under the function $f(t)$ by a series of trapezoids, as shown in Fig. I-40. Let the integral of $f(t)$ evaluated at $t = kT$ be
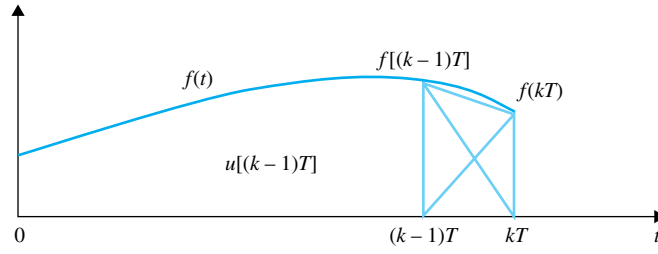
Figure I-40 Trapezoidal-integration rule.

designated as $u(kT)$. Then,

$$u(kT) = u[(k-1)T] + \frac{T}{2}\{f(kT) - f[(k-1)T]\} \tag{I-237}$$

where the area under $f(t)$ for $(k-1)T \le t < kT$ is approximated by the area of the trapezoid in the interval. Taking the z-transform on both sides of Eq. (I-237), we have the transfer function of the digital integrator as

$$G_I(z) = K_I \frac{U(z)}{F(z)} = \frac{K_I T(z+1)}{2(z-1)} \tag{I-238}$$

where K_I is the proportional constant.

Forward-Rectangular Integration

For the forward-rectangular integration, we approximate the area under $f(t)$ by rectangles, as shown in Fig. I-41. the integral of $f(t)$ at $t = kT$ is approximated by

$$u(kT) = u[(k-1)T] + Tf(kT) \tag{I-239}$$

By taking the z-transform on both sides of Eq. (I-141), the transfer function of the digital integrator using the forward-rectangular rule is

$$G_I(z) = K_I \frac{U(z)}{F(z)} = \frac{K_I Tz}{z-1} \tag{I-240}$$

Backward-Rectangular Integration

For the backward-rectangular integration, the digital approximation rule is illustrated in Fig. I-42. The integral of $f(t)$ at $t = kT$ is approximated by

$$u(kT) = u[(k-1)T] + Tf[(k-1)T] \tag{I-241}$$

The z-transfer function of the digital integrator using the backward-rectangular integration rule is

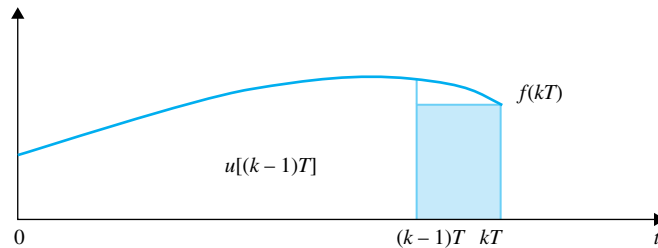$$G_I(z) = K_I \frac{U(z)}{F(z)} = \frac{K_I T}{z-1} \tag{I-242}$$

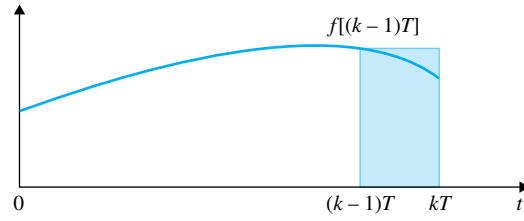**Figure I-41** Forward-rectangular integration rule.

Figure I-42 Backward-rectangular integration rule.

By combining the proportional, derivative, and integration operations described before, the digital PID controller is modeled by the following transfer functions.

Trapezoidal Integration

$$G_c(z) = \frac{\left(K_P + \dfrac{TK_I}{2} + \dfrac{K_D}{T}\right)z^2 + \left(\dfrac{TK_I}{2} - K_P - \dfrac{2K_D}{T}\right)z + \dfrac{K_D}{T}}{z(z-1)} \qquad \text{(I-243)}$$

Forward-Rectangular Integration

$$G_c(z) = \frac{\left(K_P + \dfrac{K_D}{T} + TK_I\right)z^2 - \left(K_P + \dfrac{2K_D}{T}\right)z + \dfrac{K_D}{T}}{z(z-1)} \qquad \text{(I-244)}$$

Backward-Rectangular Integration

$$G_c(z) = \frac{\left(K_P + \dfrac{K_D}{T}\right)z^2 + \left(TK_I - K_P - \dfrac{2K_D}{T}\right)z + \dfrac{K_D}{T}}{z(z-1)} \qquad \text{(I-245)}$$

When $K_I = 0$, the transfer function of the digital PD controller is

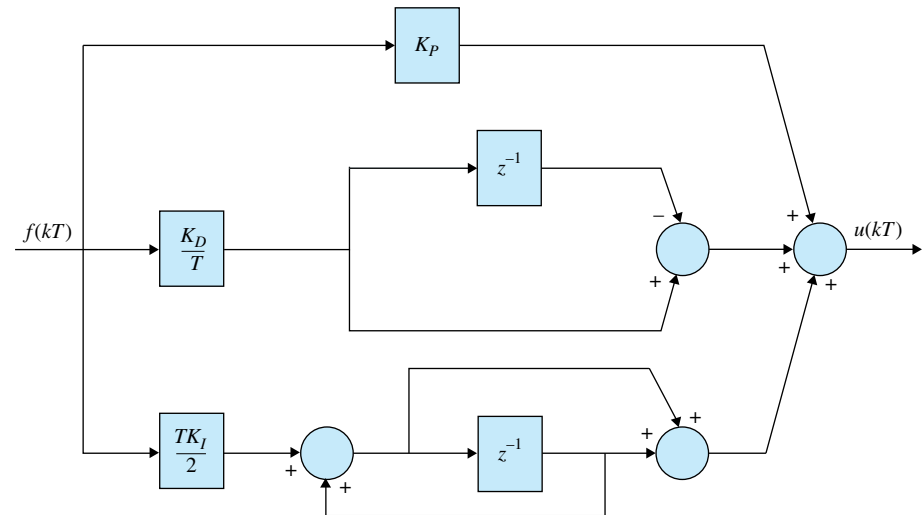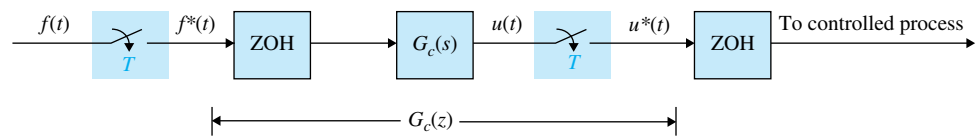$$G_c(z) = \frac{\left(K_P + \dfrac{K_D}{T}\right)z - \dfrac{K_D}{T}}{z} \qquad \text{(I-246)}$$

Figure I-43 Block diagram of a digital-program implementation of the PID controller.

Figure I-44 Realization of a digital controller by an analog controller with sample-and-hold units.

Once the transfer function of a digital controller is determined, the controller can be implemented by a digital processor or computer. The operator z^{-1} is interpreted as a time delay of T seconds. In practice, the time delay is implemented by storing a variable in some storage location in the computer and then taking it out after T seconds have elapsed. Figure I-43 illustrates a block diagram representation of the digital program of the PID controller using the trapezoidal-integration rule.

I-10-4 Digital Implementation of Lead and Lag Controllers

In principle, any continuous-data controller can be made into a digital controller simply by adding sample-and-hold units at the input and the output terminals of the controller and selecting a sampling frequency as small as is practical. Figure I-44 illustrates the basic scheme with $G_c(s)$, the transfer function of the continuous-data controller, and $G_c(z)$, the equivalent digital controller. The sampling period T should be sufficiently small so that the dynamic characteristics of the continuous-data controller are not lost through the digitization. The system configuration in Fig. I-44 actually suggests that given the continuous-data controller $G_c(s)$, the equivalent digital controller $G_c(z)$ can be obtained by the arrangement shown. On the other hand, given the digital controller $G_c(z)$, we can realize it by using an analog controller $G_c(s)$ and sample-and-hold units, as shown in Fig. I-44.

► **EXAMPLE I-25** As an illustrative example, consider that the continuous-data controller in Fig. I-44 is represented by the transfer function

$$G_c(s) = \frac{s + 1}{s + 1.61} \tag{I-247}$$

From Fig. I-44, the transfer function of the digital controller is written

$$G_c(z) = \frac{U(z)}{F(z)} = (1 - z^{-1})\mathcal{Z}\left[\frac{s + 1}{s(s + 1.61)}\right] \tag{I-248}$$

$$= \frac{z - (0.62e^{-1.61T} + 0.38)}{z - e^{-1.61T}}$$

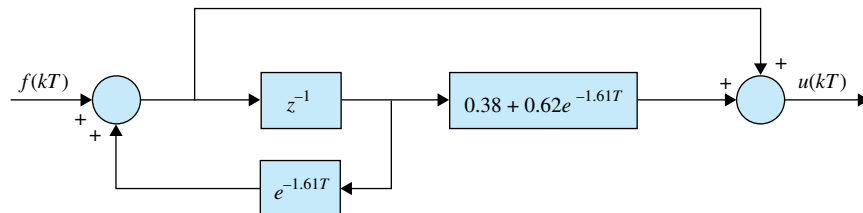The digital-program implementation of Eq. (I-248) is shown in Fig. I-45.

Figure I-45 Digital-program realization of Eq. (I-248). ◄

▶ I-11 DIGITAL CONTROLLERS

• One advantage of the digital controller is that its program can be easily altered.

Digital controllers can be realized by digital networks, digital computers, microprocessors, or digital signal processors (DSPs). A distinct advantage of digital controllers implemented by microprocessors or DSPs is that the control algorithm contained in the controller can be easily altered by changing the program. Changing the components of a continuous-data controller is rather difficult once the controller has been built.

I-11-1 Physical Realizability of Digital Controllers

The transfer function of a digital controller can be expressed as

$$G_c(z) = \frac{E_2(z)}{E_1(z)} = \frac{b_0 + b_1 z^{-1} + \cdots + b_m z^{-m}}{a_0 + a_1 z^{-1} + \cdots + a_n z^{-n}} \tag{I-249}$$

where n and m are positive integers. The transfer function $G_c(z)$ is said to be physically realizable if its output does not precede any input. This means that the series expansion of $G_c(z)$ should not have any positive powers in z. In terms of the $G_c(z)$ given in Eq. (I-249), if $b_0 \neq 0$, then $a_0 \neq 0$. If $G_c(z)$ is expressed as

$$G_c(z) = \frac{b_m z^m + b_{m-1} z^{m-1} + \cdots + b_1 z + b_0}{a_n z^n + a_{n-1} z^{n-1} + \cdots + a_1 z + a_0} \tag{I-250}$$

then the physical realizability requirement is $n \geq m$.

The decomposition techniques presented in Chapter 5 can be applied to realize the digital controller transfer function by a digital program. We consider that a digital program is capable of performing arithmetic operations of addition, subtraction, multiplication by a constant, and shifting. The three basic methods of decomposition for digital programming are discussed in the following sections.

Digital Program by Direct Decomposition
Applying direct decomposition to Eq. (I-249), we have the following equations:

$$E_2(z) = \frac{1}{a_0}(b_0 + b_1 z^{-1} + \cdots + b_m z^{-m})X(z) \tag{I-251}$$

$$X(z) = \frac{1}{a_0}E_1(z) - \frac{1}{a_0}(a_1 z^{-1} + a_2 z^{-2} + \cdots + a_n z^{-n})X(z) \tag{I-252}$$

Figure I-46 shows the signal flow graph of a direct digital program of Eq. (I-249) by direct decomposition for $m = 2$ and $n = 3$. The branches with gains of z^{-1} represent time delays or shifts of one sampling period.
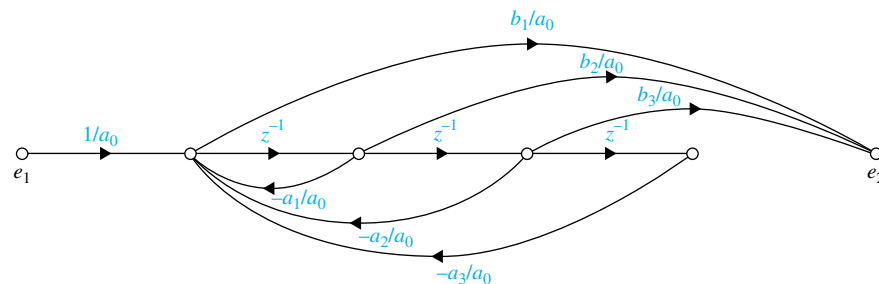

Figure I-46 Signal-flow graph of digital program by direct decomposition of Eq. (I-249) with $n = 3$ and $m = 2$.

Digital Program by Cascade Decomposition
The transfer function $G_c(z)$ can be written as a product of first- or second-order transfer functions, each realizable by a simple digital program. The digital program of the overall transfer function is then represented by these simple digital programs connected in cascade. Equation (I-249) is written in factored form as

$$G_c(z) = G_{c1}(z)G_{c2}(z) \cdots G_{cn}(z) \tag{I-253}$$

where the individual factors can be expressed as

Real Pole and Zero

$$G_{ci}(z) = K_i \frac{1 + c_i z^{-1}}{1 + d_i z^{-1}} \tag{I-254}$$

Complex Conjugate Poles (No Zeros)

$$G_{ci}(z) = \frac{K_i}{1 + d_{i1} z^{-1} + d_{i2} z^{-2}} \tag{I-255}$$

Complex Conjugate Poles with One Zero

$$G_{ci}(z) = K_i \frac{1 + c_i z^{-1}}{1 + d_{i1} z^{-1} + d_{i2} z^{-2}} \tag{I-256}$$

and several other possible forms up to the second order.

Digital Program by Parallel Decomposition
The transfer function in Eq. (I-249) can be expanded into a sum of simple first- or second-order terms by partial-fraction expansion. These terms are then realized by digital programs connected in parallel.

▶ **EXAMPLE I-26** Consider the following transfer function of a digital controller.

$$G_c(z) = \frac{E_2(z)}{E_1(z)} = \frac{10(1 + 0.5z^{-1})}{(1 - z^{-1})(1 - 0.2z^{-1})} \tag{I-257}$$

Since the leading coefficients of the numerator and denominator polynomials in z^{-1} are all constants, the transfer function is physically realizable. The transfer function $G_c(z)$ is realized by the three types of digital programs discussed earlier.

Direct Digital Programming
Equation (I-257) is written

$$G_c(z) = \frac{E_2(z)}{E_1(z)} = \frac{10(1 + 0.5z^{-1})X(z)}{(1 - z^{-1})(1 - 0.2z^{-1})X(z)} \tag{I-258}$$

Expanding the numerator and denominator of the last equation and equating, we have

$$E_2(z) = (10 + 5z^{-1})X(z) \tag{I-259}$$
$$X(z) = E_1(z) + 1.2z^{-1}X(z) - 0.2z^{-2}X(z) \tag{I-260}$$

The last two equations are realized by the digital program shown in Fig. I-47.

Cascade Digital Programming
The right-hand side of Eq. (I-257) is divided into two factors in one of several possible ways.

$$G_c(z) = \frac{E_2(z)}{E_1(z)} = \frac{1 + 0.5z^{-1}}{1 - z^{-1}} \frac{10}{1 - 0.2z^{-1}} \tag{I-261}$$
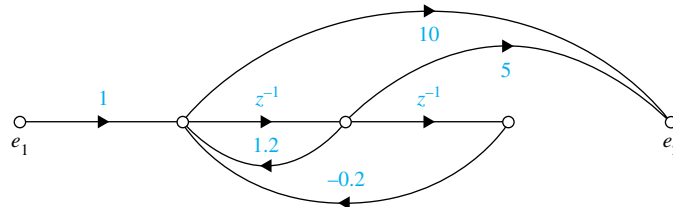
Figure I-47 Direct digital program of Eq. (I-257).

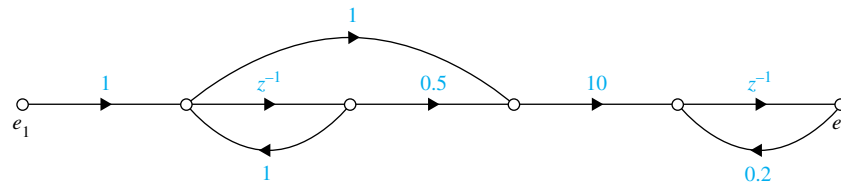Figure I-48 shows the signal flow graph of the cascade digital program of the controller.

Figure I-48 Cascade digital program of Eq. (I-257).

Parallel Digital Programming

The right-hand side of Eq. (I-257) is expanded by partial fraction into two separate terms.

$$G_c(z) = \frac{E_2(z)}{E_1(z)} = \frac{18.75}{1 - z^{-1}} - \frac{8.75}{1 - 0.2z^{-1}} \tag{I-262}$$

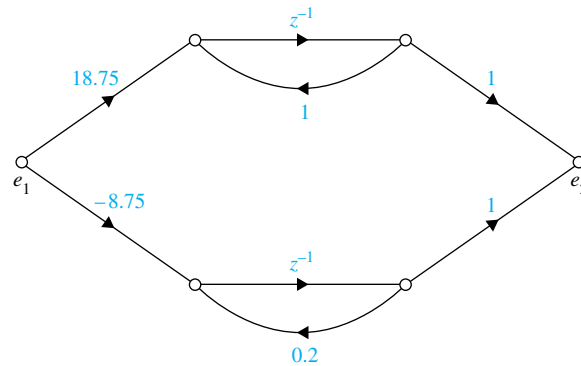Figure I-49 shows the signal flow graph of the parallel digital program of the controller.

Figure I-49 Parallel digital program of Eq. (I-257). ◀

▶ I-12 DESIGN OF DISCRETE-DATA CONTROL SYSTEMS IN THE FREQUENCY DOMAIN AND THE *z*-PLANE

The *w*-transformation introduced in Section I-5 can be used to carry out the design of discrete-data control systems in the frequency domain. Once the transfer function of the controlled process is transformed into the *w*-domain, all the design techniques for continuous-data control systems can be applied to the design of discrete-data systems.

I-12-1   Phase-Lead and Phase-Lag Controllers in the *w*-Domain

Just as in the *s*-domain, the single-stage phase-lead and phase-lag controllers in the *w*-domain can be expressed by the transfer function

$$G_c(w) = \frac{1 + a\tau w}{1 + \tau w} \tag{I-263}$$

where $a > 1$ corresponds to phase lead and $a < 1$ corresponds to phase lag. When *w* is replaced by $j\omega_w$, the Bode plots of Eq. (I-263) are identical to those of Figs. 10-28 and 10-45 for $a > 1$ and $a < 1$, respectively. Once the controller is designed in the *w*-domain, the *z*-domain controller is obtained by substituting the *w*-transformation relationship in Eq. (I-163); that is,

$$w = \frac{2}{T}\frac{z - 1}{z + 1} \tag{I-264}$$

The following example illustrates the design of a discrete-data control system using the *w*-transformation in the frequency domain and the *z*-plane.

▶ **EXAMPLE I-27**   Consider the sun-seeker control system described in Section 4-9, and shown in Fig. 10-29. Now let us assume that the system has discrete data so that there is a ZOH in the forward path. The sampling period is 0.01 second. The transfer function of the controlled process is

$$G_p(s) = \frac{2500}{s(s + 25)} \tag{I-265}$$

The *z*-transfer function of the forward path, including the sample-and-hold is,

$$G_{h0}G_p(z) = (1 - z^{-1})\mathscr{Z}\left(\frac{2500}{s^2(s + 25)}\right) \tag{I-266}$$

Carrying out the *z*-transform in the last equation with $T = 0.01$ second, we get

$$G_{h0}G_p(z) = \frac{0.1152z + 0.106}{(z - 1)(z - 0.7788)} \tag{I-267}$$

The closed-loop transfer function of the discrete-data system is

$$\frac{\Theta_o(z)}{\Theta_r(z)} = \frac{G_{h0}G_p(z)}{1 + G_{h0}G_p(z)} = \frac{0.1152z + 0.106}{z^2 - 1.6636z + 0.8848} \tag{I-268}$$

The unit-step response of the uncompensated system is shown in Fig. I-50. The maximum overshoot is 66 percent.

Let us carry out the design in the frequency domain using the *w*-transformation of Eq. (I-162),

$$z = \frac{(2/T) + w}{(2/T) - w} \tag{I-269}$$

Substituting Eq. (I-269) into Eq. (I-268), we have

$$G_{h0}G_p(w) = \frac{100(1 - 0.005w)(1 + 0.000208w)}{w(1 + 0.0402w)} \tag{I-270}$$

The Bode plot of the last equation is shown in Fig. I-51. The gain and phase margins of the uncompensated system are 6.39 dB and 14.77°, respectively.

Phase-Lag Controller Design in the Frequency Domain
Let us first design the system using a phase-lag controller with the transfer function given in Eq. (I-263) with $a < 1$. Let us require that the phase margin of the system be at least 50°.
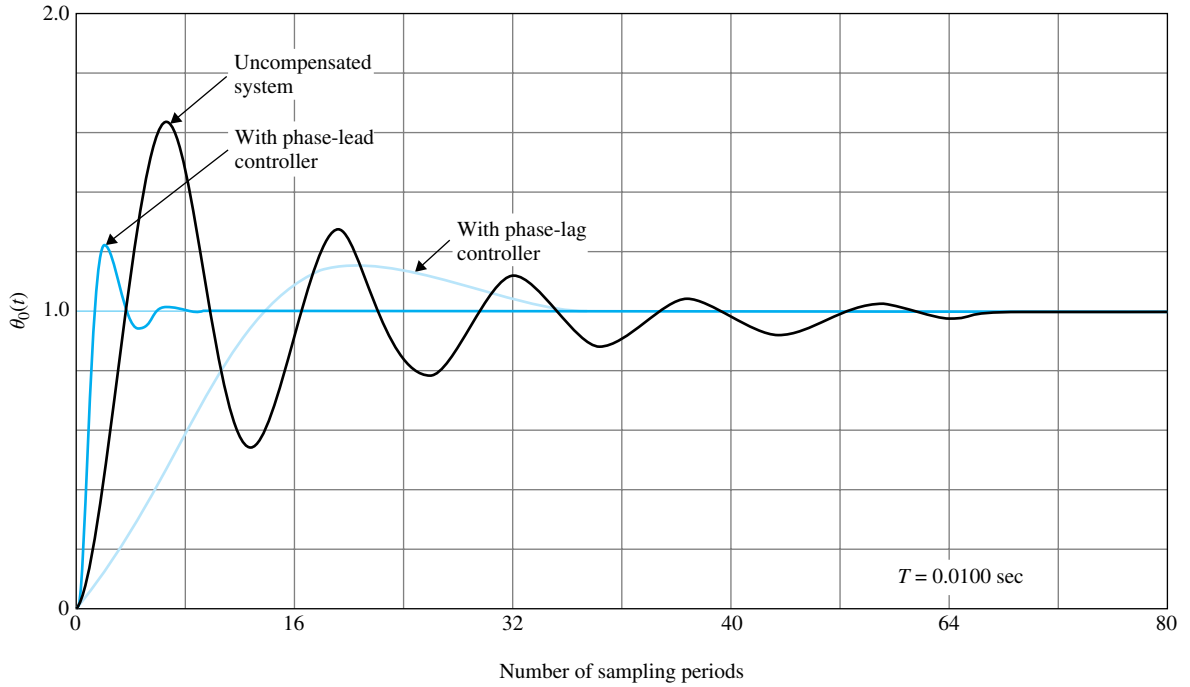
Figure I-50 Step responses of discrete-data sun-seeker system in Example I-27.

From the Bode plot in Fig. I-51, a phase margin of 50° can be realized if the gain crossover point is at $\omega_w = 12.8$ and the gain of the magnitude curve of $G_{ho}G_p(j\omega_w)$ is 16.7 dB.

Thus, we need -16.7 dB of attenuation to bring the magnitude curve down so that it will cross the 0-dB axis at $\omega_w = 12.8$. We set

$$20\log_{10} a = -16.7 \text{ dB} \tag{I-271}$$

from which we get $a = 0.1462$. Next, we set $1/a\tau$ to be at least one decade below the gain crossover point at $\omega_w = 12.8$. We set

$$\frac{1}{a\tau} = 1 \tag{I-272}$$

Thus,

$$\frac{1}{\tau} = a = 0.1462 \tag{I-273}$$

The phase-lag controller in the w-domain is

$$G_c(w) = \frac{1 + a\,\tau w}{1 + \tau w} = \frac{1 + w}{1 + 6.84w} \tag{I-274}$$

Substituting the z-w-transform relation, $w = (2/T)(z - 1)/(z + 1)$, in Eq. (I-274), the phase-lag controller in the z-domain is obtained,

$$G_c(z) = 0.1468\,\frac{z - 0.99}{z - 0.9985} \tag{I-275}$$

The Bode plot of the forward-path transfer function with the phase-lag controller of Eq. (I-274) is shown in Fig. I-51. The phase margin of the compensated system is improved to 55°. The unit-step
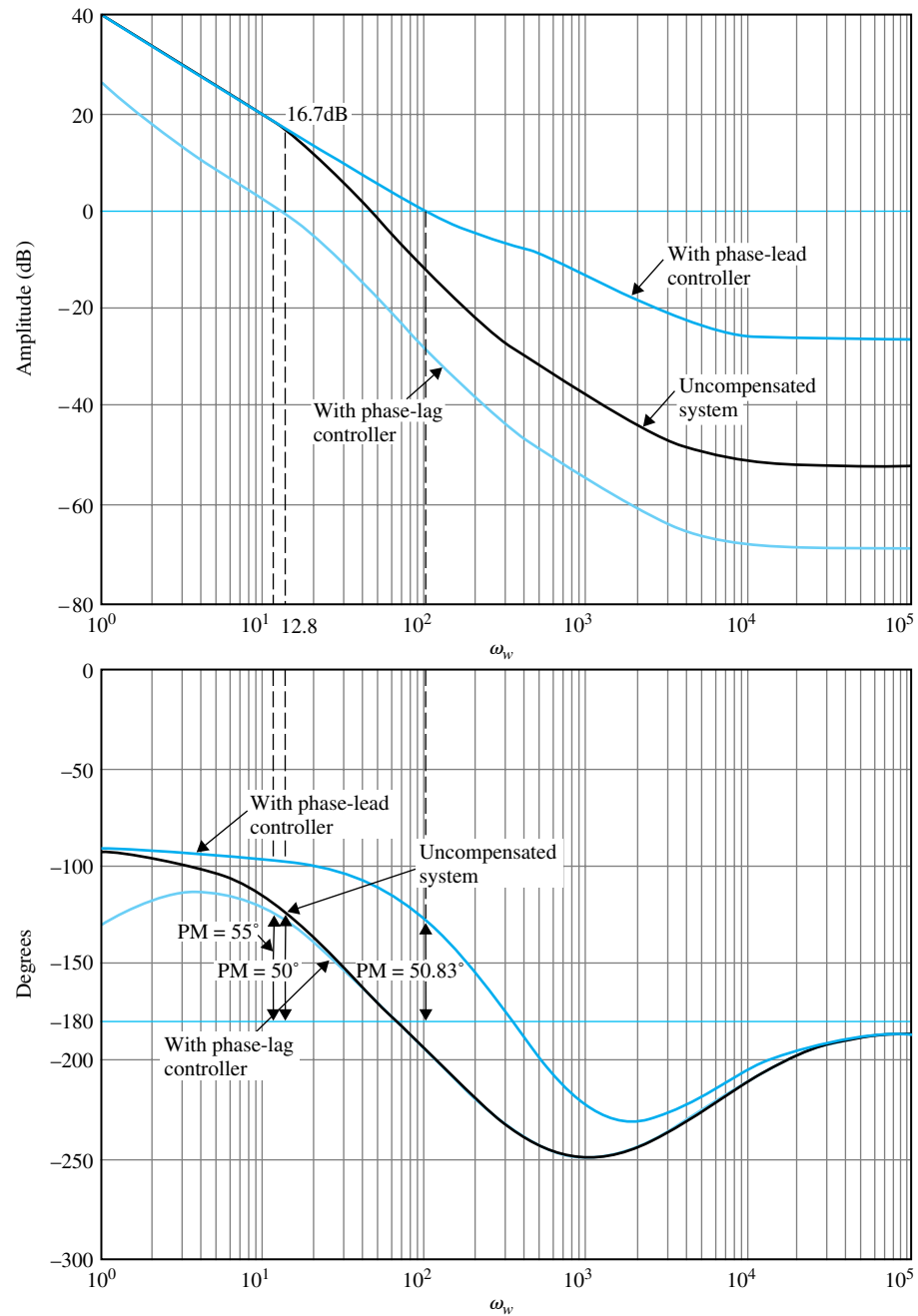
Figure I-51 Bode plots of discrete-data sun-seeker system in Example I-27.

response of the phase-lag compensated system is shown in Fig. I-50. The maximum overshoot is reduced to 16 percent.

Phase-Lead Controller Design in the Frequency Domain

A phase-lead controller is obtained by using $a > 1$ in Eq. (I-263). The same principle for the design of phase-lead controllers of continuous-data systems described in Chapter 10 can be applied here. Since the slope of the phase curve near the gain crossover is rather steep, as shown in Fig. I-51, it is expected that some difficulty may be encountered in designing a phase-lead controller for the

system. Nevertheless, we can assign a relatively large value for a, rather than using the amount of phase lead required as a guideline.

Let us set $a = 20$. The gain of the controller at high values of ω_w is

$$20\log_{10} a = 20\log_{10} 20 = 26 \text{ dB} \tag{I-276}$$

From the design technique outlined in Chapter 10, the new gain crossover should be located at the point where the magnitude curve is at $-26/2 = -13$ dB. Thus, the geometric mean of the two corner frequencies of the phase-lead controller should be at the point where the magnitude of $G_{ho}G_p(j\omega)$ is -13 dB. From Fig. I-51 this is found to be at $\omega_w = 115$. Thus,

$$\frac{1}{\tau} = 115\sqrt{a} = 514 \tag{I-277}$$

The w-domain transfer function of the phase-lead controller is

$$G_c(w) = \frac{1 + a\tau w}{1 + \tau w} = \frac{1 + 0.03888w}{1 + 0.001944w} \tag{I-278}$$

The transfer function of the phase-lead controller in the z-domain is

$$G_c(z) = \frac{8.7776z - 6.7776}{1.3888z + 0.6112} \tag{I-279}$$

The Bode plot of the phase-lead compensated system is shown in Fig. I-51. The phase margin of the compensated system is 50.83°. The unit-step response of the phase-lead compensated system is shown in Fig. I-50. The maximum overshoot is 27 percent, but the rise time is faster.

Digital PD-Controller Design in the z-Plane

The digital PD controller is described by the transfer function in Eq. (I-246), and is repeated as

$$G_c(z) = \frac{\left(K_P + \dfrac{K_D}{T}\right)z - \dfrac{K_D}{T}}{z} \tag{I-280}$$

To satisfy the condition that $G_c(1) = 1$ so that $G_c(z)$ does not affect the steady-state error of the system, we set $K_P = 1$. Applying the digital PD controller as a cascade controller to the sun-seeker system, the forward-path transfer function of the compensated system is

$$G_c(z)G_{ho}G_p(z) = \frac{(1 + 100K_D)z - 100K_D}{z} \frac{0.1152z + 0.106}{(z - 1)(z - 0.7788)} \tag{I-281}$$

We can use the root-contour method to investigate the effects of varying K_D. The characteristic equation of the closed-loop system is

$$z(z^2 - 1.6636z + 0.8848) + 11.52K_D(z - 1)(z + 0.9217) = 0 \tag{I-282}$$

Dividing both sides of the last equation by the terms that do not contain K_D, the equivalent forward-path transfer function with K_D appearing as a multiplying factor is

$$G_{eq}(z) = \frac{11.52K_D(z - 1)(z + 0.9217)}{z(z^2 - 1.6636z + 0.8848)} \tag{I-283}$$

The root contours of the system for $K_D > 0$ are shown in Fig. I-52. These root contours show that the effectiveness of the digital PD controller is limited for this system, since the contours do not dip low enough toward the real axis. In fact, we can show that the best value of K_D from the standpoint of overshoot is 0.022, and the maximum overshoot is 28 percent.

Digital PI-Controller Design in the z-Plane

The digital PI controller introduced in Section I-10-3 can be used to improve the steady-state performance by increasing the system type and, at the same time, improve the relative stability by using
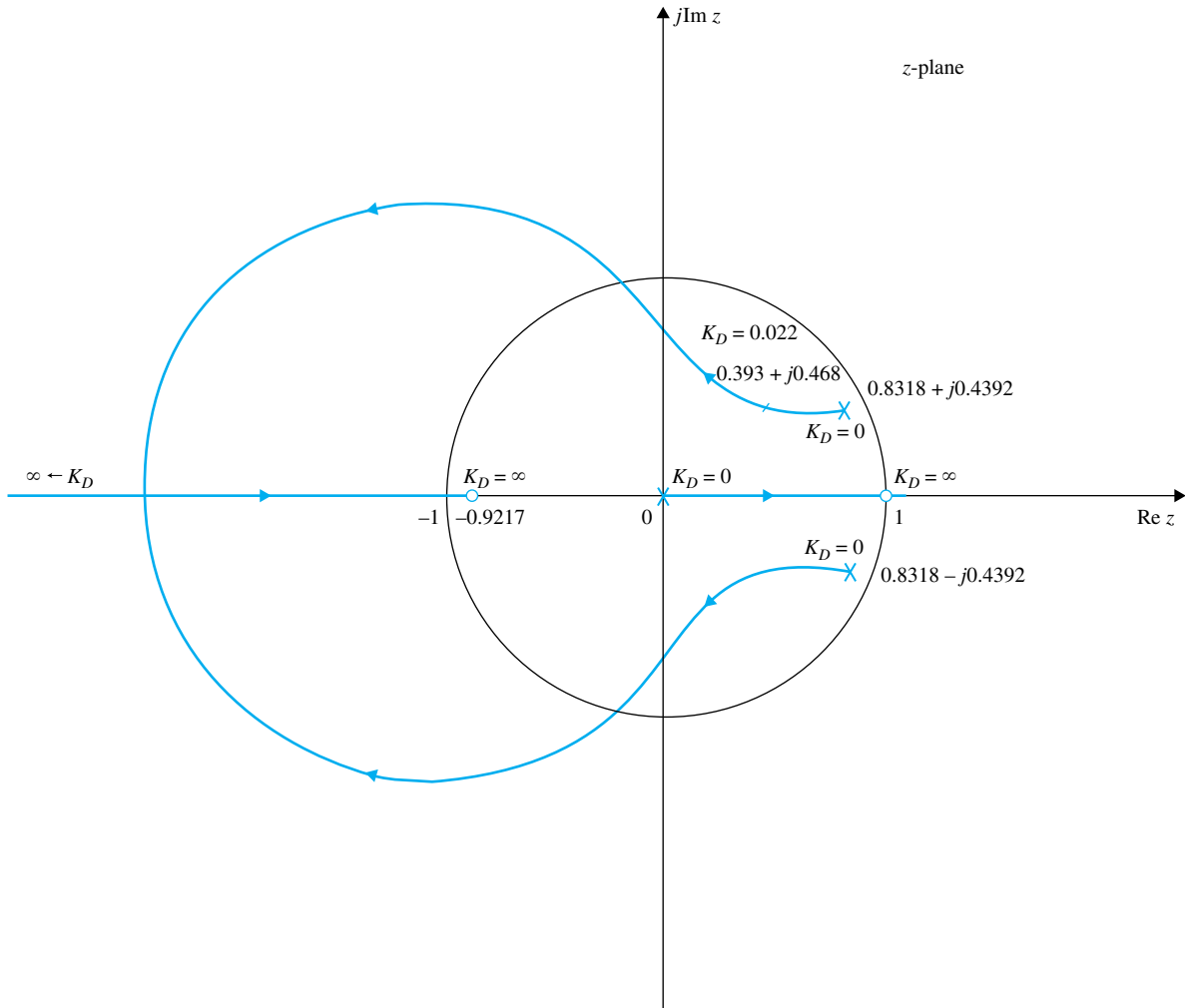
Figure I-52 Root contours of sun-seeker system in Example I-27 with digital PD controller. K_D varies.

the *dipole* principle. Let us select the backward-rectangular integration implementation of the PID controller given by Eq. (I-245). With $K_D = 0$, the transfer function of the digital PI controller becomes

$$G_c(z) = \frac{K_P z - (K_P - K_I T)}{z - 1} = K_P \frac{z - \left(1 - \dfrac{K_I T}{K_P}\right)}{z - 1} \tag{I-284}$$

The principle of the dipole design of the PI controller is to place the zero of $G_c(z)$ very close to the pole at $z = 1$. The effective gain provided by the controller is essentially equal to K_P.

To create a root-locus problem, the transfer function in Eq. (I-267) is written

$$G_{ho}G_p(z) = \frac{K(z + 0.9217)}{(z - 1)(z - 0.7788)} \tag{I-285}$$

where $K = 0.1152$. The root loci of the system are drawn as shown in Fig. I-53. The roots of the characteristic equation when $K = 0.1152$ are $0.8318 + j0.4392$ and $0.8318 - j0.4392$. As shown earlier, the maximum overshoot of the system is 66 percent. If K is reduced to 0.01152, the
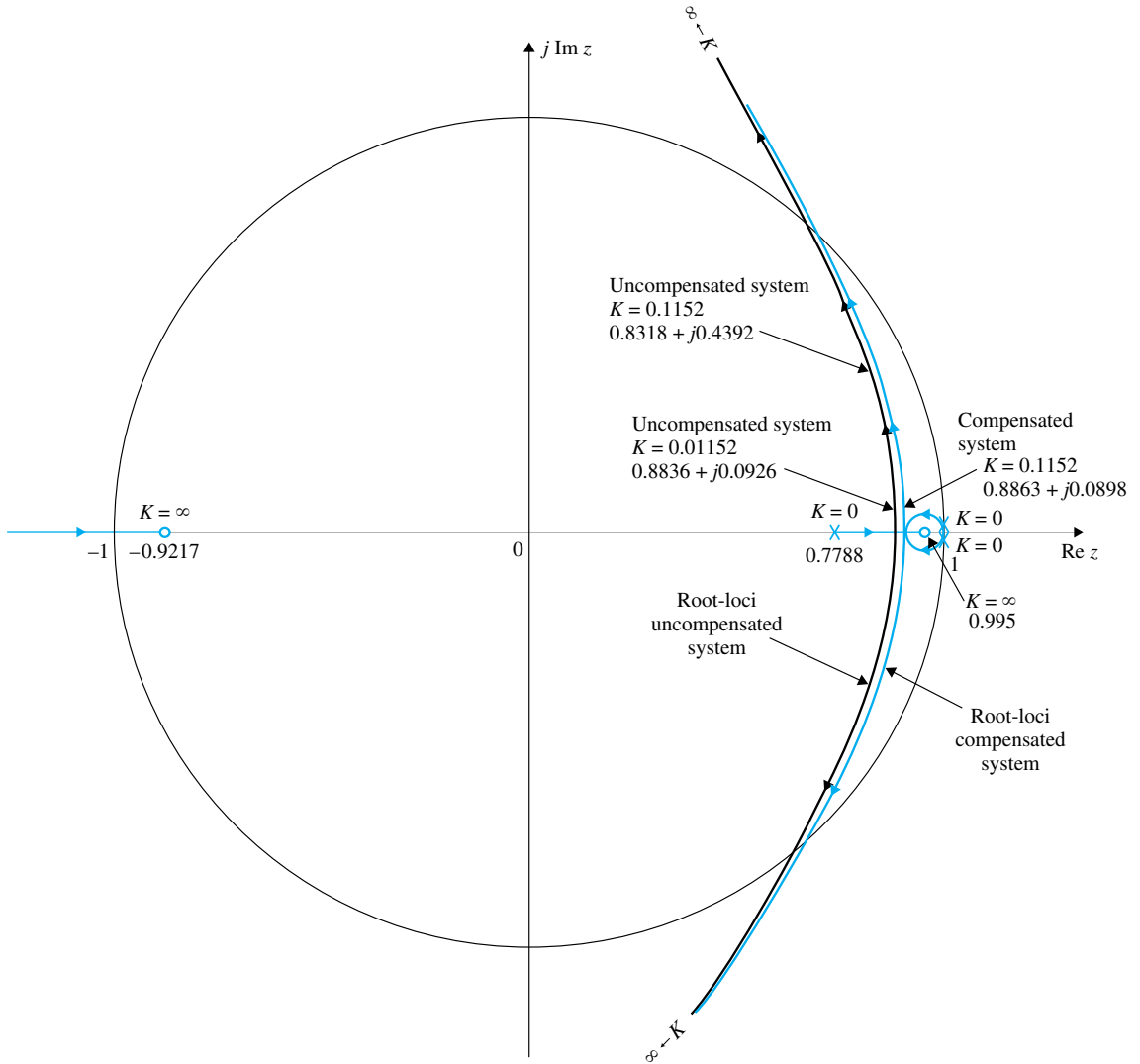
Figure I-53 Root loci of sun-seeker system in Example I-27 with and without digital PI controller.

characteristic equation roots are at $0.8836 + j0.0926$ and $0.8836 - j0.0926$. The maximum overshoot is reduced to only 3 percent.

We can show that if the gain in the numerator of Eq. (I-265) is reduced to 250, the maximum overshoot of the system would be reduced to 3 percent. This means to realize a similar improvement on the maximum overshoot, the value of K_P in Eq. (I-284) should be set to 0.1. At the same time, we let the zero of $G_c(z)$ be at 0.995. Thus,

$$G_c(z) = 0.1\frac{z - 0.995}{z - 1} \tag{I-286}$$

The corresponding value of K_I is 0.05. The forward-path transfer function of the system with the PI controller becomes

$$G_c(z)G_{ho}G_p(z) = \frac{0.1K(z + 0.995)(z + 0.9217)}{(z - 1)^2(z - 0.7788)} \tag{I-287}$$

where $K = 0.1152$. The root loci of the compensated system are shown in Fig. I-53. When $K = 0.1152$, the two dominant roots of the characteristic equation are at $0.8863 + j0.0898$ and $0.8863 - j0.0898$. The third root is at 0.9948, which is very close to the pole of $G_c(z)$ at $z = 1$, and thus the effect on the transient response is negligible. We can show that the actual maximum overshoot of the system with the forward-path transfer function in Eq. (I-287) is approximately 8 percent.

This design problem simply illustrates the mechanics of designing a phase-lead and phase-lag controller using the w-transformation method in the frequency domain and digital PD and PI controllers in the z-plane. No attempt was made in optimizing the system with respect to a set of performance specifications. ◀

▶ I-13 DESIGN OF DISCRETE-DATA CONTROL SYSTEMS WITH DEADBEAT RESPONSE

One difference between a continuous-data control system and a discrete-data control system is that the latter is capable of exhibiting a **deadbeat response**. A deadbeat response is one that reaches the desired reference trajectory in a minimum amount of time without error. In contrast, a continuous-data system reaches the final steady-state trajectory or value theoretically only when time reaches infinity. The switching operation of sampling allows the discrete-data systems to have a finite transient period. Figure I-54 shows a typical deadbeat response of a discrete-data system subject to a unit-step input. The output response reaches the desired steady state with zero error in a minimum number of sampling periods without intersampling oscillations.

H. R. Sirisena [10] showed that given a discrete-data control system with the controlled process described by

$$G_{h0}G_p(z^{-1}) = \frac{Q(z^{-1})}{P(z^{-1})} \tag{I-288}$$

for the system to have a deadbeat response to a step input, the transfer function of the digital controller is given by

$$G_c(z) = \frac{P(z^{-1})}{Q(1) - Q(z^{-1})} \tag{I-289}$$

where $Q(1)$ is the value of $Q(z^{-1})$ with $z^{-1} = 1$.

The following example illustrates the design of a discrete-data system with deadbeat response using Eq. (I-289).
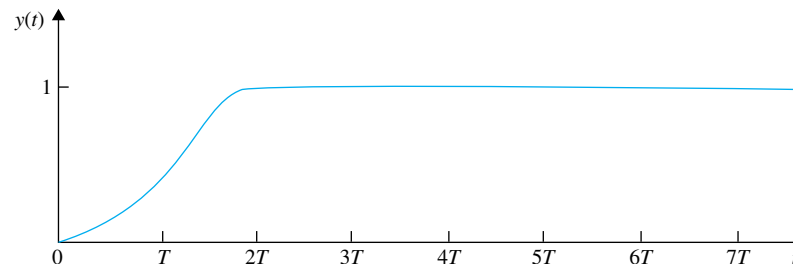

Figure I-54   A typical deadbeat response to a unit-step input.

▶ **EXAMPLE I-28** Consider the discrete-data sun-seeker system discussed in Example I-27. The forward-path transfer function of the uncompensated system is given in Eq. (I-207) and is written as

$$G_{ho}G_p(z^{-1}) = \frac{Q(z^{-1})}{P(z^{-1})} = \frac{0.1152z^{-1}(1 + 0.9217z^{-1})}{(1 - z^{-1})(1 - 0.7788z^{-1})} \tag{I-290}$$

Thus,

$$Q(z^{-1}) = 0.1152z^{-1}(1 + 0.9217z^{-1}) \tag{I-291}$$

$$P(z^{-1}) = (1 - z^{-1})(1 - 0.7788z^{-1}) \tag{I-292}$$

and $Q(1) = 0.22138$.

The digital controller for a deadbeat response is obtained by using Eq. (I-289).

$$G_c(z^{-1}) = \frac{P(z^{-1})}{Q(1) - Q(z^{-1})} = \frac{(1 - z^{-1})(1 - 0.7788z^{-1})}{0.22138 - 0.1152z^{-1} - 0.106z^{-2}} \tag{I-293}$$

Thus,

$$G_c(z) = \frac{(z - 1)(z - 0.7788)}{0.22138z^2 - 0.1152z - 0.106} \tag{I-294}$$

The forward-path transfer function of the compensated system is

$$G_c(z)G_{ho}G_p(z) = \frac{0.1152(z + 0.9217)}{0.22138z^2 - 0.1152z - 0.106} \tag{I-295}$$

The closed-loop transfer function of the compensated system is

$$\frac{\Theta_o(z)}{\Theta_r(z)} = \frac{G_c(z)G_{ho}G_p(z)}{1 + G_c(z)G_{ho}G_p(z)} \tag{I-296}$$

$$= \frac{0.0.5204(z + 0.9217)}{z^2}$$

For a unit-step function input, the output transform is

$$\Theta_o(z) = \frac{0.5204(z + 0.9217)}{z(z - 1)} \tag{I-297}$$

$$= 0.5204z^{-1} + z^{-2} + z^{-3} + \cdots$$

Thus, the output response reaches the unit-step input in two sampling periods.

To show that the output response is without intersampling ripples, we evaluate the output velocity of the system; that is, $\omega_o(t) = d\theta_o(t)/dt$.

The z-transfer function of the output velocity is written

$$\frac{\Omega_o(z)}{\Theta_r(z)} = \frac{G_c(z)(1 - z^{-1})\mathcal{Z}\left[\dfrac{2500}{s(s + 25)}\right]}{G_c(z)G_{ho}G_p(z)} \tag{I-298}$$

$$= \frac{100(z - 1)}{z^2}$$

The output velocity response due to a unit-step input is

$$\Omega_o(z) = \frac{100}{z} = 100z^{-1} \tag{I-299}$$

• The root sensitivity of a system with deadbeat response is poor.

Thus, the output velocity becomes zero after the second sampling period, which proves that the position response is deadbeat without intersampling ripples. The responses of $\theta_o(t)$ and $\omega_o(t)$ are shown in Fig. I-55. The characteristic of a system with deadbeat response is that the poles of the closed-
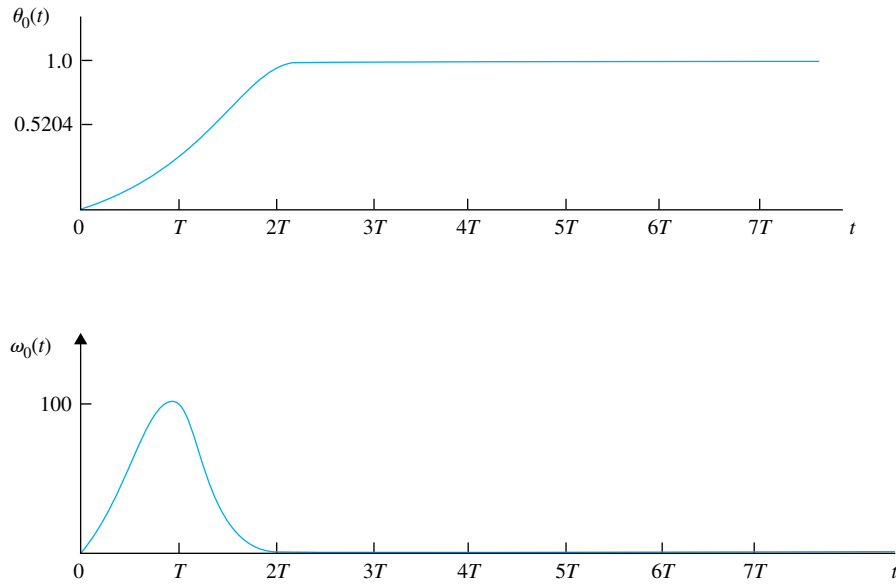
Figure I-55 Output position and velocity responses of discrete-data sun-seeker system in Example I-28.

loop transfer function are all at $z = 0$. Since these are multiple-order poles, from the standpoint of root sensitivity discussed in Chapter 8, the root sensitivity of a system with deadbeat response is very high. ◀

▶ I-14 POLE-PLACEMENT DESIGN WITH STATE FEEDBACK

Just as for continuous-data systems, pole-placement design through state feedback can be applied to discrete-data systems. Let us consider the discrete-data system described by the following state equation:

$$\mathbf{x}[(k + 1)T] = \mathbf{A}\mathbf{x}(kT) + \mathbf{B}u(kT) \tag{I-300}$$

where $\mathbf{x}(kT)$ is an $n \times 1$ state vector, and $u(kT)$ is the scalar control. The state-feedback control is

$$u(kT) = -\mathbf{K}\mathbf{x}(kT) + r(kT) \tag{I-301}$$

where $\mathbf{K}$ is the $1 \times n$ feedback matrix with constant-gain elements. By substituting Eq. (I-301) into Eq. (I-300), the closed-loop system is represented by the state equation

$$\mathbf{x}[(k + 1)T] = (\mathbf{A} - \mathbf{B}\mathbf{K})\mathbf{x}(kT) \tag{I-302}$$

Just as in the continuous-data case treated in Section 10-12, we can show that if the pair [$\mathbf{A}$, $\mathbf{B}$] is completely controllable, a matrix $\mathbf{K}$ exists that can give an arbitrary set of eigenvalues of $(\mathbf{A} - \mathbf{B}\mathbf{K})$; that is, the n roots of the characteristic equation

$$|z\mathbf{I} - \mathbf{A} + \mathbf{B}\mathbf{K}| = 0 \tag{I-303}$$

can be arbitrarily placed. The following example illustrates the design of a discrete-data control system with state feedback and pole placement.

▶ **EXAMPLE I-29** Consider that the sun-seeker system described in Example 10-9 is subject to sampled data so that the state diagram of the system without feedback is shown in Fig. I-56(a). The sampling period is 0.01 second. The dynamics of the ZOH are represented by the branch with a transfer function of $1/s$. The closed-loop system with state feedback for the time interval $(kT) \leq t \leq (k + 1)T$ is portrayed by the state diagram shown in Fig. I-56(b), where the feedback gains k_1 and k_2 form the feedback matrix

$$\mathbf{K} = \begin{bmatrix} k_1 & k_2 \end{bmatrix} \tag{I-304}$$

Applying the SFG gain formula to Fig. I-56(b), with $X_1(s)$ and $X_2(s)$ as outputs and $x_1(kT)$ and $x_2(kT)$ as inputs, we have

$$X_1(s) = \left[\frac{1}{s} - \frac{2500k_1}{s^2(s + 25)}\right]x_1(kT) + \left[\frac{1}{s(s + 25)} - \frac{2500k_2}{s^2(s + 25)}\right]x_2(kT) \tag{I-305}$$

$$X_2(s) = \frac{-2500k_1}{s(s + 25)}x_1(kT) - \frac{2500k_2}{s(s + 25)}x_2(kT) + \frac{1}{s + 25}x_2(kT) \tag{I-306}$$

Taking the inverse Laplace transform on both sides of Eqs. (I-305) and (I-306) and letting $t = (k + 1)T$, we have the discrete-data state equations as

$$x_1[(k + 1)T] = (1 - 0.1152k_1)x_1(kT) + (0.2212 - 0.1152k_2)x_2(kT)$$
$$x_2[(k + 1)T] = -22.12k_1x_1(kT) + (0.7788 - 22.12k_2)x_2(kT) \tag{I-307}$$

Thus, the coefficient matrix of the closed-loop system with state feedback is

$$\mathbf{A} - \mathbf{BK} = \begin{bmatrix} 1 - 0.1152k_1 & 0.2212 - 0.1152k_2 \\ -22.12k_1 & 0.7788 - 22.12k_2 \end{bmatrix} \tag{I-308}$$

The characteristic equation of the closed-loop system is

$$|z\mathbf{I} - \mathbf{A} + \mathbf{BK}| = \begin{vmatrix} z - 1 + 0.1152k_1 & -0.2212 + 0.1152k_2 \\ 22.12k_1 & z - 0.7788 + 22.12k_2 \end{vmatrix} \tag{I-309}$$

$$= z^2 + (-1.7788 + 0.1152k_1 + 22.12k_2)z + 0.7788 + 4.8032k_1 - 22.12k_2 = 0$$

Let the desired location of the characteristic equation roots be at $z = 0, 0$. The conditions on k_1 and k_2 are

$$-1.7788 + 0.1152k_1 + 22.12k_2 = 0 \tag{I-310}$$
$$0.7788 + 4.8032k_1 - 22.12k_2 = 0 \tag{I-311}$$

Solving for k_1 and k_2 from the last two equations, we get

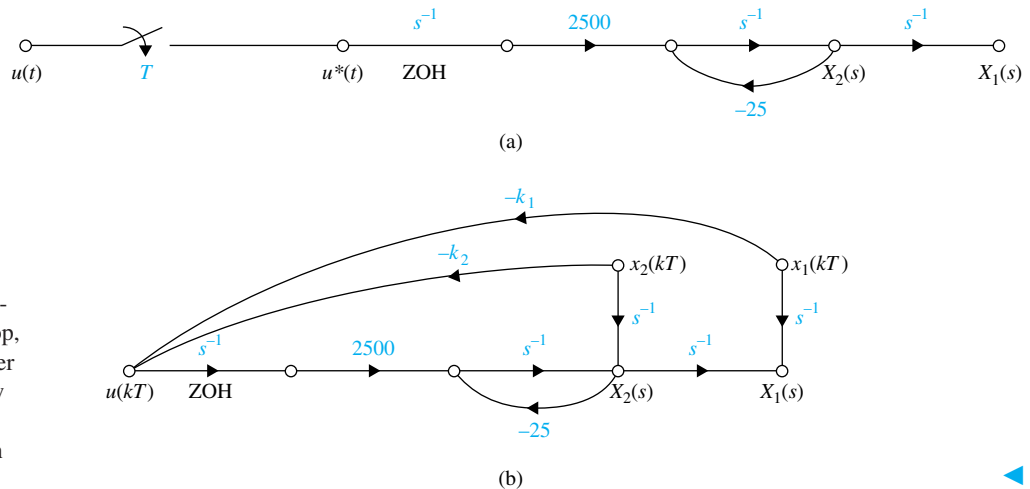$$k_1 = 0.2033 \quad \text{and} \quad k_2 = -0.07936 \tag{I-312}$$

Figure I-56 (a) Signal-flow graph of open-loop, discrete-data, sun-seeker system. (b) Signal-flow graph of discrete-data, sun-seeker system with state feedback.

►REFERENCES

1. B. C. Kuo, *Digital Control Systems*, 2nd ed., Oxford University Press, New York, 1992.
2. M. L. Cohen, "A Set of Stability Constraints on the Denominator of a Sampled-Data Filter," *IEEE Trans. Automatic Control*, Vol. AC-11, pp. 327–328, April 1966.
3. E. I. Jury and J. Blanchard, "A Stability Test for Linear Discrete Systems in Table Form," *IRE Proc.*, Vol. 49, No. 12, pp. 1947–1948, December 1961.
4. E. I. Jury and B. D. O. Anderson, "A Simplified Schur-Cohen Test," *IEEE Trans. Automatic Control*, Vol. AC-18, pp. 157–163, April 1973.
5. R. H. Raible, "A Simplification of Jury's Tabular Form," *IEEE Trans. Automatic Control*, Vol. AC-19, pp. 248–250, June 1974.
6. E. I. Jury, *Theory and Application of the z-Transform Method*, John Wiley & Sons, New York, 1964.
7. G. F. Franklin, J. D. Powell, and M. L. Workman, *Digital Control of Dynamic Systems*, 2nd ed., Addison-Wesley, Reading, MA. 1990.
8. K. OGATA, *Discrete-Time Control Systems*, Prentice Hall, Englewood Cliffs, NJ, 1987.
9. C. L. Phillips and H. T. Nagle, Jr., *Digital Control System Analysis and Design*, Prentice Hall, Englewood Cliffs, NJ, 1984
10. H. R. Sirisena, "Ripple-Free Deadbeat Control of SISO Discrete Systems," *IEEE Trans. Automatic Control*, Vol. AC-30, pp. 168–170, February 1985.

►PROBLEMS

I-1. Find the z-transforms of the following functions.

(a) $f(k) = ke^{-3k}$ **(b)** $f(k) = k\sin 2k$

(c) $f(k) = e^{-2k}\sin 3k$ **(d)** $f(k) = k^2 e^{-2k}$

• z-transforms

I-2. Determine the z-transforms of the following sequences.

(a) $f(kT) = kT\sin 2kT$

(b) $f(k) = \begin{cases} 1 & k = 0, 2, 4, 6, \ldots, \text{even integers} \\ -1 & k = 1, 3, 5, 7, \ldots, \text{odd integers} \end{cases}$

• Partial-fraction expansion, z-transform

I-3. Perform the partial-fraction of the following functions, if applicable, and then find the z-transforms using the z-transform table.

(a) $F(s) = \dfrac{1}{(s + 5)^3}$ **(b)** $F(s) = \dfrac{1}{s^3(s + 1)}$

(c) $F(s) = \dfrac{10}{s(s + 5)^2}$ **(c)** $F(s) = \dfrac{5}{s(s^2 + 2)}$

• Inverse z-transform

I-4. Find the inverse z-transforms $f(k)$ of the following functions. Apply partial-fraction expansion to $F(z)$ and then use the z-transform table.

(a) $F(z) = \dfrac{10z}{(z - 1)(z - 0.2)}$ **(b)** $F(z) = \dfrac{z}{(z - 1)(z^2 + z + 1)}$

(c) $F(z) = \dfrac{z}{(z - 1)(z + 0.85)}$ **(d)** $F(z) = \dfrac{10}{(z - 1)(z - 0.5)}$

• z-transform, final-value theorem

I-5. Given that $\mathcal{Z}[f(k)] = F(z)$, find the value of $f(k)$ as k approaches infinity without obtaining the inverse z-transform of $F(z)$. Use the final-value theorem of the z-transform if it is applicable.

(a) $F(z) = \dfrac{0.368z}{(z - 1)(z^2 - 1.364z + 0.732)}$ **(b)** $F(z) = \dfrac{10z}{(z - 1)(z + 1)}$

(c) $F(z) = \dfrac{z^2}{(z - 1)(z - 0.5)}$ **(d)** $F(z) = \dfrac{z}{(z - 1)(z - 1.5)}$

Check the answers by carrying out the long division of $F(z)$ and express it in a power series of z^{-1}.

• z-transform solutions

I-6. Solve the following difference equations by means of the z-transform.

(a) $x(k + 2) - x(k + 1) + 0.1x(k) = u_s(k)$ $\qquad x(0) = x(1) = 0$

(b) $x(k + 2) - x(k) = 0$ $\qquad x(0) = 1, \quad x(1) = 0$

I-7. This problem deals with the application of the difference equations and the z-transform to a loan-amortization problem. Consider that a new car is purchased with a load of P_0 dollars over a period of N months at a monthly interest rate of r percent. The principal and interest are to be paid back in N equal payments of u dollars each.

(a) Show that the difference equation that describes the loan process can be written as

$$P(k + 1) = (1 + r)P(k) - u$$

where $P(k)$ = amount owed after the kth period, $k = 0, 1, 2, \dots, N$.
$P(O) = P_0$ = initial amount borrowed
$P(N) = 0$ (after N periods, owe nothing)

The last two conditions are also known as the boundary conditions.

(b) Solve the difference equation in part (a) by the recursive method, starting with $k = 0$, then $k = 1, 2, \dots$, and substituting successively. Show that the solution of the equation is

$$u = \frac{(1 + r)^N P_0 r}{(1 + r)^N - 1}$$

(c) Solve the difference equation in part (a) by using the z-transform method.

(d) Consider that $P_0 = \$15,000$, $r = 0.01$ (1 percent per month), and $N = 48$ months. Find u, the monthly payment.

I-8. Perform the partial-fraction expansion to the following z-transfer functions.

(a) $G(z) = \dfrac{5z}{(z - 1)(z - 0.1)}$ **(b)** $G(z) = \dfrac{10z(z - 0.2)}{(z - 1)(z - 0.5)(z - 0.8)}$

(c) $G(z) = \dfrac{z}{(z - 1)(z - 0.5)^2}$ **(d)** $G(z) = \dfrac{2z}{(z - 1)(z^2 - z + 1)}$

(d) Find $y(t)$ for $t \geq 0$ when the input is a unit-step function. Use $G_4(s)$ as determined in part (b).

I-9. A linear time-invariant discrete-data system has an output that is described by the time sequence

$$y(kT) = 1 - e^{-2kT} \qquad k = 0, 1, 2, \dots$$

when the system is subject to an input sequence described by $r(kT) = 1$ for all ≥ 0. Find the transfer function $G(z) = Y(z)/R(s)$.

I-10. Find the transfer functions $Y(z)/R(z)$ of the discrete-data systems shown in Fig. IP-10. The sampling period is 0.5 second.

I-11. It is well known that the transfer function of an analog integrator is

$$G(s) = \frac{Y(s)}{X(s)} = \frac{1}{s}$$

where $X(s)$ and $Y(s)$ are the Laplace transforms of the input and the output of the integrator, respectively. There are many ways of implementing integration digitally. In a basic computer course, the rectangular integration is described by the schemes shown in Fig. IP-10. The continuous signal $x(t)$ is approximated by a staircase signal; T is the sampling period. The integral of $x(t)$, which is the area under $x(t)$, is approximated by the area under the rectangular approximation signal.

(a) Let $y(kT)$ denote the digital approximation of the integral of $x(t)$ from $t = 0$ to $t = kT$. Then $y(kT)$ can be written as

$$y(kT) = y[(k - 1)T] + Tx(kT) \tag{1}$$

where $y[(k - 1)T]$ denotes the area under $x(t)$ from $t = 0$ to $t = (k - 1)T$. Take the z-transform on both sides of Eq. (1) and show that the transfer function of the digital integrator is

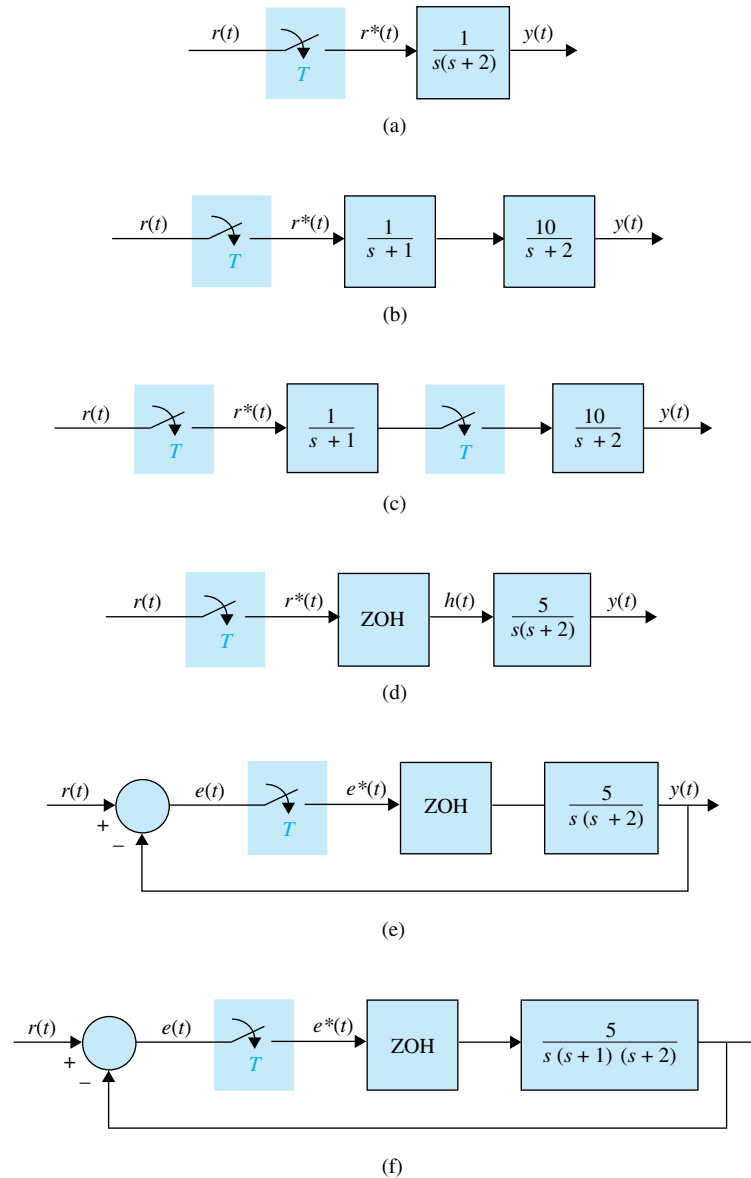$$G(z) = \frac{Y(z)}{X(z)} = \frac{Tz}{z - 1}$$

Figure IP-10

(b) The rectangular integration described in Fig. IP-11(a) can be interpreted as a sample-and-hold operation, as shown in Fig. IP-11(b). The signal $x(t)$ is first sent through an ideal sampler with sampling period T. The output of the sampler is the sequence $x(0)$, $x(T)$, ..., $x(kT)$, ... These numbers are then sent through a "backward" hold device to give the rectangle of height $x(kT)$ during the time interval from $(k - 1)T$ to kT. Verify the result obtained in part (a) for $G(z)$ using the "backward" sample-and-hold interpretation.

(c) As an alternative, we can use a "forward" rectangular hold, as shown in Fig. IP-11(c). Find the transfer function $G(z)$ for such a rectangular integrator.

• Vector-matrix discrete state equations

I-12. The block diagram of a sampled-data system is shown in Fig. IP-12. The state equations of the controlled process are

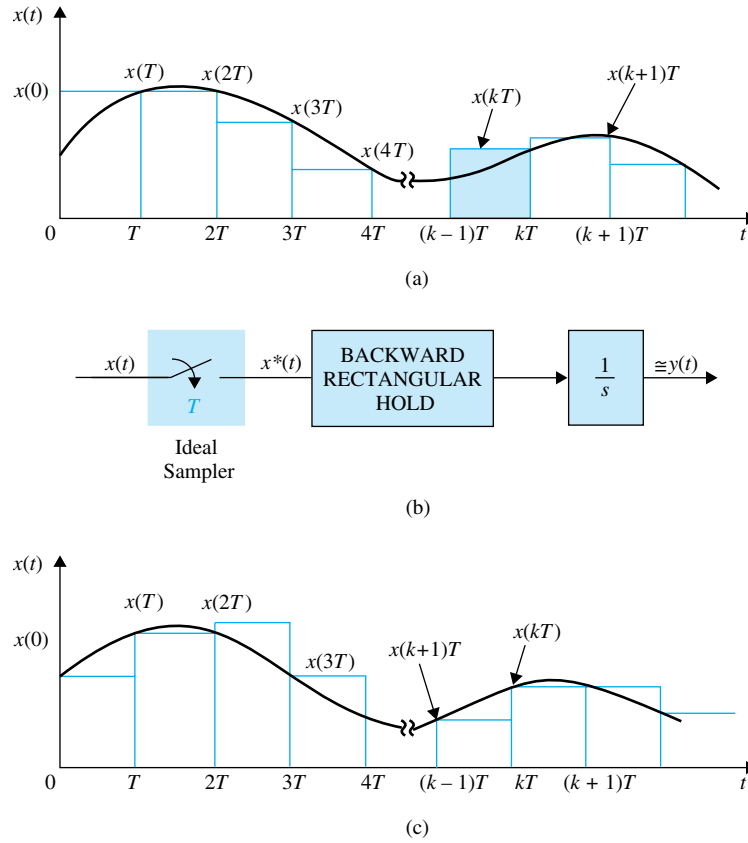$$\frac{dx_1(t)}{dt} = x_2(t) \qquad \frac{dx_2(t)}{dt} = -2x_1(t) - 3x_2(t) + h(t)$$

Figure IP-11

where $h(t)$ is the output of the sample-and-hold; that is, $u(t)$ is constant during the sampling period T.

(a) Find the vector-matrix discrete state equations in the form of

$$\mathbf{x}[(k + 1)T] = \phi(T)\mathbf{x}(kT) + \theta(T)u(kT)$$

(b) Find $\mathbf{x}(NT)$ as functions of $\mathbf{x}(0)$ and $u(kT)$ for $k = 0, 1, 2, \dots N$.
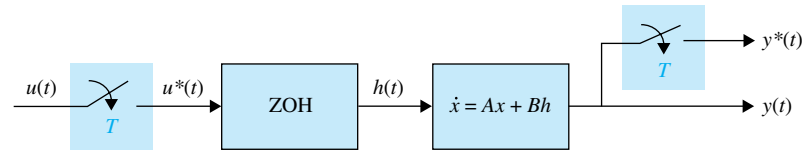

Figure IP-12

• Vector-matrix discrete state equations

I-13. Repeat Problem I-12 for the linear sampled-data system with the following state equations.

$$\frac{dx_1(t)}{dt} = x_1(t) \qquad \frac{dx_2(t)}{dt} = u(t)$$

The sampling period is 0.001 second.

• Discrete-data system, transfer function

I-14. (a) Find the transfer function $\mathbf{X}(z)/U(z)$ for the system described in Problem I-12.

(b) Find the characteristic equation of the system described in Problem I-12.

• Discrete-data system, transfer function

I-15. (a) Find the transfer function $\mathbf{X}(z)/U(z)$ for the system described in Problem I-13.

(b) Find the characteristic equation and its roots of the system described in Problem I-13.

• Digital control, state-diagram characteristic equation

I-16. Draw a state diagram for the digital control system represented by the following dynamic equations:

$$\mathbf{x}(k+1) = \mathbf{A}\mathbf{x}(k) + \mathbf{B}u(k) \qquad y(k) = x_1(k)$$

$$\mathbf{A} = \begin{bmatrix} 0 & 1 & -1 \\ 0 & 1 & 2 \\ 5 & 3 & -1 \end{bmatrix} \qquad \mathbf{B} = \begin{bmatrix} 0 \\ 0 \\ 1 \end{bmatrix}$$

Find the characteristic equation of the system.

• Digital control, state diagram, transfer function

I-17. The state diagram of a digital control system is shown in Fig. IP-17. Write the dynamic equations.
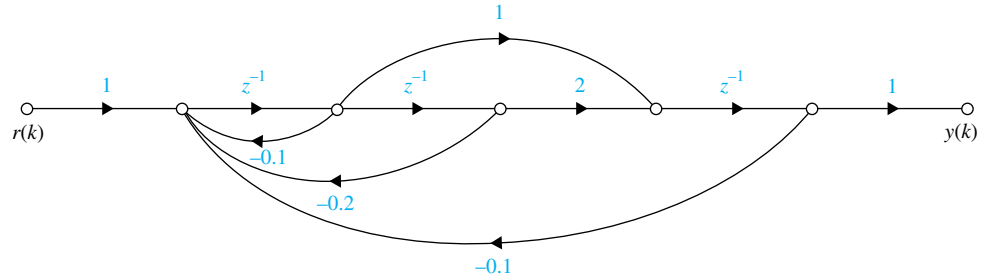
Find the transfer function $Y(z)/R(z)$.

Figure IP-17

• Sampled-data system, state equations, state diagram

I-18. The block diagram of a sampled-data system is shown in Fig. IP-18. Write the discrete state equations of the system. Draw a state diagram for the system.
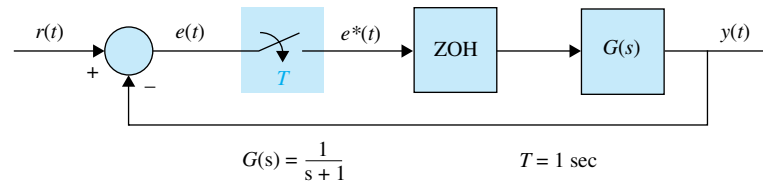

Figure IP-18

$$G(s) = \frac{1}{s+1} \qquad T = 1 \text{ sec}$$

• Stability of discrete-data systems

I-19. Apply the w-transform to the following characteristic equations of discrete-data control systems, and determine the conditions of stability (asymptotically stable, marginally stable, or unstable) using the Routh-Hurwitz criterion.

(a) $z^2 + 1.5z - 1 = 0$ **(b)** $z^3 + z^2 + 3z + 0.2 = 0$

(c) $z^3 - 1.2z^2 - 2z + 3 = 0$ **(d)** $z^3 - z^2 - 2z + 0.5 = 0$

Check the answers by solving for the roots of the equations using a root-finding computer program.

• Stability of digital control system

I-20. A digital control system is described by the state equation

$$x(k+1) = (0.368 - 0.632K)x(k) + Kr(k)$$

where $r(k)$ is the input, and $x(k)$ is the state variable. Determine the values of K for the system to be asymptotically stable.

• Stability of digital control system

I-21. The characteristic equation of a linear digital control system is

$$z^3 + z^2 + 1.5Kz - (K + 0.5) = 0$$

Determine the values of K for the system to be asymptotically stable.

I-22. The block diagram of a discrete-data control system is shown in Fig. IP-22.

(a) For $T = 0.1$ second, find the values of K so that the system is asymptotically stable at the sampling instants.

(b) Repeat part (a) when the sampling period is 0.5 second.

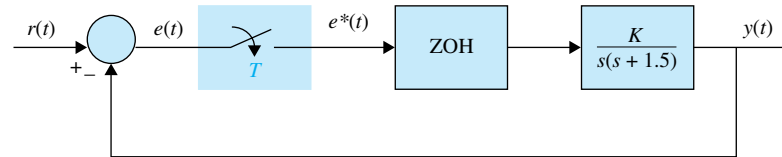**(c)** Repeat part (a) when the sampling period is 1.0 second.

Figure IP-22

I-23. Use a root-finding computer program to find the roots of the following characteristic equations of linear discrete-data control systems, and determine the stability condition of the systems.

(a) $z^3 + 2z^2 + 1.2z + 0.5 = 0$ **(b)** $z^3 + z^2 + z - 0.5 = 0$

(c) $0.5z^3 + z^2 + 1.5z + 0.5 = 0$ **(d)** $z^4 + 0.5z^3 + 0.25z^2 + 0.1z - 0.25 = 0$

I-24. The block diagram of a sampled-data control system is shown in Fig. IP-24.

(a) Derive the forward-path and the closed-loop transfer functions of the system in z-transforms. The sampling period is 0.1 second.

(b) Compute the unit-step response $y(kT)$ for $k = 0$ to 100.

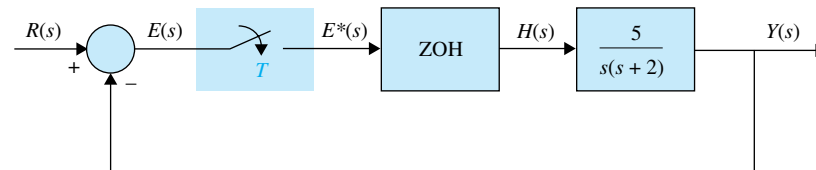**(c)** Repeat parts (a) and (b) for $T = 0.05$ second.

Figure IP-24

I-25. The block diagram of a sampled-data control system is shown in Fig. IP-25.

(a) Find the error constants K_p^*, K_v^*, and K_a^*.

(b) Derive the transfer functions $Y(z)/E(z)$ and $Y(z)/R(z)$.

(c) For $T = 0.1$ second, find the critical value of K for system stability.

(d) Compute the unit-step response $y(kT)$ for $k = 0$ to 50 for $T = 0.1$ second and $K_t = 5$.

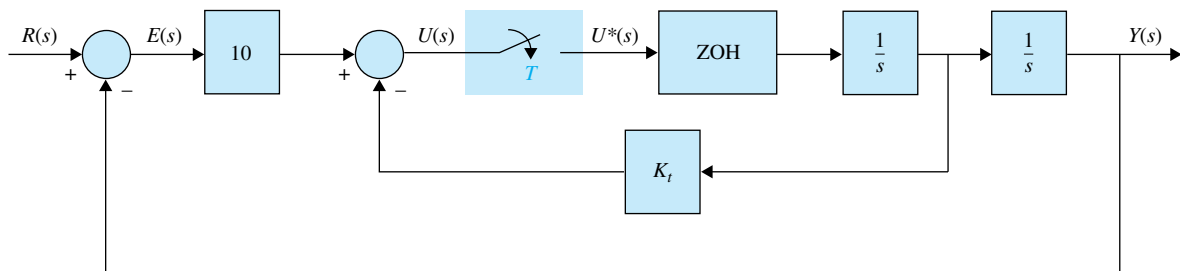**(e)** Repeat part (d) for $T = 0.1$ second and $K_t = 1$.

Figure IP-25

I-26. The forward-path dc-motor control system described in Problem 5-33 is now incorporated in a digital control system, as shown in Fig. IP-26(a). The microprocessor takes the information from the encoder and computes the velocity information. This generates the sequence of numbers, $\omega(kT)$ $k = 0, 1, 2, \ldots$. The microprocessor then generates the error signal $e(kT) = r(kT) - \omega(kT)$. The digital control is modeled by the block diagram shown in Fig. IP-26(b). Use the parameter values given in Problem 5-33.

(a) Find the transfer function $\Omega(z)/E(z)$ with the sampling period $T = 0.1$ second.

(b) Find the closed-loop transfer function $\Omega(z)/R(z)$. Find the characteristic equation and its roots. Locate these roots in the z-plane. Show that the closed-loop system is unstable when $T = 0.1$ second.

(c) Repeat parts (a) and (b) for $T = 0.01$ and 0.001 second. Use any computer simulation program.

(d) Find the error constants K_p^*, K_v^*, and K_a^*. Find the steady-state error $e(kT)$ as $k \to \infty$ when the input $r(t)$ is a unit-step function, a unit-ramp function, and a parabolic function $t^2 u_s(t)/2$.

(a)

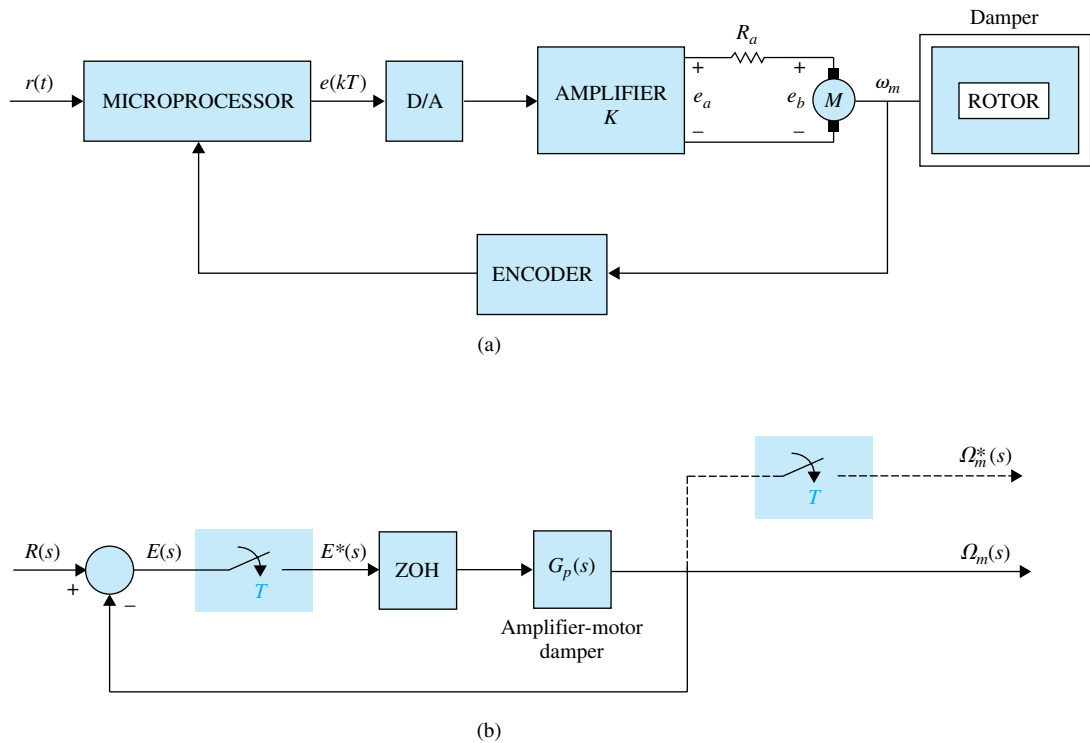

(b)

Figure IP-26

I-27. The block diagram of a sampled-data control system is shown in Fig. IP-27.

(a) Construct the root loci in the z-plane for the system for $K \geq 0$, without the zero-order hold, when $T = 0.5$ second, and then with $T = 0.1$ second. Find the marginal values of K for stability.

$$G(s) = \frac{K}{s(s + 5)}$$

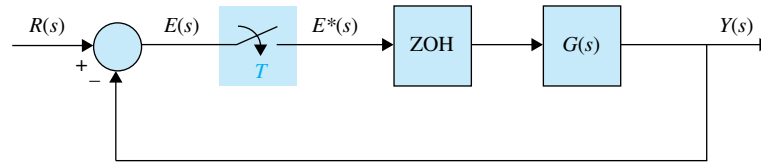**(b)** Repeat part (a) when the system has a zero-order-hold, as shown in Fig. IP-27.

Figure IP-27

I-28. The system shown in Fig. IP-27 has the following transfer function.

$$G(s) = \frac{Ke^{-0.1s}}{s(s + 1)(s + 2)}$$

Construct the root loci in the z-plane for $K \geq 0$, with $T = 0.1$ second.

I-29. The characteristic equations of linear discrete-data control systems are given in the following equations. Construct the root loci for $K \geq 0$. Determine the marginal value of K for stability.

(a) $z^3 + Kz^2 + 1.5Kz - (K + 1) = 0$

(b) $z^2 + (0.15K - 1.5)z + 1 = 0$

(c) $z^2 + (0.1K - 1)z + 0.5 = 0$

(d) $z^2 + (0.4 + 0.14K)z + (0.5 + 0.5K) = 0$

(e) $(z - 1)(z^2 - z + 0.4) + 4 \times 10^{-5}K(z + 1)(z + 0.7) = 0$

I-30. The forward-path transfer function of a unity-feedback discrete-data control system with sample-and-hold is

$$G_{ho}G(z) = \frac{0.0952z}{(z - 1)(z - 0.905)}$$

The sampling period is $T = 0.1$ second.

(a) Plot the plot of $G_{ho}G(z)$ and determine the stability of the closed-loop system.

(b) Apply the w-transformation of Eq. (I-226) to $G_{ho}G(z)$ and plot the Bode plot of $G_{ho}G(w)$. Find the gain and phase margins of the system.

I-31. Consider that the liquid-level control system described in Problem 6-13 is now subject to sample-and-hold operation. The forward-path transfer function of the system is

$$G_{ho}G(z) = \frac{1 - e^{-Ts}}{s}\left(\frac{16.67N}{s(s + 1)(s + 12.5)}\right)$$

The sampling period is 0.05 second. The parameter N represents the number of inlet valves. Construct the Bode plot of $G_{ho}G(w)$ using the w-transformation of Eq. (I-226), and determine the limiting value of N (integer) for the closed-loop system to be stable.

I-32. Find the digital equivalents using the following integration rules for the controllers given. (a) Backward-rectangular integration rule, (b) forward-rectangular integration rule, and (c) trapezoidal-integration rule. Use the backward-difference rule for derivatives.

(i) $G_c(s) = 2 + \dfrac{200}{s}$ **(ii)** $G_c(s) = 10 + 0.1s$ **(iii)** $G_c(s) = 1 + 0.2s + \dfrac{5}{s}$

I-33. A continuous-data controller with sample-and-hold units is shown in Fig. IP-33. The sampling period is 0.1 second. Find the transfer function of the equivalent digital controller. Draw a digital-program implementation diagram for the digital controller. Carry out the analysis for the following continuous-data controllers.

(a) $G_c(s) = \dfrac{10}{s + 12}$ **(b)** $G_c(s) = \dfrac{10(s + 1.5)}{(s + 10)}$

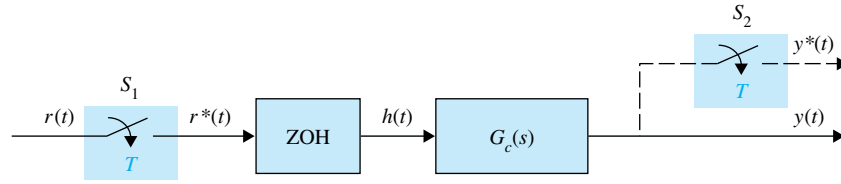**(c)** $G_c(s) = \dfrac{s}{s + 1.55}$ **(d)** $G_c(s) = \dfrac{1 + 0.4s}{1 + 0.01s}$

Figure IP-33

• Physical realizability of digital transfer functions

I-34. Determine which of the following digital transfer functions are physically realizable.

(a) $G_c(z) = \dfrac{10(1 + 0.2z^{-1} + 0.5z^{-2})}{z^{-1} + z^{-2} + 1.5z^{-3}}$

(b) $G_c(z) = \dfrac{1.5z^{-1} - z^{-2}}{1 + z^{-1} + 2z^{-2}}$

(c) $G_c(z) = \dfrac{z + 1.5}{z^3 + z^2 + z + 1}$

(d) $G_c(z) = z^{-1} + 0.5z^{-3}$

(e) $G_c(z) = 0.1z + 1 + z^{-1}$

(f) $G_c(z) = \dfrac{z^{-1} + 2z^{-2} + 0.5z^{-3}}{z^{-1} + z^{-2}}$

• Inventory-control system with digital PD controller

I-35. The transfer function of the process of the inventory-control system described in Problem 10-17 is

$$G_p(s) = \frac{4}{s^2}$$

The block diagram of the system with a PD controller and sample-and-hold is shown in Fig. IP-35. Find the transfer function of the digital PD controller using the following equation,

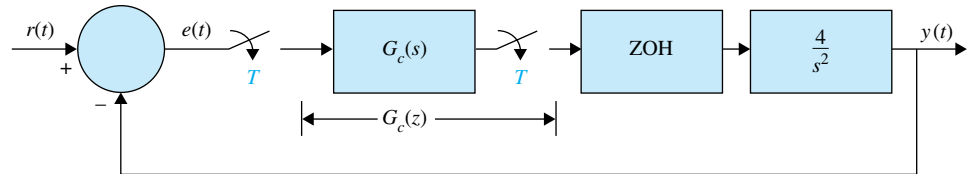$$G_c(z) = \frac{\left(K_P + \dfrac{K_D}{T}\right)z - \dfrac{K_D}{T}}{z}$$

Figure IP-35

Select a sampling period T so that the maximum overshoot of $y(kT)$ will be less than 1 percent.

• Inventory-control system with digital PD controller

I-36. Figure IP-35 shows the block diagram of the inventory-control system described in Problem 10-17 with a digital PD controller. The sampling period is 0.01 second. Consider that the digital PD controller has the transfer function

$$G_c(z) = K_P + \frac{K_P(z - 1)}{T_z}$$

(a) Find the values of K_P and K_D so that two of the three roots of the characteristic equation are at 0.5 and 0.5. Find the third root. Plot the output response $y(kT)$ for $k = 0, 1, 2, \ldots$.

(b) Set $K_P = 1$. Find the value of K_D so that the maximum overshoot of $y(kT)$ is a minimum.

• Inventory-control system with digital phase-lead controller

I-37. For the inventory-control system described in Problem I-36, design a phase-lead controller using the w-transformation so that the phase-margin of the system is at least 60°. Can you design a phase-lag controller in the w-domain? If not, explain why not.

• Aircraft attitude control system with digital controller

I-38. The process transfer function of the second-order aircraft attitude control system described in Problem 10-5 is

$$G_p(s) = \frac{4500K}{s(s + 361.2)}$$

Consider that the system is to be compensated by a series digital controller $G_c(z)$ through a sample-and-hold.

(a) Find the value of K so that the discrete ramp-error constant K_v^* is 100.

(b) With the value of K found in part (a), plot the unit-step response of the output $y^*(t)$ and find maximum overshoot.

(c) Design the digital controller so that the output is a deadbeat response to a step input. Plot the unit-step response.

• Sun-seeker system with digital controller; deadbeat response

I-39. The sun-seeker system described in Example I-5 is considered to be controlled by a series digital controller with the transfer function $G_c(z)$. The sampling period is 0.01 second. Design the controller so that the output of the system is a deadbeat response to a unit-step input. Plot the unit-step response of the designed system.

• Sun-seeker system with state feedback

I-40. Design the state-feedback control for the sun-seeker system in Example I-5 so that the characteristic equation roots are at $z = 0.5, 0.5$.

• State-feedback control

I-41. Consider the digital control system

$$\mathbf{x}[(k+1)T] = \mathbf{A}\mathbf{x}(kT) + \mathbf{B}u(kT)$$

where

$$\mathbf{A} = \begin{bmatrix} 0 & 1 \\ -1 & -1 \end{bmatrix} \qquad \mathbf{B} = \begin{bmatrix} 0 \\ 1 \end{bmatrix}$$

The state-feedback control is described by $u(kT) = -\mathbf{K}\mathbf{x}(kT)$, where $\mathbf{K} = [k_1 \quad k_2]$. Find the values of k_1 and k_2 so that the roots of the characteristic equation of the closed-loop system are at 0.5 and 0.7.